TOLUENIUM AND OTHER GASEOUS METHYLBENZENIUM IONS: COMPLEX INTERPLAY OF PROTONATED ARENES AND CYCLO-OLEFINS

Dietmar Kuck[1]*
Department of Chemistry, Bielefeld University, Bielefeld, Germany

Received 1 March 2020; accepted 14 April 2020

The development of the current knowledge of the gas-phase chemistry of protonated methylbenzenes, such as toluenium, xylenium and mesitylenium ions, their higher congeners as well as of their mostly cyclo-olefinic isomers by mass spectrometric methodology is presented. Starting from the observation of the characteristic expulsion of dihydrogen from metastable $C_7H_9^+$ ions, which is associated with the release of large amounts of kinetic energy, and the composite C- and H-scrambling prior to the loss of methane, in particular, insights into the isomerization scenario of various isomeric $C_7H_9^+$, $C_8H_{11}^+$, and $C_9H_{13}^+$ ions, based on a large variety of independent techniques, are discussed. Besides isotope labeling and metastable ion methodology, these include flowing afterglow mass spectrometry, gas-phase titration and infrared spectroscopy of mass-selected ions. The particularly complex energy hypersurface of isomerizing and fragmenting toluenium ions, which has been elaborated in various reports over the years, is presented in a combined way to assess the role of protonated cycloheptatriene, norbornadiene, and 6-methylfulvene as well as a number of further $C_7H_9^+$ isomers. The formation and nature of $C_7H_9^+$ ions generated by fragmentation of various hydrocarbon precursors, such as monoterpenes and adamantane, is also addressed. The contribution of infrared multiphoton dissociation spectroscopy (IRMPD) and tagged-ion infrared photodissociation (IRPD) of the gaseous $C_7H_9^+$ ions as compared to the wealth of previous understanding of their chemistry is commented on as well. Finally, remarkable parallels of the gas-phase chemistry of methylbenzenium ions and the role of such species within the cavities of acidic zeolite catalysts in the course of the industrially important methanol-to-hydrocarbon reaction are discussed. © 2020 John Wiley & Sons Ltd. Mass Spec Rev

Keywords: *gas-phase ion chemistry; methylbenzenes, protonated; cyclo-olefins, protonated; toluenium ions; xylenium ions; isomerization; scrambling, H and C; kinetic energy release; metastable ions; titration, gas phase; IR spectroscopy of gaseous ions; MTH reaction*

I. INTRODUCTION

Protonated toluene, $C_7H_9^+$ ($[\mathbf{1}+H]^+$, Scheme 1), representing the simplest alkylbenzenium ion and, thus, a prototypical species in the realm of electrophilic aromatic substitution, has fascinated scientists working on the fundamentals of organic chemists for many decades. After half a century of growing understanding of the role of Pfeiffer-Wizinger (or Wheland) intermediates as nowadays generally accepted σ-complexes, governing the course of electrophilic aromatic substitution reactions in solution, the following about five decades have brought about comprehensive details of the properties of toluenium ions in all of the three states of aggregation. Starting in 1958 with the first report by Doering et al. (1958), protonation of methylbenzenes in strong acids and especially in superacid solvents at low temperatures was studied by ^{1}H nuclear magnetic resonance (NMR) spectroscopy and provided a compellingly stringent picture of the regioselective addition of a proton to an energetically favorable ring position. Olah et al. (1972) demonstrated in 1972 that the *para*-toluenium ion, *p*-$[\mathbf{1}+H]^+$, is the most stable among the four possible tautomers and prevails at −97 °C. Equilibration of *p*-$[\mathbf{1}+H]^+$ with the *ortho*- and *meta*-tautomers, *o*-$[\mathbf{1}+H]^+$ and *m*-$[\mathbf{1}+H]^+$, was deduced from the coalescence of the signals of the ^{1}H NMR spectra recorded at higher temperatures (Fig. 1). Using ^{13}C NMR spectroscopy, Fărcaşiu et al. proved the coexistence of the *para*- and *ortho*-tautomers of protonated toluene and protonated ethylbenzene (ethylbenzenium ion) in superacidic solution (Fărcaşiu, Melchior, & Craine, 1977; Fărcaşiu, 1982). Notably, the existence of the *ipso*-protonated form, *i*-$[\mathbf{1}+H]^+$, the prototype of all alkylbenzenium ions that are necessarily formed in alkylation and de-alkylation processes, was never observed by NMR spectroscopy. Solid-state methylbenzenium ion salts were already prepared in the 1960s and characterized in acid-free solution (Olah, 1965; Brookhart, Anet, & Winstein, 1966). However, only in 2003 Reed and his associates succeeded to synthesize a *para*-toluenium carborane salt, $\{p\text{-}[\mathbf{1}+H]^+\ CB_{11}H_6Br_6^-\}$, as well as related methylbenzenium ion salts, including the parent benzenium congener, and to characterize their solid-sate structures by X-ray diffraction, in addition to NMR spectroscopy (Reed et al., 2003). In combination with nowadays available high-performance spectroscopic techniques, such as high-resolution ^{1}H and ^{13}C NMR

Correspondence to: Dietmar Kuck, Department of Chemistry, Bielefeld University, Universitätsstraße 25, 33615 Bielefeld, Germany. E-mail: dietmar.kuck@uni-bielefeld.de

*Dedicated to Professor Einar Uggerud.

[Correction added after online publication on 19 January 2021: "Copyright" has been updated]

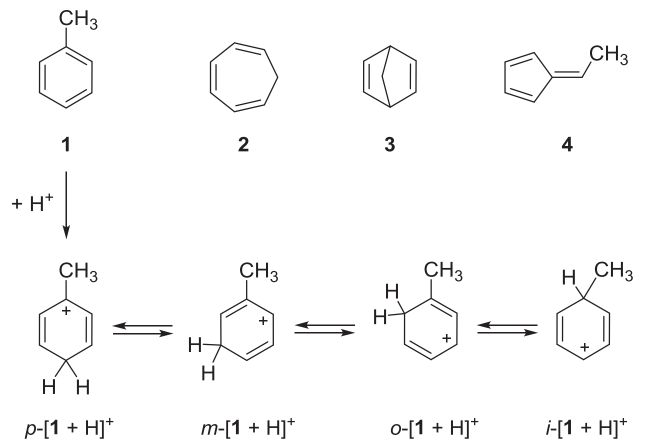

SCHEME 1. Protonation of toluene (**1**) giving the *para*-toluenium ion, p-[**1**+H]$^+$, at low temperatures in solution but the rapidly interconverting tautomers p-[**1**+H]$^+$ to i-[**1**+H]$^+$ under ambient temperature and/or in the gas phase. Also shown are some cyclo-olefinic isomers of **1**: cycloheptatriene (**2**), norbornadiene (**3**), and 6-methylfulvene (**4**), the conjugate acids of which interconvert with ions [**1**+H]$^+$ in the gas phase.

spectroscopy, in particular, benzenium salts can be considered well understood in the condensed states of matter. Figure 1 illustrates these key insights into the static and dynamic nature of toluenium ions.

Gas-phase toluenium ions and related lower alkylbenzenium ions have a separate story—and, in fact, comprise a very rich and multifaceted chemistry. It combines the world of gas-phase acid-base chemistry of arenes with that of gaseous protonated olefins and cyclo-olefins, electrophilic aromatic substitution with catalysis, and gas-phase ion chemistry with analytical chemistry. This review tells the story of gaseous toluenium ions and related protonated aromatic and olefinic hydrocarbons starting from the very beginning of organic mass spectrometry through the present state of knowledge, which is characterized by a long way from electron impact (nowadays electron ionization [EI]) mass spectrometry to sophisticated gas-phase methodology, such as ion-molecule reactions and infrared photodissociation spectroscopy of mass-selected ions.

II. GASEOUS TOLUENIUM IONS IN EI AND CHEMICAL IONIZATION (CI) MASS SPECTROMETRY

A. Early Structural Implications

Gaseous $C_7H_9^+$ ions (m/z 93) give rise to prominent peaks in the mass spectra of toluene and other C_7H_8 isomers. The formation of the [M+H]$^+$ molecular ions of such simple hydrocarbons is well known since this ionization method was established by Munson and Field in 1966 (Munson & Field, 1966; Munson & Field, 1967). Since then, the occurrence of intense m/z 93 peaks in the CI mass spectra of toluene and alkyltoluenes, indicating the respective [M+H]$^+$ molecular ions or, respectively, [M+H–alkene]$^+$ fragment ions, is well known (Herman & Harrison, 1981). However, $C_7H_9^+$ ions were observed even before the advent of the CI method in the EI mass spectra of certain olefins and cyclo-olefins. In 1958, Friedman and Wolf studied the abundant formation of $C_7H_9^+$ ions from various terpene hydrocarbons under EI conditions and discussed the possible role of the *para*-toluenium ion and some isomers, including protonated cycloheptatriene, [**2**+H]$^+$, as key intermediates of the overall fragmentation (Friedman & Wolf, 1958). Harrison and coworkers observed intense m/z 93 peaks in the EI mass spectra of 1,3-cyclooctadiene, 1,2-dimethylcyclopentadiene and 1-methyl-1,4-cyclohexadiene and related olefins (Harrison et al., 1965). By comparison with the spectra of the corresponding alkylbenzenes and measurements of the appearance energies, they concluded that "the major fragment ions from the

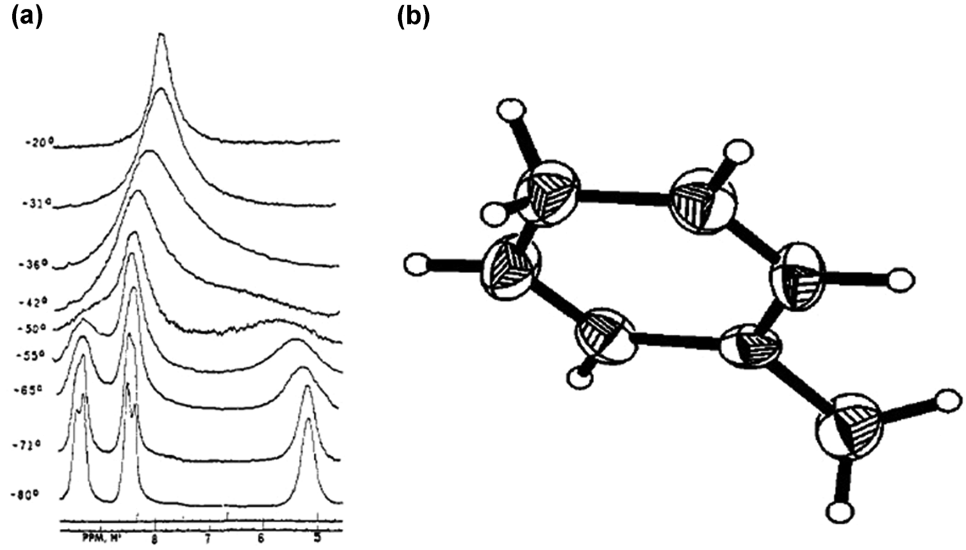

FIGURE 1. (**a**) Temperature-variable ^{1}H NMR spectra of the toluenium ion in superacidic solution, showing the three specific benzenium ring resonances of p-[**1**+H]$^+$ at −80°C and their coalescence due to the dynamic equilibrium with the other tautomers (Olah et al., 1972). (**b**) Oblique view on the solid-state structure of p-[**1**+H]$^+$ present in the toluenium ion salt {p-[**1**+H]$^+ \cdot CB_{11}H_6Br_6^-$} (ORTEP plot); the carborane counterion is not shown (Reed et al., 2003). Adapted with permission from *The Journal of the American Chemical Society* 1972;94:2034–2043 (**a**) and 2003;125:1796–1804 (**b**). Copyright 2020 American Chemical Society.

methylcyclopentadienes do not retain the cyclopentadienyl structure but undergo rearrangement, probably to form a cyclic benzenium-type ion" (Harrison et al., 1965). Thus, the structure of protonated toluene was tentatively assigned to the $C_7H_9^+$ ions (*m*/*z* 93) ions. The EI mass spectra of terpenes are known for long time to exhibit prominent peaks at *m*/*z* 93 (Reed, 1963). An early study by Schwarz et al. (1976) pointed to the formation of a common structure of the $C_7H_9^+$ ions formed from various monoterpenes, while even later work by Basic and Harrison (1991) suggested the prevalent formation of protonated cycloheptatriene, [**2**+H]$^+$. These early investigations clearly show that the gas-phase chemistry of the *m*/*z* 93 fragment ions appearing in the EI mass spectra of unsaturated hydrocarbons had attracted some interest, in part because of the obvious structural parallels to the long-known isomerization of $C_7H_7^+$ (*m*/*z* 91) and $C_7H_8^{\bullet+}$ (*m*/*z* 92) ions generated from alkylbenzenes (Grubb, 1963; Meyer & Harrison, 1965; Howe & McLafferty, 1971). However, as compared to the $C_7H_9^+$ ions, these direct *m*/*z*-scale neighbors in the hydrocarbon ion gallery gained much more general attention over the decades (Bursey, Bursey, & Kingston, 1973; Kuck, 1990a, 1990b, 2005c; Lifshitz, 1994).

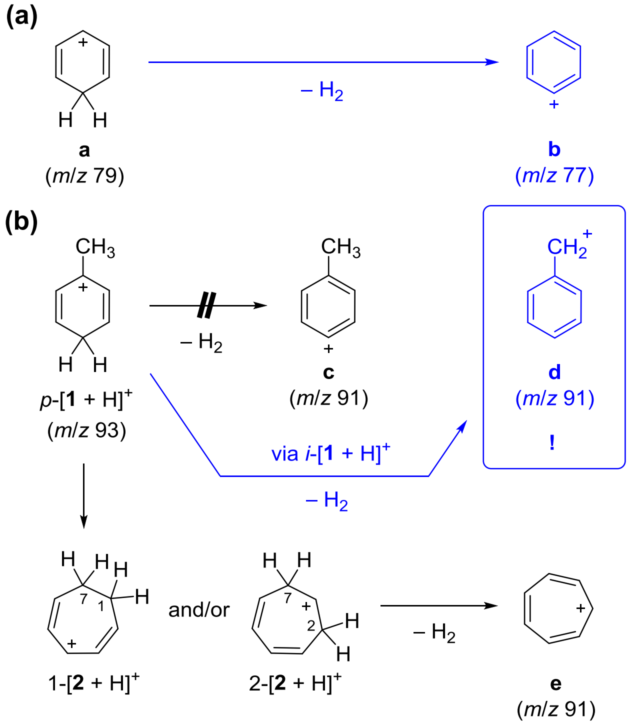

SCHEME 2. Mechanistically contrasting elimination of H_2 (**a**) from the parent benzenium ion, **a**, giving the phenyl cation, **b**, by 1,1-elimination, and (b) from the *para*-toluenium ion, *p*-[**1**+H]$^+$. Early work suggested ring expansion of ions [**1**+H]$^+$ to the dihydrotropylium ions 1-[**2**+H]$^+$ and/or 2-[**2**+H]$^+$ followed by 1,2- or 1,3-elimination of H_2, respectively, to give the tropylium ion, **e** (Williams & Hvistendahl, 1974b; Hvistendahl & Williams, 1975). While 1,1-elimination of H_2 from [**1**+H]$^+$ was excluded by experiment, 1,2-elimination via the *ipso*-tautomer, *i*-[**1**+H]$^+$, giving the benzylium ion, **d**, was suggested in later work (Kuck, Schneider, & Grützmacher, 1985). The actually occurring pathways are depicted in blue color (see text).

B. Unimolecular Fragmentation of $C_7H_9^+$ Ions

$C_7H_9^+$ ions (*m*/*z* 93) generated from various precursors exhibit a highly specific unimolecular fragmentation behavior. Similar to the parent benzenium ion, $C_6H_7^+$ (*m*/*z* 79, **a**, Scheme 2), they undergo elimination of dihydrogen. In fact, the *m*/*z* 93 peaks appearing in the standard EI and CI mass spectra are accompanied by more or less intense peaks at *m*/*z* 91, similar to the twin peaks at *m*/*z* 79 and *m*/*z* 77 of alkylbenzenes and related cyclo-olefinic hydrocarbons (Grubb, 1963; Kuck, 1990; Kuck, 1990; Kuck & Mormann, 2000). In addition, $C_7H_9^+$ ions eliminate methane, a minor but most important fragmentation channel, which enables a deeper insight into their isomerization behavior that precedes fragmentation. Nevertheless, the features of the dihydrogen elimination from gaseous $C_7H_9^+$ ions represented a most inspiring observation, which was interpreted by Williams and Hvistendahl in terms of the Woodward-Hoffman rules (Woodward & Hoffmann, 1969; Williams & Hvistendahl, 1974a, 1974b; Hvistendahl & Williams, 1975). The unimolecular reaction $C_7H_9^+ \rightarrow C_7H_7^+ + H_2$ is accompanied by the release of an unusually large amount of kinetic energy, $T_{\text{kin}} = 0.87 - 0.99\ \text{eV} = 85 - 97\ \text{kJ/mol}$, as indicated by a strongly broadened and even dish-shaped peak in the mass-selected ion kinetic energy (MIKE) spectra of metastable $C_7H_9^+$ ions (Fig. 2b) (Cooks et al., 1973; Williams & Hvistendahl, 1974b; Kuck, Schneider, & Grützmacher, 1985). In contrast, the apparently analogous reaction of benzenium ion, $C_6H_7^+ \rightarrow C_6H_5^+ + H_2$, is associated with a negligibly small kinetic energy release (KER), as reflected by a narrow peak with Gaussian shape in the MIKE spectrum (Fig. 2a) (Williams & Hvistendahl, 1974b; Kuck, Schneider, & Grützmacher, 1985). This striking difference inspired Williams and Hvistendahl to suggest that both processes occur through orbital-symmetry-controlled but fundamentally different mechanisms. The H_2 loss from $C_6H_7^+$ should occur by a symmetry-allowed 1,1-elimination from the endocyclic methylene unit to give the phenyl cation, $C_6H_5^+$ (*m*/*z* 77, **b**, Scheme 2). This implies that the reverse reaction, namely the 1,1-addition of H_2 to the phenyl cation, should require only little, if any, activation energy. Thus, the transition state for the forward reaction of the $C_6H_7^+$ ion cannot transmit appreciable amounts of "reverse activation energy" into the fragments as they separate from each other on-the-fly within the ion beam. This situation gives rise to narrow peaks with Gaussian peak shape in a sector-field mass spectrometer. If the H_2 loss from the $C_7H_9^+$ ions took place by the same 1,1-elimination mechanism, narrow peak shapes should be observed as well and the tolyl cation, for example the *para*-isomer (**c**, Scheme 2), corresponding to the *para*-toluenium ion, *p*-[**1**+H]$^+$, as the reacting tautomer, should be formed. To rationalize the extremely large KER observed in the case of the $C_7H_9^+$ ions, Williams and Hvistendahl proposed that the actual fragmentation occurs by a symmetry-forbidden 1,2-elimination of H_2 from the dihydrotropylium ion, that is, more specifically, from the C^1-protonated cycloheptatriene, 1-[**2**+H]$^+$. Alternatively, 1,3-elimination of H_2 from the 1,3-dihydrotropylium ion (C^2-protonated cycloheptatriene, 2-[**2**+H]$^+$) was also inferred (Williams & Hvistendahl, 1974b; Hvistendahl & Williams, 1975). Instead of a tolyl cation, such as ion **c**, the tropylium cation (**e**, Scheme 2) would be the $C_7H_7^+$ product in these cases. Due to orbital-symmetry control, such a mechanism would require a high-energy transition state and, as a consequence, a large reverse activation barrier towards 1,2-addition of dihydrogen to the tropylium ion, **e**. Undoubtedly this mechanistic model provided an elegant explanation for the origin of the large KER associated with

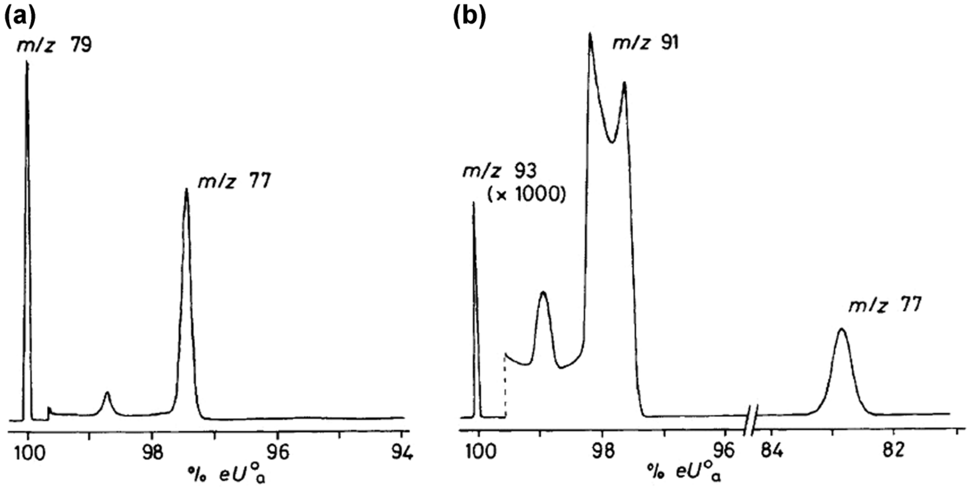

FIGURE 2. Mass-analyzed ion kinetic energy (MIKE) spectra of mass selected metastable ions (**a**) $C_6H_7^+$ (*m/z* 79) showing the elimination of H_2 to give $C_6H_5^+$ (*m/z* 77) as a narrow peak with Gaussian peak shape, and (**b**) $C_7H_9^+$ (*m/z* 93) showing the elimination of H_2 to give $C_7H_7^+$ (*m/z* 91) as a broad, dished-top peak and the elimination of CH_4 to give $C_6H_7^+$ (*m/z* 77) as a narrow peak with Gaussian peak shape. The ions were generated from the dihydrobenzoic and dihydrotoluic acids (see text) (Kuck, Schneider, & Grützmacher, 1985). Reproduced by permission of The Royal Society of Chemistry.

the H_2 elimination from the $C_7H_9^+$ ions. The putative formation of the tropylium ion, **e**, for a long time being notoriously considered in many textbooks as the ubiquitous form of the gaseous $C_7H_7^+$ ion formed upon fragmentation of alkylbenzenes and other toluene derivatives (Watson & Sparkman, 2007), and the attractiveness of the Woodward-Hoffmann rules may have dwarfed the possibility that the other well-known $C_7H_7^+$ isomer, benzylium ion (**d**, Scheme 2) may be formed instead or along with the tropylium ion **e**. As a matter of fact, it turned out that it is this latter route which is pursued during the elimination of H_2 from gaseous $C_7H_9^+$ ions. As will be discussed in detail in this review, our nowadays understanding of the isomerization and fragmentation behavior of gaseous $C_7H_9^+$ ions is much more elaborate and comprehensive.

Notably, the elimination of methane from the $C_7H_9^+$ ions is associated with only a minor KER, as revealed by our own investigations on that topic published in 1985 (Kuck, Schneider, & Grützmacher, 1985). The corresponding peak in the MIKE spectrum has a Gaussian shape and the value $T_{\text{kin}} = 34\,\text{meV} = 3.3\,\text{kJ/mol}$ was determined (Fig. 2b). This indicates that the CH_4 molecule is lost by 1,1-elimination, akin the loss of H_2 from the parent benzenium ion **a** (Fig. 2a), as already mentioned above. However, the fragmentation channel $C_7H_9^+ \rightarrow C_6H_5^+ + CH_4$ turned out to be much more informative than the competing, and dominating, expulsion of H_2. Extensive isotope labeling of the toluenium ions was the key technique and this was combined with a (then) novel and well viable EI-based technique for the generation of the gaseous ions that had been developed in our laboratory and applied at first to the study of the fragmentation of protonated α,ω-diphenylalkanes (Kuck, Bäther, & Grützmacher, 1979; Kuck, Bäther, & Grützmacher, 1985).

Our original idea was triggered by a long-known synthesis route of cycloheptatriene, **2**, and many various cycloheptatriene derivatives, which is depicted in Scheme 3 (Nelson, Fassnacht, & Piper, 1961; Kuck, 2015). Birch reduction of benzoic acid (**5**) giving 1,4-dihydrobenzoic acid (**6**) and subsequent conversion of the carboxyl group yields 1,4-dihydrobenzyl alcohol (**7**). In acidic media, this alcohol undergoes dehydration with concomitant Wagner-Meerwein rearrangement leading to cycloheptatriene, **2**. Amusingly, this solution-phase process involves (possibly tautomeric) dihydrotropylium ions, such as 1-[**2**+H]$^+$. More importantly, Birch reduction of **6** (and its deuterium-labeled isotopologs) not only opens an elegant synthesis access to the corresponding dihydrobenzoic acids but also to various 1-alkyl-substituted derivatives, such as the homolog **8** in the simplest case. This is achieved by quenching of the reaction mixture by addition of an appropriate alkyl halide, such as methyl iodide or $^{13}CH_3I$ or CD_3I in the cases of **8a** and **8b**, respectively (see below) (Kuck, Schneider, & Grützmacher, 1985). As another variant, starting from *ortho*-, *meta*- or *para*-toluic acids (**9–11**), or higher congeners of **5**, the synthesis of the corresponding methyl-1,4-dihydrobenzoic acids (**12–14**), or the respective congeners, can be carried out (Mormann & Kuck, 2002; Sekiguchi et al., 2009). As expected, the EI mass spectra of 1,4-dihydrobenzoic acid, **6**, and its various alkylated derivatives all exhibit the loss of the carboxyl radical as the by far dominating fragmentation channel and, in fact, the MIKE spectra of the corresponding $[M–CO_2H]^+$ ions reveal the fragmentation behavior of (alkyl)benzenium ions thus generated by directed EI-induced fragmentation of the dihydrobenzoic acid precursors. Instead of the acids, the corresponding (more volatile) methyl esters can be easily synthesized by treatment of crude acids with diazomethane (Mormann & Kuck, 2002) or by acid-catalyzed esterification with methanol carried out in the case of methyl dihydrobenzoic acids (Schröder et al., 2004).

The fragmentation of the parent benzenium ion, **a**, generated from 1,4-dihydrobenzoic acid, **6**, was found to be identical with that of $C_6H_7^+$ ions obtained from other sources and use of deuterium-labeled isotopologs confirmed the fast equilibration (complete scrambling) of the seven protons prior to fragmentation (Kuck, Schneider, & Grützmacher, 1985; Kuck, 2000, 2002, 2005a, 2005b, 2007). A study by Schröder et al. published in 2004 used the same synthesis approach to regioselective deuterium-labeled methyl dihydrobenzoates as precursors. Photoionization mass spectrometry confirmed the

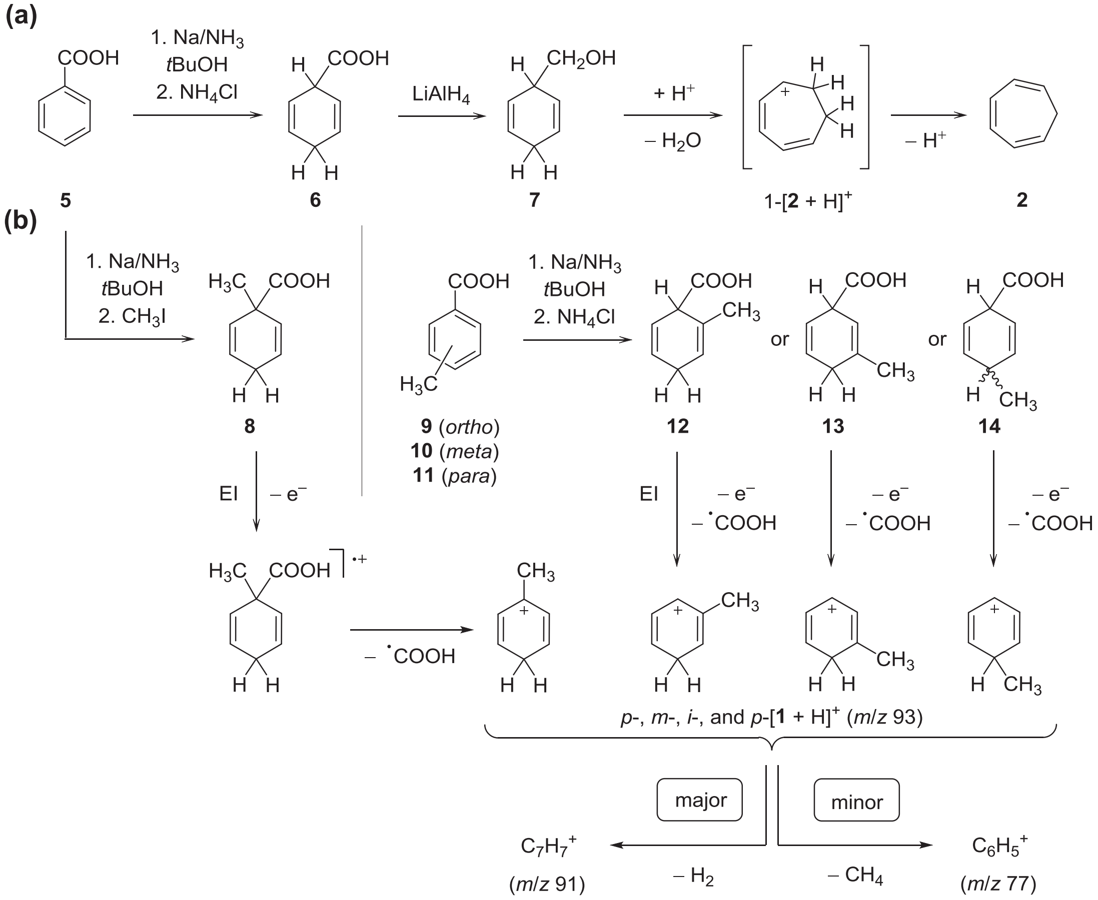

SCHEME 3. (**a**) Synthesis of cycloheptatriene, **2**, by consecutive Birch and alanate reduction of benzoic acid, **5**, and subsequent dehydration with concomitant ring expansion via the dihydrotropylium ion 1-[**2**+H]$^+$ as a reactive intermediate. (**b**) Synthesis of 1-methyl-1,4-dihydrobenzoic acid, **8**, from **5** and of the isomeric 1,4-dihydrotoluic acids **12**–**14** from the corresponding isomeric toluic acids **9**–**11** as precursors for the putatively specific generation of the tautomeric toluenium ions [**1**+H]$^+$ by EI-induced loss of $^{\bullet}$COOH. All tautomers eliminate dihydrogen and methane in similar ratios (Kuck D, unpublished results; see also Kuck, Schneider, & Grützmacher, 1985; Nelson, Fassnacht, & Piper, 1961; Mormann & Kuck, 2002; Kuck, 2015).

complete scrambling behavior and excluded earlier claims on delayed scrambling or other "structural memory effects" (Mason, Williams, & Anderson, 1995; DePuy, Gareyev, & Fornarini, 1997; Schröder et al., 2004). In fact, our original expectation that selectively deuterium-labeled dihydrobenzoic acids would be suitable precursors to generate benzenium and toluenium ions with well-defined protonation sites was futile. It proved to be inappropriate for the specific conversion of, for example, 1-methyl-1,4-dihydrobenzoic acid, **8**, into the *para*-toluenium ion, *p*-[**1**+H]$^+$, or of each of the *ortho*-, *meta*-, and *para*-methyl isomers **9**–**11** into the corresponding toluenium tautomers *m*-[**1**+H]$^+$, *o*-[**1**+H]$^+$ *and i*-[**1**+H]$^+$, as depicted in Scheme 3. Nowadays, the simple reason has multiply been confirmed: The intramolecular H/D equilibration in the parent benzenium ion, **a**, and its alkyl derivatives by fast proton ring walk cannot be suppressed due to the low energy barrier (see below) (Kuck, 1990a, 2002, 2005a). In fact, we found that the $C_7H_9^+$ ions generated from the four isomeric precursors **8**–**11** all eliminate dihydrogen and methane in somewhat different but quite similar relative amounts (Kuck D, unpublished results). However, the strategy turned out to be constructive with alkyldihydrobenzoic acid derivatives that contain ω-phenylalkyl residues and, thus, an additional, flexibly attached (neutral) aromatic ring (Kuck, Bäther, & Grützmacher, 1979; Kuck, Bäther, & Grützmacher, 1985). Also, our original dihydrobenzoic acid approach strategy triggered further fruitful studies in the long term (Kuck et al., 1985; Kuck, 2012, 2015). Nevertheless, it appears that future efforts in competent laboratories using cold precursor ions and photo-induced fragmentation could bring further progress.

Notwithstanding these limitations, it appears that our early work on the gas-phase chemistry of the toluenium ion generated from 1-methyl-1,4-dihydrobenzoic acid, **8**, has been particularly inspiring (Kuck, Schneider, & Grützmacher, 1985). It may be justified to discuss this complex situation in detail here again, because later work by other authors nicely confirmed and complemented our early findings (see below). Starting with the fragmentation behavior of the [α-^{13}C]-labeled toluenium isotopomer [**1a**+H]$^+$ generated from [1-^{13}C]-1-methyl-1,4-dihydrobenzoic acid, **8a**, allows the most straightforward access to a complex scenario, termed "composite scrambling" (Scheme 4) (Kuck, 2002). EI-induced fragmentation of the

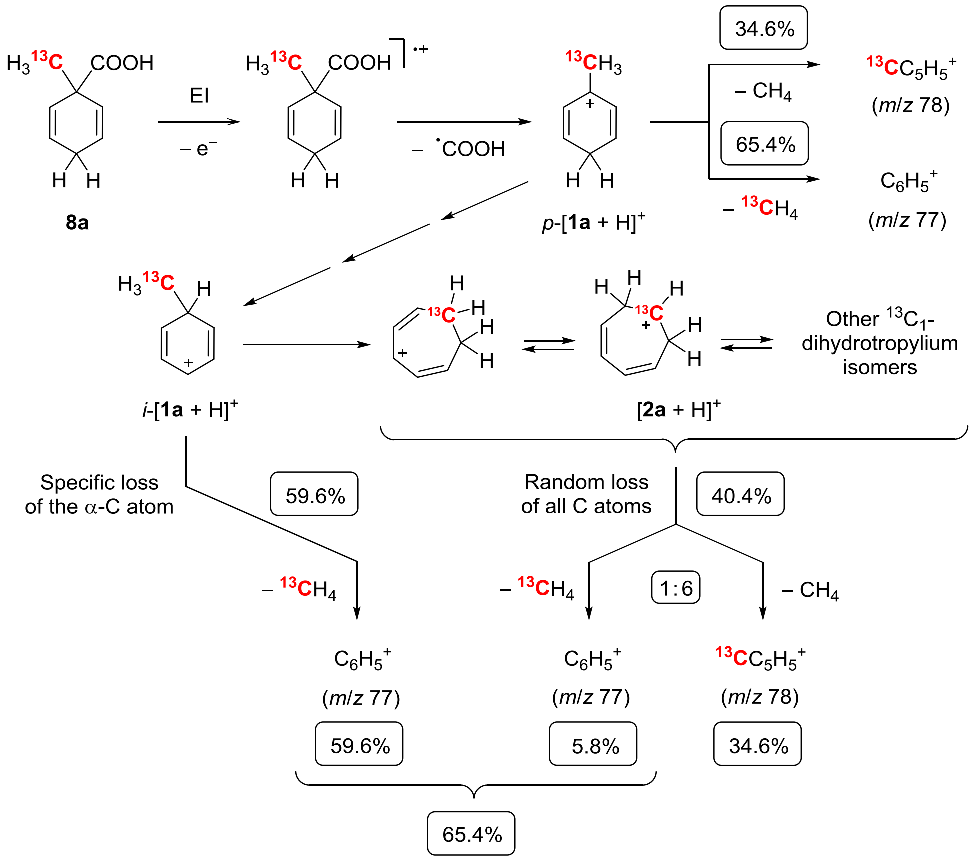

SCHEME 4. Generation of the α-^{13}C-labeled toluenium ion *p*-[**1a**+H]$^+$ from 1-^{13}C-1,4-dihydrobenzoic acid, **8a**, and elimination of methane isotopologs from the metastable ion including specific (59.6%) and random loss (40.4%) of the α-C atom via the *ipso*-tautomer *i*-[**1a**+H]$^+$ and corresponding dihydrotropylium ions [**2a**+H]$^+$ (Kuck, Schneider, & Grützmacher, 1985).

molecular radical cation **8a**$^{\bullet+}$ gives rise to the α-^{13}C-toluenium ion *p*-[**1a**+H]$^+$ and the mixture of fast interconverting tautomers, including the *ipso*-isomer, *i*-[**1a**+H]$^+$. The MIKE spectrum of ions [**1a**+H]$^+$ reveals the elimination of methane from the metastable $^{13}CC_6H_9^+$ ions in the ratio [$^{13}CH_4$]/[CH_4] = 34.6:65.4, indicating skeletal rearrangement prior to fragmentation. Since it is reasonable to assume ring expansion to the dihydrotropylium isomers with concomitant fast and complete H scrambling and, thus, symmetrization of the ion, we postulated that the observed loss of $^{13}CH_4$ corresponds to a 6/7 fraction of those ions that undergo this process prior to fragmentation. The "hidden" 1/7 fraction of these ions eliminates CH_4 (34.6%:6 = 5.8%). As a consequence, the skeletal rearrangement comprises a fraction of 34.6% + 5.8% = 40.4% of the dissociating ions, whereas the other 59.6% undergo specific elimination of the original α-C atom as methane. It is intriguing that both the C-random and the C$^{\alpha}$-specific elimination channels should involve *ipso*-toluenium ions as the actually dissociating species that have distinct origins.

Admittedly, the above interpretation of a neither-specific-nor-random loss of $^{13}CH_4$ and CH_4 appears quite venturous. However, strong corroboration came from the analysis of the MIKE spectra of three deuterium-labeled toluenium ion isotopologs (Kuck, Schneider, & Grützmacher, 1985). Two of them are particularly compelling and revealed the composite scrambling scenario (Kuck, 2002): The metastable ions [**1b**+H]$^+$ generated from corresponding 1-trideuteromethyl-1,4-dihydrobenzoic acid **8b** eliminate all of the four possible C(H,D)$_4$ isotopologs in the ratio [CHD_3]/[CH_2D_2]/[CH_3D]/[CH_4] = 40.6:32.5:21.9:4.9, again clearly nonspecific but far distinct from the statistical ratio. This experimentally observed distribution is reproduced in Figure 3. However, assuming that a 40.4% fraction of the $C_7H_6D_3^+$ ions would undergo complete H/D scrambling along with complete C scrambling, as postulated above, results in a distribution pattern of [CHD_3]/[CH_2D_2]/[CH_3D]/[CH_4] = 1.9:14.4:19.2:4.8, which matches almost perfectly at the upper-mass end of the experimental distribution (namely, at *m/z* 80 and *m/z* 79). In turn, the remainder of the C(H,D)$_4$ isotopologs involving the original α-C atom contain 38.7% of the original α-D atoms of the methyl group but also some *ring*-H atoms. Overall, this C-specific fraction appears in the ratio of [CHD_3]/[CH_2D_2]/[CH_3D]/[CH_4] = 38.7:18.1:2.7:0.1, indicating a slow and incomplete exchange between the original methyl and ring hydrogen atoms. In other words, a ~40% fraction of the toluenium ions undergo complete C and H scrambling, another ~40% fraction of the ions eliminate the original constituents of the methyl group, and the remainder fraction of ~20% suffers slow hydrogen exchange between the methyl group and the benzenium ring.

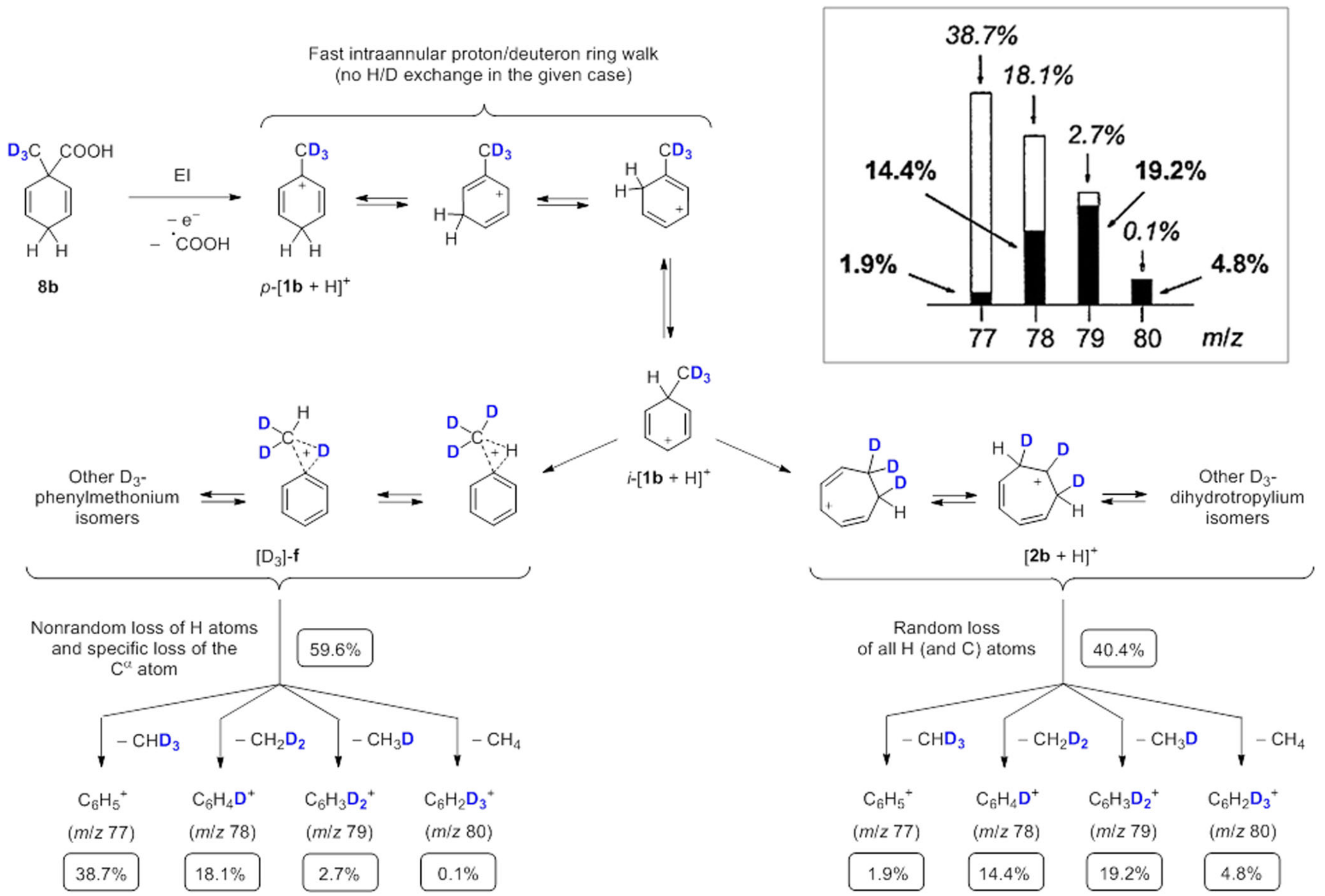

FIGURE 3. Fragmentation of the metastable [α,α,α-D_3]-labeled toluenium ions [**1b**+H]$^+$ generated from 1-trideuteromethyl-1,4-dihydrobenzoic acid, **8b**, by elimination of methane isotopologs, including the loss of $C^\alpha(H,D)_4$ after partial H/D scrambling via the phenylmethonium ions [D_3]-**f** (59.6%) and the random loss of $C(H,D)_4$ via the dihydrotropylium ion isotopologs [**2b**+H]$^+$ (40.4%). The insert shows the experimental pattern of $C_6(H,D)_5^+$ isotopologs and a visualization of the contributions from the two fractions of $C_7H_6D_3^+$ ions that undergo composite scrambling (Kuck, Schneider, & Grützmacher, 1985; Kuck, 2002). Insert reproduced from ref. Kuck (2002) with permission of Elsevier.

This is expressed in Figure 3 by the key role of the phenylmethonium ion, [D_3]-**f** in the present case, generated from the *ipso*-toluenium tautomer *i*-[**1b**+H]$^+$ as the key intermediate for both the specific and the random fragmentation channels.

Another set of deuterium-labeled toluenium ions [**1c**+H]$^+$, was generated from [2,3,4,5,6-D_5]-1-methyl-1,4-dihydrobenzoic acid (**8c**, synthesized and used as a mixture of stereoisomers). The distribution pattern of the methane elimination from the metastable $C_7H_4D_5^+$ ions is reproduced in Figure 4. The analysis of the experimental ratio $[CD_4]/[CHD_3]/[CH_2D_2]/[CH_3D]/[CH_4] = 2.0:14.3:36.7:40.8:6.1$ results in the same interpretation but provides an additional insight. First, the fraction (40.4%) of the ions that fragment after complete C and H/D scrambling gives rise to the "statistical" distribution of methane isotopologs, $[CD_4]/[CHD_3]/[CH_2D_2]/[CH_3D]/[CH_4] = 1.5:12.8:19.3:6.4:0.3$, which fits perfectly into the observed pattern at the lower-mass end (in this case at *m/z* 78 and *m/z* 79). This again leaves the fraction of C-specific methane elimination of 59.6% that appears in the ratio $[CD_4]/[CHD_3]/[CH_2D_2]/[CH_3D]/[CH_4] = 0.5:1.5:17.4:34.4:5.8$, again reflecting the slow and incomplete exchange between the original methyl and ring hydrogen atoms. Thus, the picture obtained for the [*ring*-D_5]-labeled ions [**1c**+H]$^+$ is a perfect and complementary confirmation of the results obtained with the [α,α,α-D_3]-toluenium ions [**1c**+H]$^+$. The additional insight consists in the observed ratio of the two peaks at *m/z* 81 and *m/z* 82 in the MIKE spectrum of the isotopologs [**1c**+H]$^+$: The loss of CH_3D and CH_4 occurs in the statistic ratio of 5:1, reflecting the fast equilibration of the ring H and D atoms (complete 1H/5D scrambling (Kuck, 2002)) within the toluenium ions prior to the C^α-specific loss of the methane isotopologs, which, in turn, is subject to the slow and incomplete H/D exchange between the methyl group and the ring. Thus, we can safely assume that the fast proton ring walk in the toluenium ions takes place as an independent isomerization process, leading to equilibration of the six hydrogen atoms of the benzenium unit before either the ring expansion to the dihydrotropylium ions [**2c**+H]$^+$ intervenes or the channel to the phenylmethonium ion, [D_5]-**f** in this case, is opened. In other words, all of the three fractions (~40%, ~ 40% and ~20%) of toluenium ions [**1c**+H]$^+$ that undergo different isomerization behavior, as deduced above, suffer the preceding proton ring walk to full extent.

The early assumption that protonated cycloheptatriene, that is, the dihydrotropylium ions, [**2**+H]$^+$, represent the central intermediate for the 1,2-elimination of dihydrogen from $C_7H_9^+$

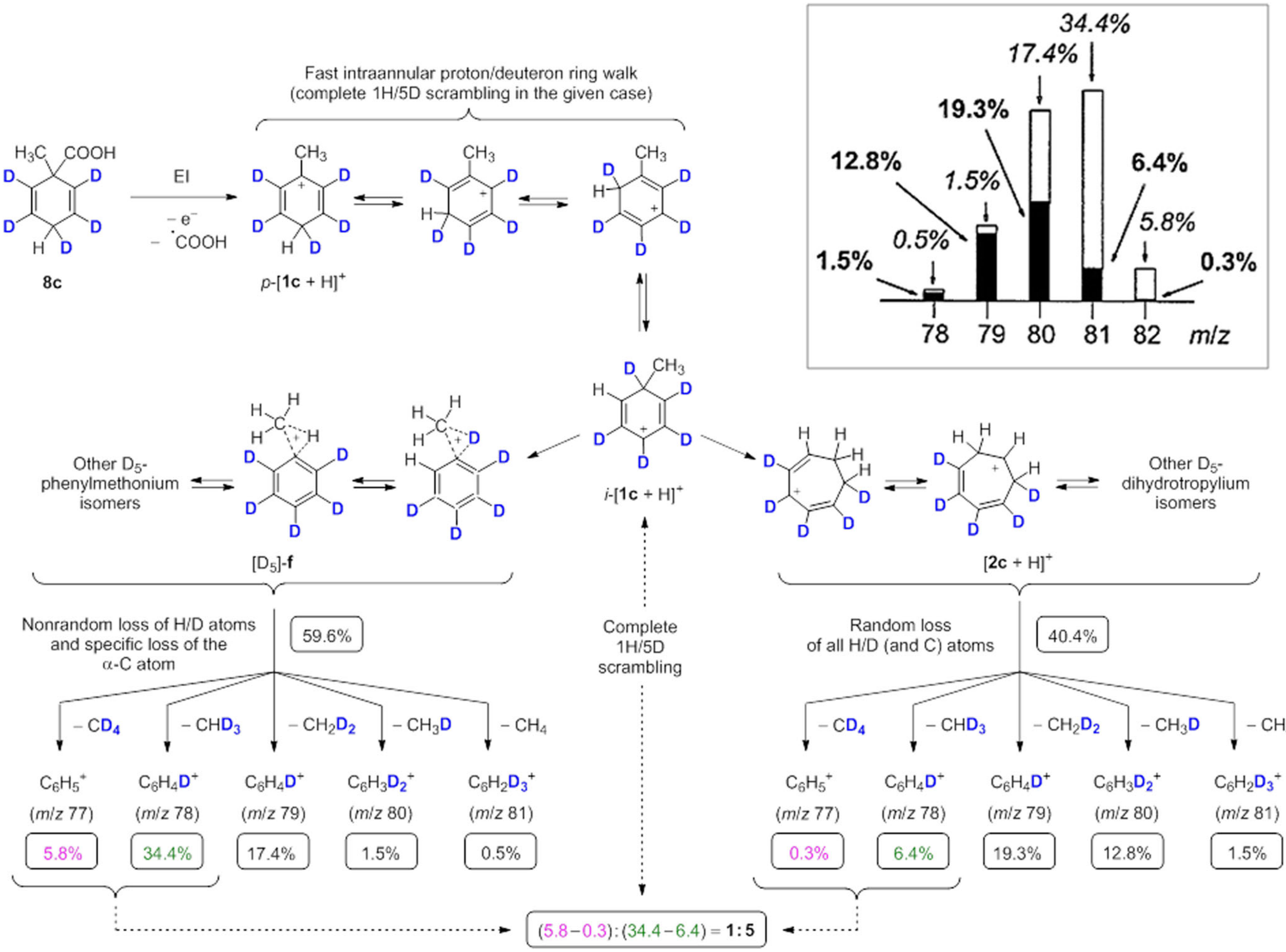

FIGURE 4. Fragmentation of the metastable *ring*-D_3-labeled toluenium ions [**1c**+H]$^+$ generated from [2,3,4,5,6-D_5]-1-methyl-1,4-dihydrobenzoic acid, **8c**, by elimination of methane isotopologs, including the loss of $C^{\alpha}(H,D)_4$ after partial H/D scrambling via phenylmethonium ions [D_5]-**f** (59.6%) and the random loss of $C(H,D)_4$ via the dihydrotropylium ion isotopologs [**2c**+H]$^+$ (40.4%). The insert shows the experimental pattern of $C_6(H,D)_5^+$ isotopologs and a visualization of the contributions from the two fractions of $C_7H_4D_5^+$ ions that undergo composite scrambling. The complete [1H/5D]-scrambling of the ring hydrogen atoms is clearly reflected from the [*m/z* 77]:[*m/z* 78] = 1:5 abundance ratio (Kuck, Schneider, & Grützmacher, 1985; Kuck, 2002). Insert reproduced from ref. Kuck (2002) with permission of Elsevier.

ions required correction in favor of *ipso*-protonated toluene, that is, the *ipso*-toluenium ion, *i*-[**1**+H]$^+$, as the actually reacting species. Similar to the original assumption based on ions [**2**+H]$^+$, expulsion of H_2 by 1,2-elimination from ions *i*-[**1**+H]$^+$ should also be associated with a high reverse activation barrier and thus give rise to large T_{kin} values. This suggestion was deduced indirectly from our insights into the mechanism of the methane elimination from the toluenium ions (Kuck, Schneider, & Grützmacher, 1985). However, a key experiment that provided strong evidence in favor 1,2-elimination from *i*-[**1**+H]$^+$ ions was carried out by Schröder, Roithová and their associates (Schröder et al., 2006). These authors subjected both ions [**1**+H]$^+$ and [**2**+H]$^+$ to infrared multiphoton dissociation (IRMPD) within the cell of an ion cyclotron resonance (ICR) mass spectrometer and reacted the $C_7H_7^+$ ions produced by H_2 expulsion to the well-established probe reaction with arenes (Dunbar, 1975; Ausloos, 1982; Zins, Pepe, & Schröder, 2010). The finding that almost the whole population of $C_7H_7^+$ ions reacted with neutral toluene by the characteristic methylene group transfer, giving methylbenzylium ions, $C_8H_9^+$ (*m/z* 105, such as **g**, Scheme 5), confirmed the formation of benzylium ion, **d**, as the product of H_2 expulsion and ruled out the formation of the tropylium ion, **e**. It can be safely excluded that the latter ion would be formed first and only then undergo the endergonic and kinetically demanding ring contraction to benzylium ion **d** (Lifshitz, 1994). The confirmation that benzylium ions, **d**, rather than tropylium ions, **e**, are the products of H_2 elimination nicely confirmed our early view (Kuck, Schneider, & Grützmacher, 1985) that a hypervalent phenylmethonium ion, $[C_6H_5\cdots CH_4]^+$ (**f**), bearing a two-electron-three center bond that involves the original C^{ipso}-C^{α} bond, is formed as a key intermediate. This species should be close to the transition state for H_2 elimination, which was calculated to lie 39–40 kcal/mol above the energy level of the *ipso*-toluenium ion, *i*-[**1**+H]$^+$, on the B3LYP/6-311+G(2d,p) level of theory (Schröder et al., 2006), as confirmed by more

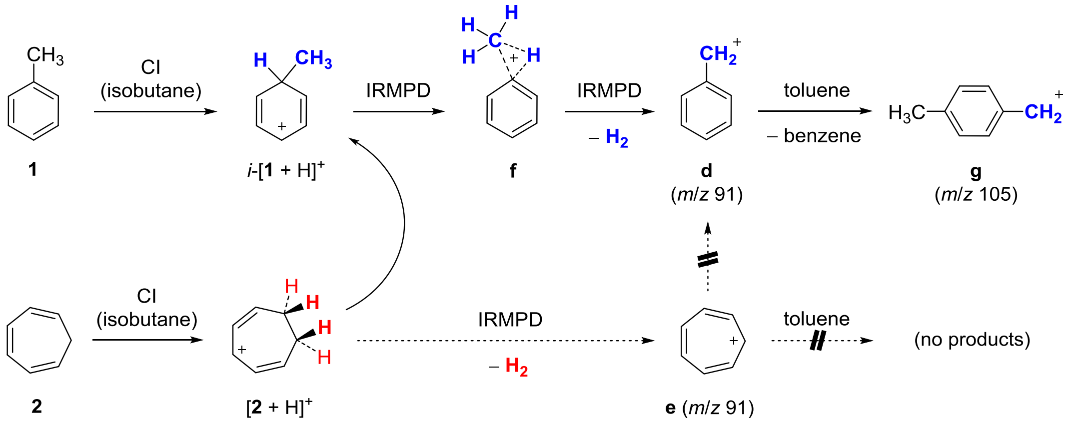

SCHEME 5. Formation of the benzylium ion, **d**, by infrared multiphoton dissociation of the $C_7H_9^+$ ions generated by chemical ionization of toluene, **1**, and cycloheptatriene, **2**, combined with the affirmative probe reaction for the benzylium ion, **d**, that generates (assumably mostly) the *para*-methylbenzylium ion, **g**. The intermediate generation of the tropylium ion, **e**, by IRMPD and subsequent ring contraction to ion **d** can be excluded (Schröder et al., 2006). The phenylmethonium ion, **f**, representing the intermediate for both H_2 and CH_4 losses, is included.

recent calculations by Wang, Bierbaum et al. using B3LYP/6-311+G(2d,2p) (Wang et al., 2018). In fact, ions *i*-[**1**+H]$^+$ can be considered a key species of the overall fragmentation of gaseous $C_7H_9^+$ ions by both 1,2-elimination of H_2 and by 1,1-elimination of CH_4. More details will be described below.

III. TOLUENIUM IONS FORMED BY BIMOLECULAR REACTIONS: METHYL CATION ATTACK ON BENZENE AND METHANE ADDITION TO THE PHENYL CATION

The recent report by Wang, Bierbaum and their associates disclosed an important and detailed complementation of the half-century-long studies of the bimolecular formation of toluenium and xylenium ions by electrophilic attack of methyl cations on benzene and toluene, respectively (Wang et al., 2018). This reaction has always been and will remain prototypical for electrophilic aromatic substitution processes and Friedel-Crafts reactions, in particular (Dewar, 1946; Taylor, 1990; Olah, 1971; March, 1992). Starting in 1970, Bursey and his associates observed the formation of $C_7H_7^+$ ions by encounter of CH_3^+ and benzene in the cell of an ICR mass spectrometer. The $C_7H_9^+$ (*m/z* 93) intermediate was not detectable due to the low-pressure conditions. The authors noted the high exothermicity (64–71 kcal/mol) of the addition/H_2-elimination sequence (Benezra, Hoffman, & Bursey, 1970). A few years later, Beauchamp was the first to state that addition of CD_3^+ ions to unlabeled benzene in the ICR cell results in the elimination of all three dihydrogen isotopologs. The abundance ratio of H_2:HD:D_2 = 15:72:13 was observed. It was deduced that either H/D scrambling within the short-lived, excited toluenium ion intermediate or ring expansion followed by formation of the tropylium ion would occur (Beauchamp, 1975). Notably, at the same time, Williams and Hvistendahl attributed the expulsion of H_2 from $C_7H_9^+$ ions to the intermediacy of the dihydrotropylium ion, as discussed above (Williams & Hvistendahl, 1974b; Hvistendahl & Williams, 1975). In 1981, Morrison and his associates studied the encounter of methyl cations and benzene in a triple-stage quadrupole (TSQ) mass spectrometer. Again, the adduct ions $C_7(H,D)_9^+$ generated from various isotopologous precursors were not observed under these conditions but apparently "complete" H/D scrambling occurred prior to dihydrogen loss and the formation of the $C_7(H,D)_7^+$ product ions. In addition to (apparent) charge exchange between the reactants, the formation of $C_6(H,D)_5^+$ ions by loss of methane was observed for the first time, accompanied with limited (that is, incomplete) H/D scrambling (Morrison, Stanney, & Tedder, 1981a, 1981b). The latter process was first interpreted as a hydride abstraction reaction by CH_3^+ from neutral benzene but the intermediacy of short-lived toluenium ions (Wheland intermediates or σ-complexes) were inferred (Morrison, Stanney, & Tedder, 1981b). Cacace and Giacomello, in one of their early investigations on the attack of electrophiles on aromatic substrates in the liquid and in the dense gas phase, addressed the reaction of tritiated methyl cations, CT_3^+, with benzene and toluene. Notably, they obtained no evidence for the formation of benzyl cations from the long-lived toluenium adduct ions, although they discussed H/D scrambling between the methyl group and the protonated aromatic ring (Cacace & Giacomello, 1978). In the light of nowadays' insights, it appears worth noting that, while the formation of toluene and the xylenes was rationalized in terms of highly exothermic electrophilic methylation reactions followed by isomerization by 1,2-C and 1,2-H shifts, the presence of sizable amounts of ethylbenzene in the product mixture from both gas-phase and liquid-phase methylation was not discussed (Cacace & Giacomello, 1978). It appears that this observation was never mentioned in later work which, in contrast to Cacace's early investigations, was based on the radiolytic technique (Cacace, 1988; Speranza, 1992; Fornarini & Crestoni, 1998).

Studies based on purely theoretical methodology were reported later in 2004. In particular, Ignatyev and Schaefer III published an investigation on the elimination of dihydrogen from the $C_7H_9^+$ intermediates formed by electrophilic attack of CH_3^+ on benzene (Ignatyev and Schaefer, 2004). It appears gratifying to note that, in their analysis, the transition state for the 1,1-elimination of H_2 closely resembles the structure of a phenylmethonium ion, $[C_6H_5\text{-}CH_4]^+$ (**f**), the intermediacy of

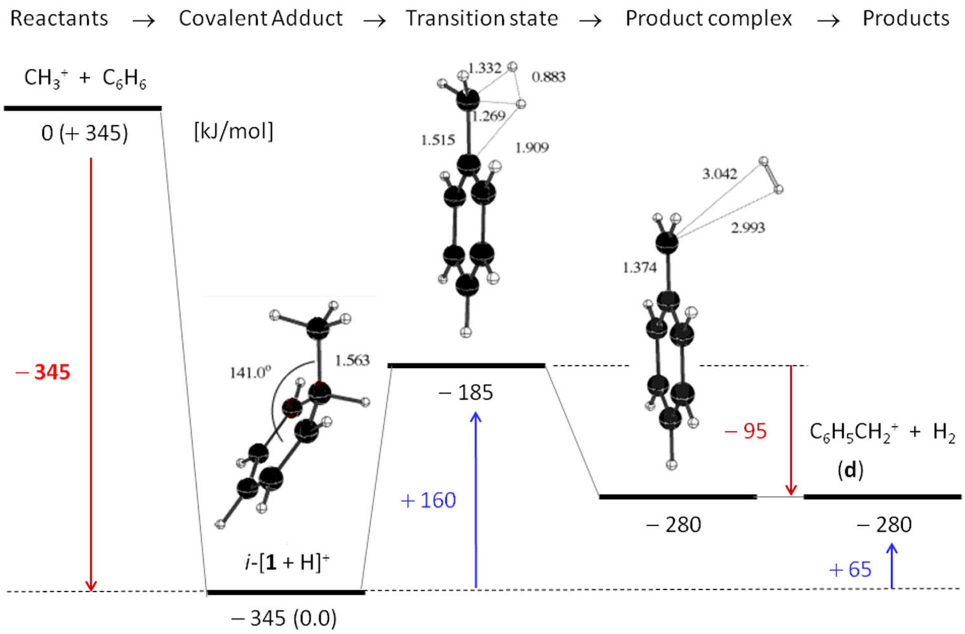

FIGURE 5. Energy profile as $\Delta E_0 = \Delta E_e + \Delta(\text{ZPVE})$ (kJ/mol) for the reaction of the methyl cation with benzene, giving the *ipso*-toluenium ions, *i*-[**1**+H]$^+$, and leading to the benzylium cation, **d**, with concomitant elimination of dihydrogen, as calculated on the B3LYP/aug-cc-pVDZ level of theory. The calculated transition state lies 95 kJ/mol, that is, almost 1.0 eV above the energy level of the products (Ignatyev & Schaefer, 2004). Adapted with permission from *The Journal of the American Chemical Society* 2004;126:14515–14526. Copyright 2020 American Chemical Society.

which was already inferred in our early experimental study on the unimolecular fragmentation of toluenium ions (Kuck, Schneider, & Grützmacher, 1985). The energy profile of the bimolecular attack is illustrated in Figure 5. The high exothermicity of the covalent C–C bond formation leading to the *ipso*-toluenium ion, *i*-[**1**+H]$^+$, is by far sufficient to surmount the relatively high barrier towards the elimination of dihydrogen. In agreement with all previous and subsequent studies, the reverse activation energy of the latter process was calculated to be almost 1.0 eV (≈97 kJ/mol), and thus matches very nicely the amount of kinetic energy released from $C_7H_9^+$ ions observed experimentally (Williams & Hvistendahl, 1974b; Kuck, Schneider, & Grützmacher, 1985). Unfortunately, the details of the methane loss from the *ipso*-toluenium ion were not addressed in Schaefer's work (Ignatyev & Schaefer, 2004), but later investigations did address this aspect (see below). Also in 2004, Hirao and his associates published a molecular dynamics study of the H_2 elimination process that illustrates the details of the C–C bond-forming step during the attack of CH_3^+ on the aromatic π-electron system (Ishikawa et al., 2004). In the two investigations discussed here, no support was found for the intermediacy of a π-complex (Ignatyev & Schaefer, 2004; Ishikawa et al., 2004). It appears that these theoretical studies present the state-of-the-art understanding of the bimolecular formation of toluenium ions from CH_3^+ and benzene. Notably, they do not comprise reaction channels other than 1,2-C and 1,2-H shifts, such as reversible ring expansion and the elimination of methane, but focused on the long-lasting question as to how much π-complexes may intervene on the way to the most stable toluenium and, in more general view, alkylbenzenium ion tautomers (Heidrich, 2002).

In view of such an extended series of experimental and theoretical studies, it is satisfying to note that experimental work on the bimolecular formation of toluenium ions under flow-tube conditions, that is, in the "dense" gas phase, has been accomplished recently in great detail (Wang et al., 2018). In fact, this work on the $C_7H_9^+$ manifold has a decades-long background (see a remark in the Acknowledgments). In that project, Wang, Bierbaum, DePuy and their associates studied both the reaction of the methyl cation with benzene and that of the phenyl cation with methane by flowing afterglow/selected ion flow/drift tube (FA-SIFT-Drift) mass spectrometry (Bierbaum, 2015; Wang et al., 2018). The $C_7H_9^+$ ions formed from the encounter of CH_3^+ and benzene were found to eliminate H_2 and CH_4 and to lose $CH_3^\bullet$ in a branching ratio of 52:39:9 (Scheme 6a). Besides the former two processes, the latter one—a homolytic C–C bond cleavage of even-electron ions producing ionized benzene, $C_6H_6^{\bullet+}$—was assigned to a high-energy fragmentation channel of the toluenium adduct ions rather than to a charge exchange reaction reported earlier (Morrison, Stanney, & Tedder, 1981a, 1981b; Cacace, 1982; Bierbaum, 2015). More importantly, the relative abundances of $C_7(H,D)_7^+$ and $C_6(H,D)_5^+$ fragment ions formed either directly after the attack of CH_3^+ or CD_3^+ to C_6H_6 or C_6D_6 or, alternatively, after CID of the respective adduct ions, $C_7H_{9-x}D_x^+$ ($x = 0$, 3, 5, or 9), gave detailed insights into the isomerization behavior of the toluenium ions and the interplay of skeletal isomerization. In this way, the extent of scrambling in the short-lived, fast-fragmenting adduct ions $C_7H_6D_3^+$ and $C_7H_3D_6^+$ was found to be significantly less than that observed for the long-lived isotopologs. Overall, the extent of scrambling in the $C_7(H,D)_9^+$ ions was neither specific nor complete. Again, this appears to be the result of a combination of H/D exchange processes, a situation very similar to the fragmentation of metastable toluenium ions in a sector-field mass spectrometer, which we termed "composite scrambling" (Kuck, Schneider, &

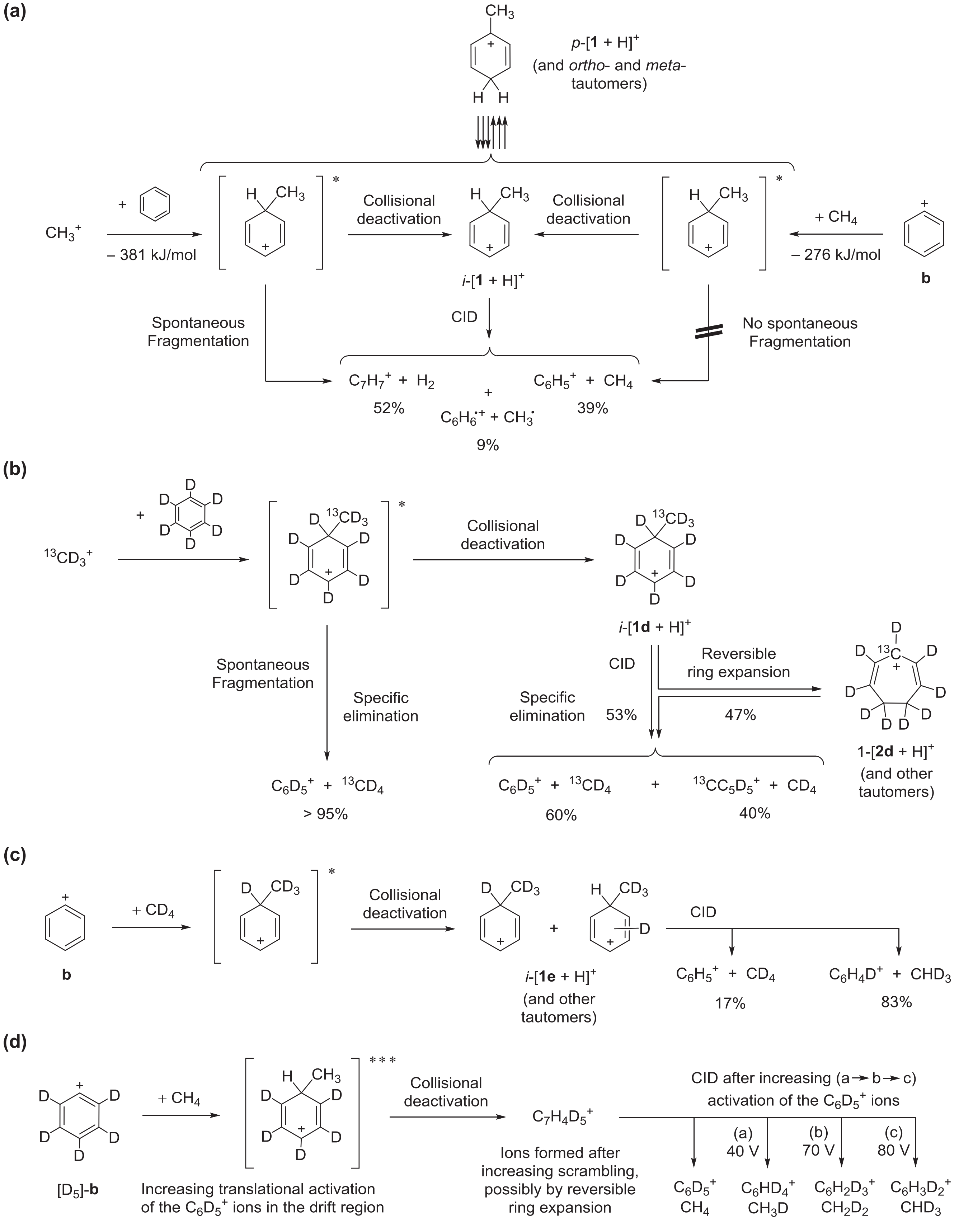

SCHEME 6 Continued.

Grützmacher, 1985; Kuck, 2002). In this context, a most telling result of the SIFT-FA work was obtained from a particular ^{13}C-labeling experiment.

When fully deuterated benzene, C_6D_6, was reacted with $^{13}CD_3^+$ ions, the short-lived adduct ions $^{13}C_1{}^{12}C_6D_9^+$ (*m/z* 103) were found to eliminate exclusively $^{13}CD_4$ (Scheme 6b). However, when the stable, long-lived adduct ions, *i*-[**1d**+H]$^+$ and its tautomers, were subjected to CID, both $^{13}CD_4$ and $^{12}CD_4$ were lost in the ratio of 60:40 (Wang et al., 2018). Strikingly, this ratio is very close to that found for the fragmentation of metastable ions $^{13}C_1{}^{12}C_6H_9^+$, [**1a**+H]$^+$ (*m/z* 94), generated from 1-[^{13}C-methyl]-1,4-dihydrobenzoic acid, **8a**, in our early study using a sector-field mass spectrometer (Scheme 4) (Kuck, Schneider, & Grützmacher, 1985; Kuck, 2002). Again, reversible ring expansion to the corresponding dihydrotropylium ions, for example, 1-[**2d**+H]$^+$, can be inferred.

The addition of methane to phenylium ions is the alternative path for the bimolecular generation of toluenium ions, first reported by Speranza, Gaspar et al. (Speranza et al., 1977). In fact, the insertion of highly reactive aryl cations into aliphatic C–H (but not into C–C) bonds of alkanes (Leung et al., 1978; Angelini, Sparapani, & Speranza, 1984) can be considered a positive probe reaction for the tolyl cation isomers, $CH_3C_6H_4^+$, such as ion **c**, of the $C_7H_7^+$ ion manifold, just as the methylene transfer reaction with arenes is a characteristic probe reaction for the isomeric benzylium ion, $C_6H_5CH_2^+$ (**d**, Scheme 5) (Dunbar, 1975; Ausloos, 1982; Kuck, 1990b). In the flowing afterglow experiments, the lower exothermicity of the CH_4 addition to the $C_6H_5^+$ ion as compared to that of the CH_3^+ ion to benzene (Scheme 6a) is evident from the lack of the spontaneous fragmentation of the exited covalent adduct in the former case. However, the methane (as well as dihydrogen) elimination via the *ipso*-toluenium ion *i*-[**1e**+H]$^+$ could be triggered by CID and, when starting from $C_6H_5^+$ and CD_4, again nicely reflected the ubiquitous fast and complete scrambling of the six ring hydrogens (Scheme 6c). In analogy, starting from the complementary isotopologs, $C_6D_5^+$ and CH_4, gave rise to the loss of CH_3D (along with CH_4). However, when the starting $C_6D_5^+$ ions were accelerated within the drift tube to generate more highly excited [C_6HD_5–CH_3]$^+$ adducts, the elimination of CH_2D_2 and even CHD_3 was observed (Scheme 6d). This clearly indicated the occurrence of H/D exchange between the ring and the methyl group with increasing internal energy, which may be due either to the slow reversible H/D exchange via the corresponding phenylmethonium intermediate, [D_5]-**f** (Fig. 4) or to the reversible skeletal isomerization by ring expansion—or to both of these mechanistic pathways. Overall, these latter findings are in excellent agreement with our earlier results (Kuck, Schneider, & Grützmacher, 1985; Kuck, 2002).

The SIFT-FA work also addressed the bimolecular formation of xylenium ions, $C_8H_{11}^+$ (*m/z* 107) by reaction of CH_3^+ ion with toluene (Wang et al., 2018). In agreement with our studies on the fragmentation of metastable xylenium ions in a sector-field mass spectrometer (see below) (Mormann & Kuck, 2002a), elimination of dihydrogen, methane and even ethene were observed. Labeling experiments were again quite telling: When the CD_3^+ ion was reacted with unlabeled toluene, spontaneous elimination of H_2 and HD was observed in unity ratio, indicating the lack of skeletal isomerization or ring/methyl H/D scrambling. The spontaneous elimination of methane reflected of the intermediacy of the two corresponding *ipso*-protonated xylene isomers [CD_3–C_6H_5–CH_3]$^+$, in similar abundances, giving rise to the loss of CH_4 (40%) and CHD_3 (34%). In addition, however, the CH_3D isotopomer was lost in significant amounts (26%) but CH_2D_2 was not. These observations pointed to the occurrence of direct, highly exothermic, hydride transfer from the benzylic C–H bond to the attacking CD_3^+ ion in the bimolecular encounter (Wang et al., 2018). In turn, the lack of the CH_2D_2 neutral excluded fast H/D scrambling. To check whether hydrogen or even carbon scrambling occurs in the long-lived xylenium ions formed under flowing afterglow conditions, the reaction of the $^{13}CD_3^+$ ion with [α,α,α-D_3]-toluene was studied by CID of the [$^{13}CD_3$–C_6H_5–CD_3]$^+$ adduct ions. Strikingly, $^{13}CHD_3$ and CHD_3 were eliminated in unity ratio. Thus, both H/D scrambling between the ring and the methyl groups and reversible ring expansion could be excluded. However, this leaves us with a discrepancy: Due to the fact that the xylenium ions eliminate not only dihydrogen and methane but also ethene, in agreement with our metastable ion studies (see below) (Mormann & Kuck, 2002a), at least a fraction of them must be subject to the ring expansion/recontraction sequence. To shine further light on this part of the subject, we turn in the following sections to extended studies on some higher analogs, homologs of the toluenium ions and their isomers.

IV. REVERSIBLE RING EXPANSION/ RECONTRACTION OF XYLENIUM IONS AND COMPOSITE SCRAMBLING

The early finding that ring expansion of toluenium ions, [**1**+H]$^+$, to dihydrotropylium ions, [**2**+H]$^+$, and the reverse reaction, the ring contraction, [**2**+H]$^+$ → [**1**+H]$^+$, represents another crucial result of the overall quite complex fragmentation scenario of gaseous $C_7H_9^+$ ions. Therefore, several studies were undertaken to reveal more details on the isomerization and fragmentation behavior of protonated toluene and cycloheptatriene and their more highly methyl-substituted derivatives. These studies represent in-depth extensions of the early work on the fragmentation of protonated cyclo-olefins (Harrison et al., 1965; Schwarz, Borchers, & Levsen, 1976; Basic & Harrison, 1991). The MIKE spectra of protonated 7-methylcycloheptatriene, [**16**+H]$^+$, and the isomeric *para*-xylenium ions, [**15**+H]$^+$, and their labeled isotopologs turned out to be particularly telling because they revealed another characteristic feature that indicates ring contraction and ring

SCHEME 6. Selected flowing afterglow/selected ion flow/drift tube (FA-SIFT-Drift) experiments and features of the isomerization and fragmentation behavior of toluenium ions generated by complementary bimolecular reactions. Both spontaneous fragmentation of the excited covalent adduct ions and their collision-induced dissociation are addressed. (**a**) Highly exothermic methylation of benzene and phenylation of methane. (**b**) Methylation: Carbon scrambling indicating that a ~47% fraction of the toluenium ions undergo reversible ring expansion. (**c**) Phenylation: The 1:5 ratio for the losses of CD_4 and CHD_3 observed upon CID indicates complete H/D scrambling at the benzenium ring. (**d**) Phenylation: Increasingly excited covalent adduct ions $C_7H_4D_5^+$ show increasing but incomplete H/D scrambling between the ring and methyl hydrogens (Wang et al., 2018).

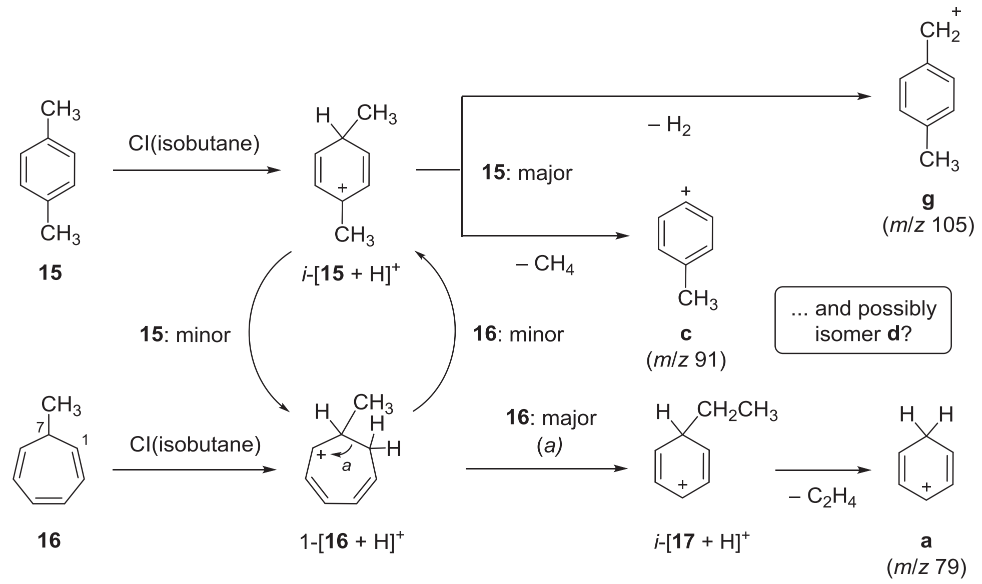

SCHEME 7. Fragmentation of long-lived *para*-xylenium ions, [**15**+H]$^+$, and methyldihydrotropylium ions, [**16**+H]$^+$, generated by protonation of *para*-xylene, **15**, and 7-methylcycloheptatriene, **18**, respectively, and their relatively slow mutual conversion by ring expansion and ring contraction. Note that the isomerization of ions [**16**+H]$^+$ is similar to that of the lower homolog [**2**+H]$^+$ but that ions [**16**+H]$^+$ rearrange preferentially to ethylbenzenium ions [**17**+H]$^+$. The most facile ring contraction step via ions 1-[**16**+H]$^+$ by Wagner-Meerwein rearrangement (*a*) is indicated (Mormann & Kuck, 1999, 2002a).

expansion, respectively. Long-lived, metastable $C_8H_{11}{}^+$ ions generated from hydrocarbons **15** and **16** eliminate ethene (Scheme 7) (Mormann & Kuck, 1999; Mormann & Kuck, 2002a). The loss of C_2H_4, which does not occur from $C_7H_9{}^+$ ions, has been known for a long time as the strongly dominant fragmentation of ethylbenzenium ions [**17**+H]$^+$ (Herman & Harrison, 1981; Kuck, 1990a). Metastable xylenium ions, such as *i*-[**15**+H]$^+$ generated from *para*-xylene, **15**, lose predominantly H_2 and CH_4 in similar amounts to give methylbenzyl ions, such as **g** (*m/z* 105) and tolyl cations, such as **c** (*m/z* 91). Elimination of ethene is a minor channel only (~10%) from this precursor. However, metastable methyldihydrotropylium ions, [**16**+H]$^+$, generated from 7-methylcycloheptatriene, **16**, under mild protonation conditions, for example by use of isobutane as the CI reactant gas, fragment in the same manner as does protonated ethylbenzene, [**17**+H]$^+$. Harsher protonation employing CI(methane) increases the relative rates of the H_2 and CH_4 losses. These observations indicate that ring contraction of ions 1-[**16**+H]$^+$ occurs preferably at the methyl-bearing site, that is, by 1,2-C shift (step *a*, Scheme 7) to give ethylbenzenium ions, [**17**+H]$^+$, but also at any unsubstituted *ring*-methylene groups of the tautomeric dihydrotropylium ions to generate xylenium ions, such as, [**15**+H]$^+$. Labeling studies with isotopologs of **16** bearing a 7-$^{13}CH_3$ or a 7-CD_3 group confirmed the highly selective ring contraction reaction [**16**+H]$^+$ → [**15**+H]$^+$.

The differentiation of characteristic H/D and other isotope exchange behavior, including "complete," "incomplete," "progressing," and "composite" scrambling (Kuck, 2002), reaches a maximum complexity in the case of $C_7H_9{}^+$ and $C_8H_{11}{}^+$ ions. As shown above, composite scrambling was clearly recognized from the fragmentation of toluenium ions, [**1**+H]$^+$, prior to elimination of methane (Kuck, Schneider, & Grützmacher, 1985). Three scrambling components were identified: (i) Fast equilibration (complete scrambling) of the six hydrogen atoms of the benzenium ring of the fraction of intact toluenium ions, (ii) fast equilibration (complete scrambling) of all carbons with concomitant complete hydrogen scrambling by reversible ring expansion to dihydrotropylium ions, (iii) slow exchange (incomplete scrambling) of the hydrogen atoms between the benzenium ring and the methyl group. This complex scenario has been confirmed and complemented with further details over the past two decades (Mormann & Kuck, 2002a; Schröder et al., 2006; Wang et al., 2018). As shown above, the flowing afterglow study on toluenium and xylenium ions generated by methylation of benzene and toluene, respectively, with $CH_3{}^+$ ions is particularly telling (Wang et al., 2018). It also shows that xylenium ions are less prone to extended skeletal rearrangements than toluenium ions, [**1**+H]$^+$. Our own work on the composite scrambling of gaseous xylenium ions, [**15**+H]$^+$, published in 2002, had also revealed this trend but, on the whole, confirmed the various isomerization channels found for toluenium ions. Nevertheless, extended isotope labeling, including the synthesis of four site-specifically ^{13}C-labeled precursors, the methyl esters, **18a** and **18b**, and the two deuterium-labeled *para*-xylenes, **15c** and **15d**, as well as the synthesis of the deuterium-labeled acids **19a** and **19b** was necessary to understand the rather complex reactions preceding the elimination dihydrogen, methane, and ethene from these $C_8H_{11}{}^+$ ions (Scheme 8) (Mormann & Kuck, 2002a, 2002b). The MIKE spectra of the [M–COOH]$^+$ ions of the latter two precursors, 1-trideuteromethyl-4-methyl-1,4-dihydrobenzoic acid, **19a**, and its 1-methyl-4-trideuteromethyl regioisomer, **19b**, are reproduced in Figure 6 (Mormann & Kuck, 2002a).

The fragmentation of long-lived, metastable xylenium ions, originally generated in the forms of *i*-[**15c**+H]$^+$ and *i'*-[**15c**+H]$^+$ from acids **19c** and **19d**, respectively, is already quite informative. The two spectra are essentially identical,

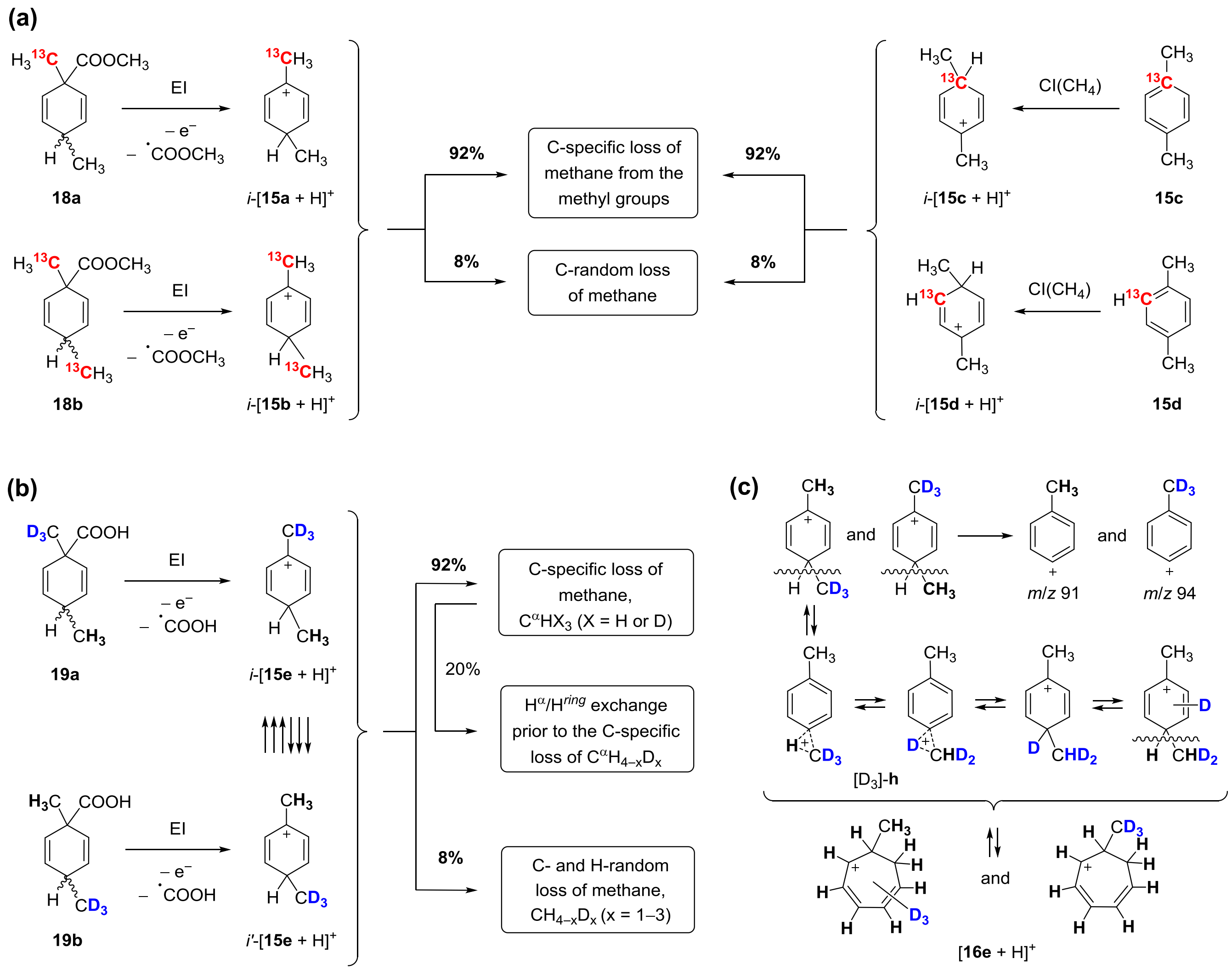

SCHEME 8. Composite scrambling of metastable xylenium ions, [**15**+H]$^+$, prior to elimination of methane. (**a**) Generation of four ^{13}C-isotopologs from by either EI-induced fragmentation of esters **18a** and **18b** or by CI(methane) of the xylenes **15c** and **15d**, fragmentation of which leads to the composite C-specific/random (92:8) scrambling model. (**b**) Based on this model, the fragmentation of the [α,α,α-D$_3$]-isotopologs [**15e**+H]$^+$ generated from acids **19a** and **19b** (see Fig. 6) reveals that a ~20% fraction among those ions that react C-specific undergoes incomplete H-scrambling between the methyl groups and the benzenium ring. (**c**) This composite scrambling behavior is sketched schematically: C-specific (top), C-specific with H$^{\alpha}$/H^{ring} scrambling (middle), complete C- and H-scrambling via reversible ring expansion (bottom) (Mormann & Kuck, 2002a).

reflecting the complete scrambling of the five hydrogen atoms at the benzenium ring. Again, the dihydrogen losses from the $C_8H_8D_3^+$ ions are associated with a large kinetic energy release ($T_{kin} \geq 1.1$ eV) (Mormann & Kuck, 2002a), as reflected by the pronounced flat-topped peaks. The deeply concave abundance pattern corresponding to the elimination of the methane isotopologs reflects qualitatively the rather slow and incomplete H/D scrambling. In contrast, the abundance pattern for the elimination of the ethene isotopologs is convex but, nevertheless, the H/D scrambling is still far from the statistical distribution of the eleven H and D atoms. Thus, to understand the scrambling scenario in metastable xylenium ions, the ^{13}C-labeling experiments were again indispensible. EI-induced fragmentation of the 1-[^{13}C]methyl-4-methyl- and 1,4-di-[^{13}C]-methyl-1,4-dihydrobenzoic acid methyl esters, **18a** and **18b**, respectively, on the one hand, and fragmentation of the two *ring*-labeled *para*-xylenes, namely the [1-^{13}C]- and the 2-[^{13}C]-isotopologs, **15c** and **15d**, after CI(CH$_4$)-ionization resulted in a consistent semiquantitative picture. In fact, the detailed analysis revealed composite scrambling in analogy to the fragmentation of metastable toluenium ions [**1**+H]$^+$ (Kuck, Schneider, & Grützmacher, 1985; Mormann & Kuck, 2002a) and in qualitative agreement with the relatively attenuated scrambling behavior of xylenium ions [**15**+H]$^+$, generated in the FA-SIFT instrument, as mentioned above (Wang et al., 2018). The details of the scrambling preceding the elimination of methane from the various xylenium ions are depicted in Scheme 8.

Most remarkably, metastable xylenium ions [**15a**+H]$^+$ (*m/z* 108) eliminate $^{13}CH_4$ and CH_4 in a ratio different from unity (45.6:54.4), a clear indication for skeletal isomerization. In line with this finding, the doubly labeled isotopologs [**15b**+H]$^+$ (*m/z* 109) undergo loss of $^{13}CH_4$ and CH_4 in the

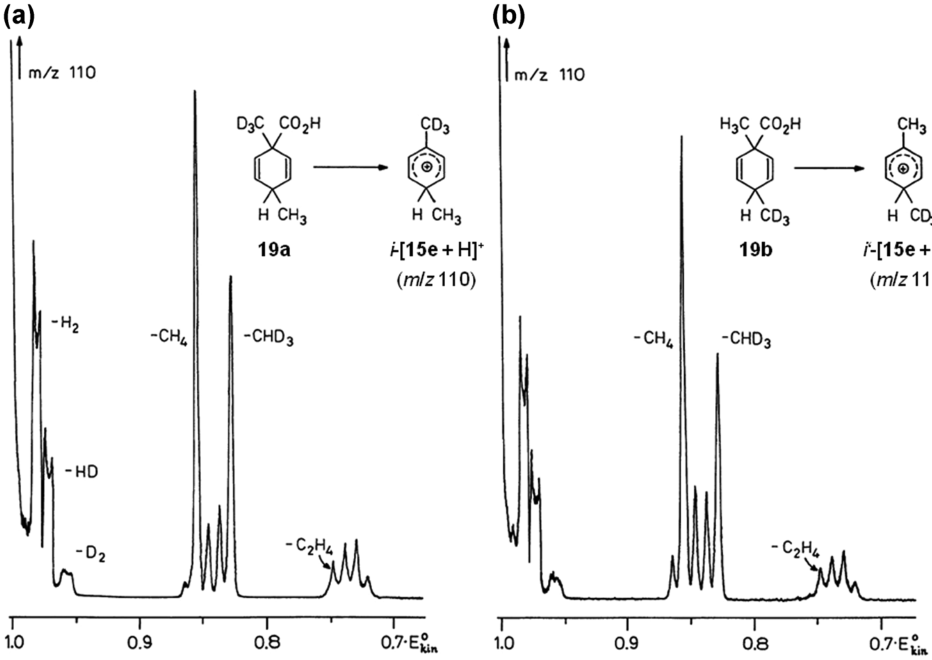

FIGURE 6. MIKE spectra of the easily interconverting [α,α,α-D_3]-xylenium ions [**15e**+H]$^+$ (*m/z* 110), generated from two regiospecifically labeled 1,4-dimethyl-1,4-dihydrobenzoic acids, **19a** and **19b**, respectively, by EI-induced loss of $^{\bullet}$COOH. Note: Slight differences of the abundance pattern are attributed to partial incorporation of D atoms into the ring of isotopologous precursor **19b** (Mormann & Kuck, 2002a). Adapted from ref. Mormann & Kuck (2002a) with permission of Elsevier.

ratio of 95.5:4.5. Strikingly, but only at first glance, the two [*ring*-^{13}C]-labeled isotopomers [**15c**+H]$^+$ and [**15d**+H]$^+$ (both *m/z* 108) expel only ~1% of $^{13}CH_4$ (Mormann & Kuck, 2002a). However, the respective ratios of 0.9:99.1 and 1.5:98.5 (about the same within experimental error) observed in these two cases agree well with all other data if we assume that 92% of the metastable xylenium ions undergo C-specific methane elimination. In other words, a fraction of 92% of the CH_4 neutral fragment contains exclusively a carbon atom that originates from one of the methyl groups. In contrast, the remaining 8% of the xylenium ions undergo complete C-scrambling, involving all of their eight carbon atoms. Thus, here again, the results of the ^{13}C-labeling experiments lay the ground for the composite scrambling model (Scheme 8a). It is again striking to recognize that the abundance pattern of the $C(H,D)_4$ neutrals eliminated from the $C_8H_8D_3^+$ ions [**15e**+H]$^+$ (Fig. 6) agrees well with this model (Mormann & Kuck, 2002a): Neglecting isotope effects, we can reconstruct this experimental pattern by assuming that the 8%-fraction of completely scrambled ions eliminate CHD_3, CH_2D_2, CH_3D, and CH_4 in the statistical ratio of 2.4:25.5:50.9:21.1, which corresponds to actual contributions of 0.2%, 2.0%, 4.1%, and 1.7%, respectively. The major, 92%-fraction of the xylenium ions [**15e**+H]$^+$ expels methane C-specifically but with concomitant slow, and thus incomplete, H/D-exchange between the methyl groups and the benzenium ring. These partially H^{α}/H^{ring}-scrambled ions comprise a fraction of ~20% overall, as shown in Scheme 8b. In analogy to the fragmentation of the deuterium-labeled toluenium ions [**1a**+H]$^+$ and [**1b**+H]$^+$ discussed above, the latter slow scrambling process is believed to occur via nonclassical tolylmethonium structures (ions [D_3]-**h**), whereas the complete C- and H-scrambling of the xylenium ions involves reversible ring expansion to methyl-substituted dihydrotropylium ions [**16e**+H]$^+$ (Scheme 8c). In summary, the isomerization and fragmentation behavior of long-lived xylenium ions resembles that of long-lived toluenium ions, but the propensity to undergo ring expansion of ions [**15**+H]$^+$ within the composite scrambling scenario is clearly decreased in comparison to ions [**1**+H]$^+$. This résumé is in complete agreement with the recent findings by Wang, Bierbaum and their associates (Wang et al., 2018). At this point, it should also be noted that the well-known isomerization of the three xylene isomers under strongly acidic conditions represents an additional background for the gas-phase isomerization of xylenium ions. It may well be that *meta*-xylenium ions, the conjugate base of which represents the most basic isomer among the three xylenes, play the major role during the elimination of methane. Gas-phase titration studies have clearly revealed the dominance of *meta*-xylenium ions in $C_8H_{11}^+$ ion mixtures generated by under various CI conditions (Nefedov et al., 1970; Büker et al., 1997).

Finally, the outcome of the various labeling experiments with regard to the characteristic and, as will be address below, quite relevant ethene loss from long-lived xylenium ions [**15**+H]$^+$, deserves some comment. First, this fragmentation channel clearly confirms the occurrence of the reversible ring expansion of the xylenium ions to the methyldihydrotropylium isomers [**16**+H]$^+$. Reversibility includes ring contraction not only to the isomeric protonated *ortho*-, *meta*-, and *para*-xylenes but also to protonated ethylbenzene [**17**+H]$^+$. Beyond any doubt, the *ipso*-ethylbenzenium ions, *i*-[**17**+H]$^+$, is the actual $C_8H_{11}^+$ species from which C_2H_4 is released eventually (Mormann & Kuck, 2002a). As mentioned above, the abundance distribution of the $C_2(H,D)_4$ neutrals eliminated from the $C_8H_8D_3^+$ isotopologs [**15e**+H]$^+$, is convex but far from the statistical pattern (Fig. 6) (Mormann & Kuck, 2002a). Again, the analysis of the fragmentation of the ^{13}C-labeled isotopologs [**15a**+H]$^+$ to [**15d**+H]$^+$ was essential for understanding the MIKE spectra of the [α,α,α-D$_3$]-labeled isotopologs [**15e**+H]$^+$ and led us to a modified composite scrambling model for the C_2H_4 loss from ions [**15**+H]$^+$. Similar to the loss of the methane isotopologs, the metastable toluenium ions [**15a**+H]$^+$ eliminate $^{13}C^{12}CH_4$ and $^{12}C_2H_4$ in a ratio of 45:55. The doubly labeled isotopologs [**15b**+H]$^+$ expel $^{13}C_2H_4$, $^{13}C^{12}CH_4$, and $^{12}C_2H_4$ in the ratio of 10:77:13 (averaged values for $^{13}C_2C_6H_{11}{}^+$ ions from different precursors, see Ref. Mormann & Kuck, 2002a). Both patterns are unsymmetrical due to the complex isomerization behavior. Furthermore, the two [*ring*-^{13}C]-labeled isotopomers [**15c**+H]$^+$ and [**15d**+H]$^+$ were found to behave identical, losing $^{13}C^{12}CH_4$ and $^{12}C_2H_4$ in ratios of ~14:86. The composite scrambling model agrees well with all these experimentally observed abundance ratios and suggests that a fraction of 75% of the metastable xylenium ions [**15**+H]$^+$, undergo specific, *irreversible* ring expansion to methyldihydrotropylium ions [**16**+H]$^+$ and subsequent recontraction to ethylbenzenium isomers [**17**+H]$^+$. As mentioned above, fast 1,2-methyl shifts at the benzenium ring of ions [**15**+H]$^+$ and even within the seven-membered ring of ions [**16**+H]$^+$ may accompany these processes. The remaining fraction (25%) of the xylenium ions undergo *reversible* ring expansion-recontraction via ions [**16**+H]$^+$ leading to complete carbon scrambling prior to the final ring contraction to ethylbenzenium ions [**17**+H]$^+$. A further refinement was suggested but does not alter this 75:25 composite scrambling model that involves both specific and random ethane elimination. A general scenario for the conversion of xylenium ions to ethylbenzenium ions with subsequent elimination of ethene deduced from the above analysis is depicted in Scheme 9.

V. TOLUENIUM AND XYLENIUM IONS FROM PROTONATED METHYLFULVENES AND COMPOSITE SCRAMBLING

It is obvious that the reversible ring expansion is a characteristic feature of gaseous toluenium and xylenium ions but it does not occur easily. Historically, the special attention on such type of isomerization processes preceding the fragmentation of gaseous $C_7H_9{}^+$ and $C_8H_{11}{}^+$ ions is certainly due to the long-established propensity of benzylium ions, $C_7H_7{}^+$, **d**, and toluene radical cations, $C_7H_8{}^{\bullet+}$, and their methyl-substituted analogs to undergo formally similar ring expansion reactions (Bursey, Bursey, & Kingston, 1973; Kuck, 1990b, 2005c; Lifshitz, 1994). However, the fact that a ring-contracted isomer of the benzenium ion, $C_6H_7{}^+$, **a**, namely C^1-protonated fulvene, is only moderately less stable than the “stabilomer” of the $C_6H_7{}^+$ ion family, is known since 1985 (Lias & Ausloos, 1985). In fact, both constitutional isomers are formed in $C_6H_7{}^+$ ion mixtures generated by various bimolecular and unimolecular reactions (Herman, Herman, & McMahon, 1991; Zhu & Gäumann, 1993; Gäumann, Zhao, & Zhu, 1994; Bouchoux, Nguyen, & Salpin, 2000). Bouchoux and his associates contributed a detailed computational study on the isomerization of tautomeric fulvenium ions to the benzenium ion and found that *ipso*-protonation (that is, protonation at C^5) of fulvene is the crucial step from which the ring expansion process takes place via a bicyclo[3.1.0]hex-2-en-4-yl cation as the key intermediate (Bouchoux, Yáñez, & Mó, 1999). Notably, all these reactions

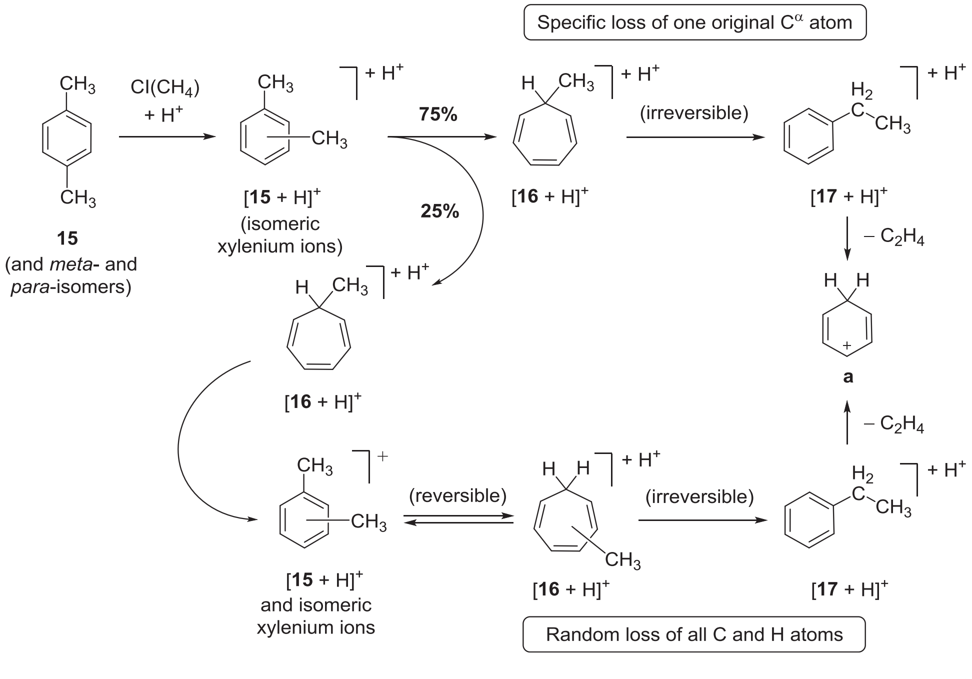

SCHEME 9. Composite scrambling of metastable xylenium ions prior to elimination of ethene. A fraction of 75% of the *para*-xylenium ions [**15**+H]$^+$, undergo specific elimination of $C^{\alpha}C^{ring}H_4$ after irreversible ring expansion and recontraction to ethylbenzenium ions [**17**+H]$^+$. A fraction of 25% of the ions suffers reversible ring expansion/recontraction involving methyldihydrotropylium ions [**16**+H]$^+$ and finally eliminates C_2H_4 after complete C and complete H scrambling (Mormann & Kuck, 2002a). It is assumed that elimination of C_2H_4 from protonated *meta*- and *ortho*-xylenium occurs along the same isomerization channels.

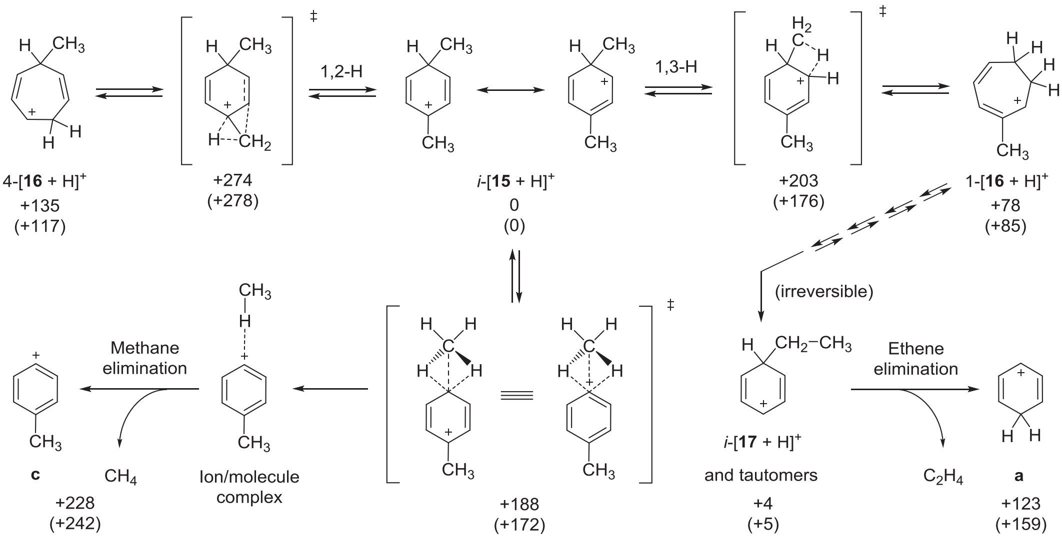

SCHEME 10. Crucial transition states on the way to methane and ethene elimination from *para*-xylenium ions $[\mathbf{15}+H]^+$, as computed for the *ipso*-tautomer, *i*-$[\mathbf{15}+H]^+$, as the starting species. Energy levels are give in kJ/mol, based on calculations at the B3LYP/6-311 G(d,p) and MP2/6-31G(d) levels of theory (Arstad, Kolboe, & Swang, 2004). Note that this isomer lies by 34 kJ/mol above the most stable isomer, viz., C^4-protonated *meta*-xylene. Initiation of the ring expansion by 1,3-H shift was calculated to be much more favorable than by 1,2-H-shift and constitutes the most favorable starting point on the way to the ethylbenzenium ions $[\mathbf{17}+H]^+$, and subsequent loss of C_2H_4. The transition state for the loss of CH_4 lies below, but not far below, the fragmentation threshold, thus rationalizing the slow H^{α}/H^{ring} exchange hydrogen observed experimentally (Mormann & Kuck, 2002a). The ion/molecule complex bound by a hydrogen bridge is implied here in analogy to computational work on toluenium ions $[\mathbf{1}+H]^+$ (Wang et al., 2018).

occur well below the fragmentation threshold for the 1,1-elimination of H_2. Therefore, it appears reasonable to assume that methyl-substituted fulvenium ions, as ring-contracted constitutional isomers, may also be involved in the complex structural rearrangements of toluenium and xylenium ions prior to the loss of H_2, CH_4 and C_2H_4.

In an impressive complement to our experimental work on the fragmentation of xylenium ions $[\mathbf{15}+H]^+$ (Mormann & Kuck, 2002a), in particular, Kolboe and his associates studied the role of methylfulvenium ions as reactive intermediates during the isomerization of xylenium ions prior to elimination of methane and ethene. They compared the ring-contraction and ring-expansion routes by in-depth theoretical calculations on the B3LYP/6-311G(d,p) and MP2/6-31G(d) level of theory (Arstad, Kolboe, & Swang, 2004). Many details of the complex isomerization scenario were confirmed by these theoretical studies. Among others, the authors showed that the transition state for the loss of methane from *para*-xylenium ions $[\mathbf{15}+H]^+$, can be described as a relatively loose complex $[CH_3\text{-}C_6H_4\cdots CH_4]^+$ with a C–C bond distance of ~1.9 Å between the two constituents. Gratifyingly, this transition state was seen as the crucial configuration that allows the experimentally observed (slow) hydrogen exchange between the methyl group and the benzenium ring, as depicted in Scheme 10. Later computational work by Wang, Bierbaum and their associates confirmed this interpretation for the case of the toluenium ions (Wang et al., 2018). According to the calculations, the H^{α}/H^{ring} scrambling in *para*-xylenium ions $[\mathbf{15}+H]^+$ competes with the ring expansion pathways to methyldihydrotropylium ions $[\mathbf{16}+H]^+$, and thus with the complete C- and H-scrambling. Based on the calculations, it was suggested that the ring expansion is initiated preferably by 1,3-H shift rather than by 1,2-H shift, as also illustrated in Scheme 10.

More specifically, the above-mentioned benzenium-to-fulvenium ion ring contraction via the bicyclo[3.1.0]hex-2-en-4-yl cation was adapted to second-next higher analog, the *ipso*-xylenium ion, *i*-$[\mathbf{15}+H]^+$, and the corresponding *anti*- and *syn*-3,6-dimethylbicyclo[3.1.0]hex-2-en-3-yl cations (not illustrated but see below for similar cases) were suggested as key intermediates on the way to ethene elimination. The calculations suggested opening of the cyclopropane ring in both the *anti*- and *syn*-isomer giving rise to methylcyclopentadienyl cations that bear pending C_2-residues (Arstad, Kolboe, & Swang, 2004). The final expulsion of C_2H_4 from these intermediates and even the ring expansion to the ethylbenzenium ions $[\mathbf{17}+H]^+$ was calculated to be very energy-demanding for either pathway (~260 kJ/mol). This is not surprising because of the unfavorable (antiaromatic) 4π-electron system of cyclopentadienyl cations. In line with intuition, ring expansion of the methylcyclopentadienyl cation to the benzenium ion was found to have an extremely high energy barrier (~370 kJ/mol above the starting ions). It is satisfying to note that the alternative isomerization channel leading to elimination of ethene via ring-expanded methyldihydrotropylium isomers was calculated to be less energy-demanding (Arstad, Kolboe, & Swang, 2004). Considering the transition states here as well, the calculations predict that the formation of the latter $C_8H_{11}{}^+$ isomers requires only ~200 kJ/mol. In agreement with all experimental evidence, the recontraction to six-membered ring isomers, including the ethylbenzenium ions $[\mathbf{17}+H]^+$, is exothermic. Nevertheless, the final elimination of ethene via this latter isomer was calculated to require ~240 kcal/mol to overcome the last barrier. Overall, the computational comparison between the ring contraction and the ring expansion paths leading to ethene elimination from the *para*-xylenium ion [**15**+H]$^+$ resulted in significant favor of the latter isomerization pathway (Arstad, Kolboe, & Swang, 2004).

In view of the intriguing alternative—ring expansion/recontraction versus ring contraction/re-expansion of gaseous toluenium and xylenium ions, a further experimental work was undertaken that started from isotopically labeled methyl-substituted fulvene derivatives (Mormann, Decker, & Kuck, 2007). Besides 6-methylfulvene (**4**) as a constitutional isomer of toluene (**1**) and cycloheptatriene (**2**) the higher analog 6,6-dimethylfulvene (**20**) as well as two ^{13}C-labeled and two deuterium-labeled isotopomers of this cyclo-olefin (**20a**–**20d**) were synthesized and protonated under CI(CH_4) conditions. The long-lived, metastable $C_7H_9^+$ ions generated from 6-methylfulvene [**4**+H]$^+$, were found to fragment in almost the same way as to those formed from toluene and cycloheptatriene. Thus, the ratio of H_2 and CH_4 elimination and the amounts of kinetic energy released from [**4**+H]$^+$ (83:17, $T_{\mathrm{kin}} = 1.03$ eV and 22.0 meV, respectively) were closely similar to the values found for the latter isomers [**1**+H]$^+$ (88:12, $T_{\mathrm{kin}} = 1.09$ and 24.5 meV) and [**2**+H]$^+$ (84:16, $T_{\mathrm{kin}} = 1.05$ and 22.3 meV) (Mormann, Decker, & Kuck, 2007). Hence, the quite different exothermicities of the protonation of the three isomers, based on their experimentally determined proton affinities, *PA*(**1**) = 784 kJ/mol (Hunter & Lias, 1998), *PA*(**2**) = 833 kJ/mol (Salpin et al., 2003), and *PA*(**4**) = 876 kJ/mol (Mormann, Salpin, & Kuck, 1999), are not or only to a little extent reflected by significant differences of the fragmentation characteristics. One may speculate that the more energy-demanding channel, namely loss of CH_4, gains abundance with increasing proton affinity or gas-phase basicity (*GB*) of the conjugate bases, hydrocarbons **1**, **2**, and **4**. Although no isotope labeling was performed with 6-methylfulvene, **4**, there is no doubt that both of the cyclo-olefinic $C_7H_9^+$ isomers rearrange by ring contraction and ring expansion, respectively, to the toluenium ions [**1**+H]$^+$, prior to elimination of H_2 and CH_4 (Mormann, Decker, & Kuck, 2007).

Insight into the isomerization of the higher analog, protonated 6,6-dimethylfulvene [**20**+H]$^+$, is much more detailed and led to another case of composite scrambling of the long-lived $C_8H_{11}^+$ ions (Mormann, Decker, & Kuck, 2007). As expected from the results of the previous studies, the elimination of H_2 and CH_4 was accompanied by the loss of C_2H_4 (Fig. 7). However, the fragmentation characteristic of ions [**20**+H]$^+$ were found to be significantly different from those of the isomeric *para*-xylenium ions [**15**+H]$^+$. The elimination of C_2H_4 (19% vs. 12%) gained abundance at the expense of the loss of CH_4 (46% vs. 59%). Interestingly, elimination of C_2H_4 from long-lived protonated 7-methylcycloheptatriene [**16**+H]$^+$, is much more abundant (66%). These differences suggest that, besides conceivable energy effects due to the significantly different proton affinities of the conjugate C_8H_{10} hydrocarbons, namely *PA*(**15**) = 796 kJ/mol (Hunter & Lias, 1998), *PA*(**16**) = 840 kcal/mol (Mormann & Kuck, 2007), and *PA*(**20**) = 878 kcal/mol (Mormann, Salpin, & Kuck, 1999; Mormann & Kuck, 2007), the mechanistic accessibility to ethylbenzenium ions [**17**+H]$^+$, from which C_2H_4 is eventually expelled, is very different. The T_{kin} values of the C_2H_4 loss from the $C_8H_{11}^+$ isomers showed the same trend as that found for the lower analogs, with that for the 6,6-dimethylfulvenium ion [**23**+H]$^+$, being largest, $T_{\mathrm{kin}} = 17.9$ meV, as compared to the corresponding values determined for ions [**1**+H]$^+$ (12.3 meV) and [**2**+H]$^+$ ($T_{\mathrm{kin}} = 16.5$ meV) (Mormann, Decker, & Kuck, 2007).

^{13}C-labeling experiments with the dimethylfulvenium ions [**20**+H]$^+$ revealed that a large fraction (95%) of the methane lost from these ions involves one of the C^{methyl} atoms, whereas a small fraction (5%) undergoes complete C-scrambling. Thus, expansion of the five-membered ring of ions [**20**+H]$^+$, giving xylenium ions and subsequent direct C-specific loss of methane, is strongly dominant, while the minor fraction of the ions suffers a slow and reversible further ring expansion to methyldihydrotropylium ions [**16**+H]$^+$. Hydrogen scrambling is much more pronounced. A 50% fraction of the ions [**20**+H]$^+$ undergoes complete scrambling of the hydrogen atoms of the ring and of (notably only) one of the methyl groups, that is, the CH_4 molecule lost contains the other methyl group specifically. The other 50% fraction of the ions suffers complete H-scrambling prior to methane loss. Thus, the scrambling behavior of the 6,6-dimethylfulvenium ions [**20**+H]$^+$ is even more C-specific than that of the *para*-xylenium ions [**15**+H]$^+$ (95% vs. 92%, see Schemes 11 and 8, respectively), but complete H-scrambling is clearly more abundant (50% vs. 12%). This finding was attributed to the higher excitation energy of ions [**15**+H]$^+$ due to the considerably higher PA of the fulvene precursor **20** and to the facile hydrogen exchange between the isopropylidene group and the cyclopentadiene ring of ions [**20**+H]$^+$ (Scheme 11).

The elimination of ethene from long-lived 6,6-dimethylfulvenium ions [**20**+H]$^+$, is much less specific. The fragmentation of the ^{13}C-labeled ions, [**20a**+H]$^+$ and [**20b**+H]$^+$, was found to be consistent with a composite C-scrambling model that comprises two fractions of $^{13}C_1{}^{12}C_7H_{11}^+$ ions: A larger one (80%) expels ethene that contains one original C^{methyl} atom together with another C-atom incorporated after complete scrambling of the remaining seven 6-methylfulvene carbon atoms. In contrast, the second fraction (20%) eliminates ethene after complete scrambling of all eight C-atoms. Again, this scrambling behavior is similar to that found for *para*-xylenium ions, [**15**+H]$^+$, for which the ratio of the fractions that react partially C-specific and completely C-random was found to be 75:25

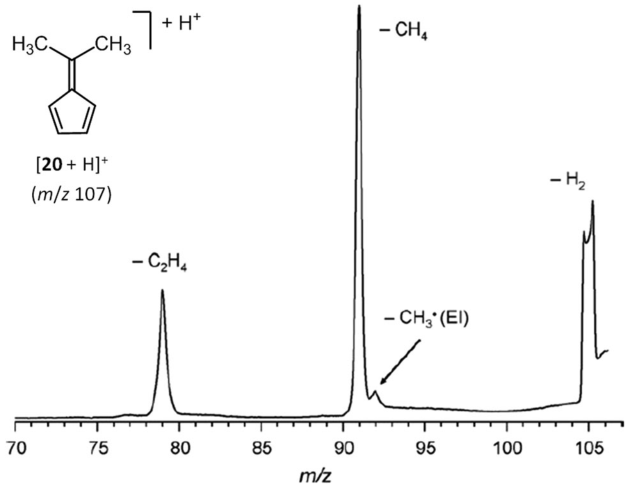

FIGURE 7. MIKE spectrum of protonated 6,6-dimethylfulvene [**20**+H]$^+$ ($C_8H_{11}^+$, *m/z* 107), generated by CI(CH_4) (Mormann, Decker, & Kuck, 2007). Adapted from ref. Mormann, Decker, & Kuck (2007) with permission of Elsevier.

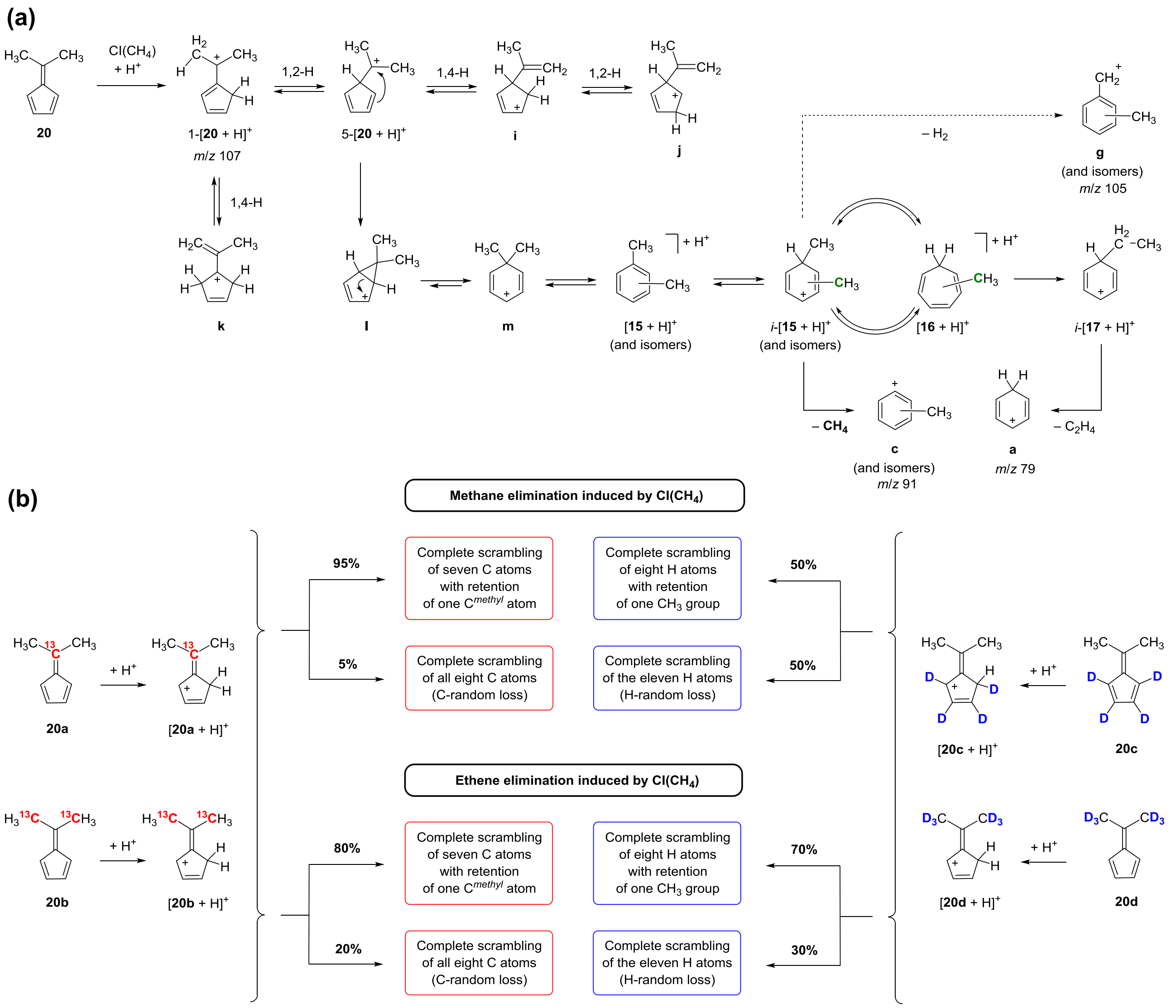

SCHEME 11. (**a**) Mechanism proposed for the isomerization of 6,6-dimethylfulvenium ions [**20**+H]$^+$ (*m*/*z* 107) by H shifts, involving ions **i**–**k**, and (in part irreversible) ring expansion reactions to xylenium ions [**15**+H]$^+$, and ethylbenzenium ions [**17**+H]$^+$, via ions **l** and **m**. (**b**) Composite C and H scrambling in the metastable $C_8H_{11}{}^+$ ions generated by protonation of isotopically labeled 6,6-dimethylfulvenes, **20a**–**20d**, by CI(CH_4) prior to elimination of methane and ethene, as deduced from the MIKE spectra. The expulsion of H_2 via ions [**15**+H]$^+$ is also indicated (Mormann, Decker, & Kuck, 2007).

(Mormann & Kuck, 2002a). Finally, the hydrogen scrambling within ions [**20c**+H]$^+$ and [**20d**+H]$^+$ prior to ethene loss was analyzed. The two experimentally observed abundance patterns were found to be consistent with composite H-scrambling when two populations of $C_8(H,D)_{11}{}^+$ ions were assumed in the ratio of 70:30. The larger one undergoes complete equilibration of the eight H/D atoms of the 6-methylfulvenium ion unit while retaining the other methyl group unscrambled, and the smaller population of ions again suffers complete scrambling of all eleven H and D atoms. Again, it is striking to note that the fractional ratios for the composite H-scrambling (70:30) and the composite C-scrambling (80:20) preceding the C_2H_4 loss from the 6,6-dimethylfulvenium ions, [**20**+H]$^+$, are similar. This finding was considered a strong indication for the occurrence of a common mechanistic isomerization pathway reflected by the H and C scrambling (Mormann, Decker, & Kuck, 2007). It was suggested that the $C_8H_{11}{}^+$ ions generated by protonation of 6,6-dimethylfulvene, **20**, readily isomerize via the bicyclic intermediate **l** to the 1,1-dimethylbenzenium ion, **m** (Scheme 11), which in turn rearranges to the related isomeric xylenium ions, including the *para*-isomer, [**15**+H]$^+$, by 1,2-C shifts. The major fraction (70–80%) of these ions undergoes a further, irreversible ring expansion to methyldihydrotropylium ions, [**16**+H]$^+$, before ring recontraction to ethylbenzenium ions, [**17**+H]$^+$, from which ethene is expelled eventually. The minor fraction (30–20%) of ions reacts reversibly. It should also be noted that, in this scenario evolving from 6,6-dimethylfulvene as the precursor, we can see the intermediacy of the (nonacidic) dimethylbenzenium ion, $C_8H_{11}{}^+$, **m**, that otherwise escapes any direct probing or observation, as an important intermediate on way from protonated 6,6-dimethylfulvene, [**20**+H]$^+$, to the protonated xylenes, [**15**+H]$^+$ (Scheme 11).

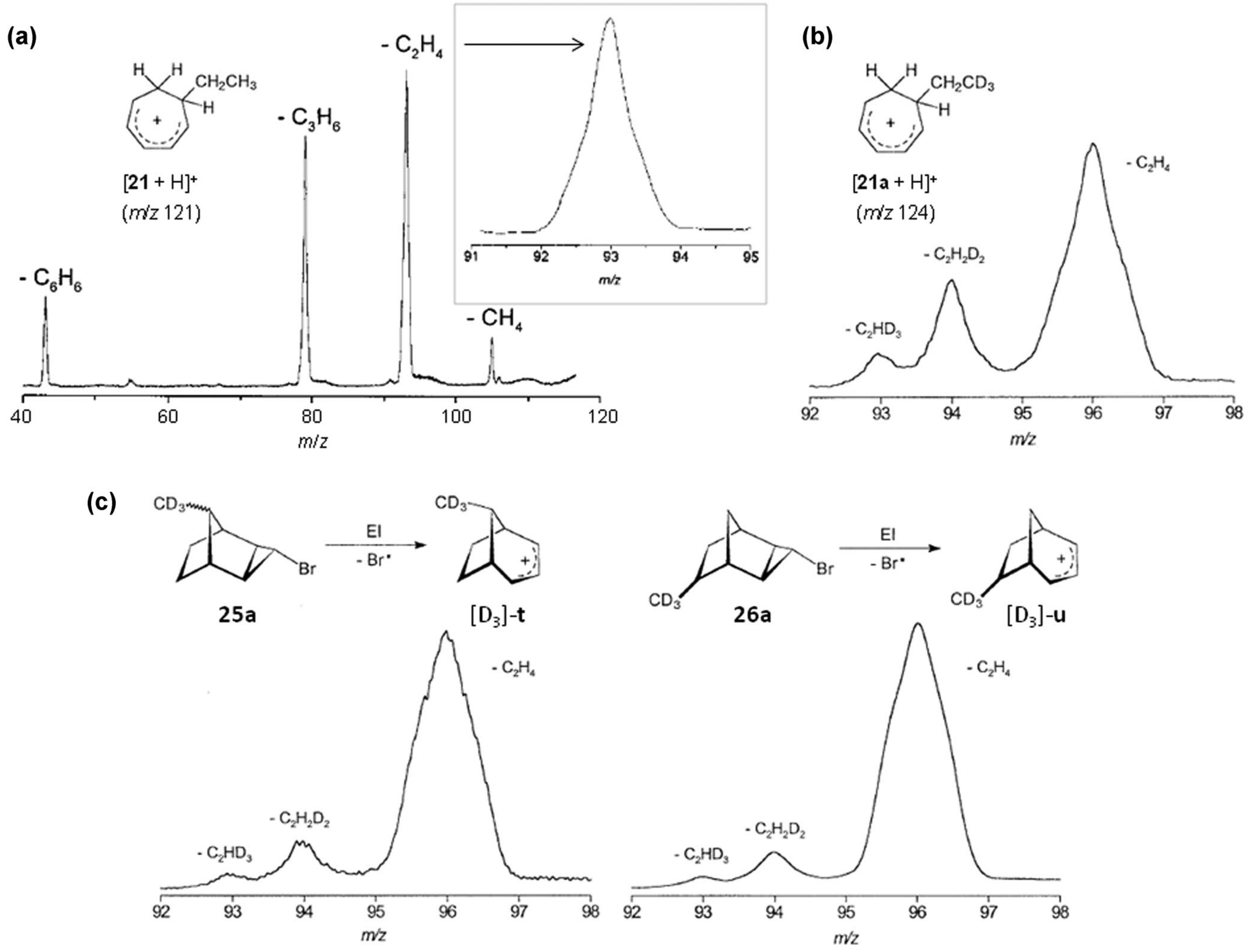

FIGURE 8. (**a**) MIKE spectrum of protonated 7-ethylcycloheptatriene, [**21**+H]$^+$ (*m/z* 121); the insert shows the magnified [M+H–C_2H_4]$^+$ signal. (**b**) Partial MIKE spectrum of protonated 7-[β,β,β-D_3]ethylcycloheptatriene, [**21a**+H]$^+$ (*m/z* 124). (**c**) Partial MIKE spectra of the [M–Br]$^+$ ions [D_3]-**t** and [D_3]-**u**, generated from the deuterium-labeled isomeric precursors **25a** and **26a**, respectively (Mormann & Kuck, 1999; Mormann & Kuck, 2001). Adapted from ref. Mormann & Kuck (1999) with permission of Wiley (**a**); adapted from ref. Mormann & Kuck (2001) with permission of Elsevier (**b**, **c**).

VI. RING CONTRACTION/RE-EXPANSION OF ALKYLCYCLOHEPTATRIENES—THE INTERPLAY OF BICYCLO[3.2.1]ALKENYL ISOMERS

The finding that proton-induced ring contraction of protonated 7-methylcycloheptatriene, [**16**+H]$^+$, gives rise to facile "chain elongation," rather than to the extrusion of another methyl group, was encountered with higher 7-alkyl derivatives as well. Thus, metastable ethyldihydrotropylium ions, [**21**+H]$^+$, as well as propyl- and isopropyldihydrotropylium ions, eliminate propene and, respectively, the corresponding C_4H_8 neutrals, in competition with benzene (Fig. 8a) (Mormann & Kuck, 1999). This behavior is a reliable probe for the intermediacy of the corresponding chain-elongated alkylbenzenium ions, which are well-known to undergo heterolysis of the C^{ipso}-C^{α} bond with selective protonation of the neutral alkene and/or benzene fragments (Leung & Harrison, 1977; Herman & Harrison, 1981; Kuck, 1990a Berthomieu et al., 1991). In the case of ions [**21**+H]$^+$, ring contraction via ion **n** (Scheme 12) leads to the *n*-propylbenzenium ions [**22**+H]$^+$ that eliminate C_3H_6 and C_6H_6 in the characteristic ratio of ~3–5. However, ring contraction of ions [**21**+H]$^+$ with concomitant excrescence of a methyl group giving rise to the isomeric ethyltoluenium ions [**23**+H]$^+$ competes to significant extent, as indicated by the loss of C_2H_4, in particular, and that of CH_4 (Scheme 12). Analysis of deuterium-labeled isotopomers of these latter isomers, and of the higher congeners in similar cases, largely confirms this scenario (Mormann & Kuck, 1999). Most interestingly, however, is the finding that the elimination of ethene from ions [**21**+H]$^+$ is bimodal: It takes place both via ethyltoluenium ions, [**23**+H]$^+$, and another, as it turned out, bicyclic intermediate. The MIKE spectrum of long-lived ions [**21**+H]$^+$ exhibits a composite peak for the [**21**+H–C_2H_4]$^+$ fragment ions, as does the corresponding spectrum of the [β,β,β-D_3]ethyl isotopologs, [**24a**+H]$^+$ (Fig. 8a and b). Besides the losses of C_2HD_3 (*m/z* 93), $C_2H_2D_2$ (*m/z* 94), and C_2H_4 (*m/z* 96) from ions [**21a**+H]$^+$, all of which are reflected by signals with similar Gaussian peak shapes ($T_{\text{kin}} = 14 \pm 1$ meV) and indicate the

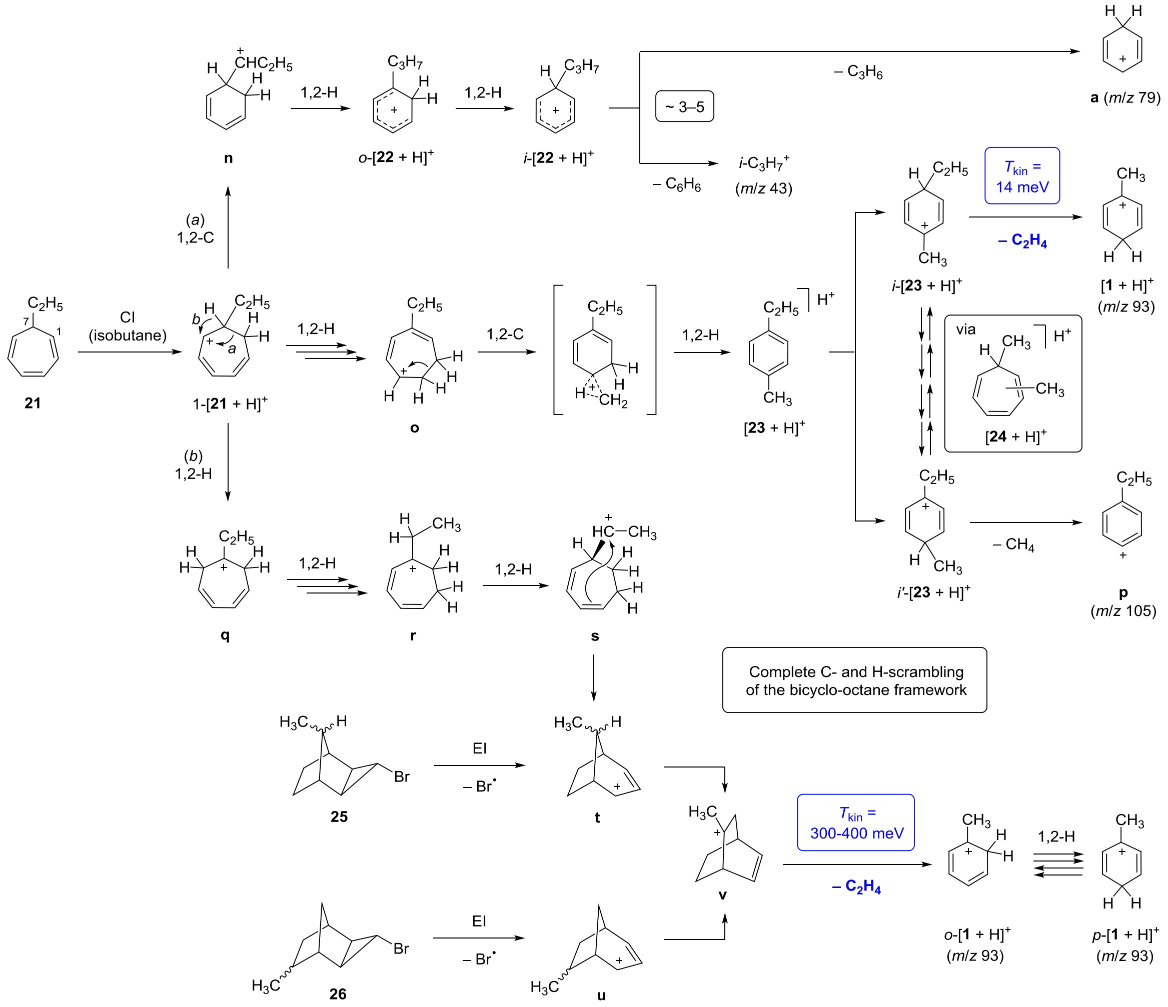

SCHEME 12. Fragmentation of protonated 7-ethylcycloheptatriene, [**21**+H]$^+$, involving isomerization by various ring contraction processes. Ring contraction to the propylbenzenium ions, [**22**+H]$^+$, via ions **n** is irreversible whereas ring contraction to the ethyltoluenium ions, [**23**+H]$^+$, via ions **o** is in part reversible and involves dimethyldihydrotropylium ions, [**24**+H]$^+$. In competition with ring contraction, a fraction of ions [**21**+H]$^+$ undergoes isomerization to bicyclo[3.2.1]oct-2-en-4-yl cations (**t**), which undergo complete C and H scrambling and eventually expel C_2H_4. This elimination is associated with a high kinetic release, in contrast to that from ions [**23**+H]$^+$ (see blue boxes). The methyl-substituted bicyclo[3.2.1]octenyl ions **t**, generated independently from **25** by EI, and **t**, formed from **26**, undergo complete C- and H-scrambling of the C_8-core prior to loss of C_2H_4, either directly or, as indicated, from the methyl-substituted bicyclo[2.2.2]octenyl isomer **v** (Mormann & Kuck, 2001).x

presence of isotopologous ethyltoluenium ions, namely $CH_3–C_6H_6^+–CH_2CD_3$ and $CH_3CH_2–C_6H_6^+–CD_3$, as reactive intermediates, the spectrum exhibits a strong contribution of [**21a**+H–C_2H_4]$^+$ ions (also with *m*/*z* 96), the formation of which is accompanied with a large kinetic energy release ($T_{\text{kin}} = 402$ meV) (Mormann & Kuck, 1999). It was concluded that this fraction of the C_2H_4 neutrals originates completely from the seven-membered ring and that it is expelled from bicyclic $C_9H_{13}^+$ intermediates, such as ion **t** (Scheme 12). To corroborate the interplay of such unusual and unexpected isomers, suitable precursors, including the tricyclic bromides **25** and **26**, of the putative methyl-substituted bicyclo[3.2.1]-oct-2-en-3-yl cations **t** and **u**, respectively, representing ethano-bridged cyclohexen-3-yl cations, were synthesized and studied by EI mass spectrometry (Fig. 8c) (Mormann & Kuck, 2001). In the same work, the lower homolog of ions **t** and **u**, lacking the methyl group, was also investigated by this approach (Mormann & Kuck, 2001).

The fragmentation behavior of the $C_9H_{13}^+$ ions generated from **25** and **26** confirmed this scenario. The [M−Br]$^+$ ions generated from the trideuteromethyl isotopologs **25a** and **26a** revealed identical characteristics for the elimination of $C_2(H,D)_4$ which, in turn, is closely similar to that found for ions [**21a**+H]$^+$. In particular, the loss of C_2H_4 from ions [D$_3$]-**t** and [D$_3$]-**u** is again bimodal, with the broad component of the signal indicating a high kinetic energy release ($T_{\text{kin}} = 300 \pm 15$ meV) (Mormann & Kuck, 2001). It was also found that the bicyclo[3.2.1]-octenyl skeleton of ions **u** and **v** undergoes complete C- and H-scrambling. Overall, it can be safely assumed that a large fraction of long-lived ethyldihydrotropylium ions, [**21a**+H]$^+$, expels ethene via the bicyclic isomers **t** and through a series of relatively labile bicyclic intermediates and after a numerous fast and reversible 1,2-H and 1,2-C shifts. While the bicyclo[3.2.1]-octenyl ion **t** was suggested to be the species from which C_2H_4 is expelled, we can also speculate that the bicyclo[2.2.2]oct-2-en-6-yl isomer **v**, a relatively stable tertiary carbenium ion, is the actually fragmenting isomer, as depicted in Scheme 12. The origin of the high amount of kinetic energy associated with the expulsion of C_2H_4 may lie in the strain energy released from the bicyclic framework during a concerted [4+2]-cycloreversion that leads to the stabilomers of the $C_7H_9^+$ ion family, namely the toluenium ions, [**1**+H]$^+$.

VII. GAS-PHASE TITRATION OF $C_7H_9^+$ ION MIXTURES

The particular complexity of the isomerization reactions of gaseous toluenium and higher methyl-substituted benzenium ions that precede fragmentation has become obvious from many experimental and theoretical studies. Most of them concerned the spontaneous or collision-induced unimolecular reactivity of the $C_7H_9^+$, $C_8H_{11}^+$ ions and their higher analogs, including those ions that can be formed by electrophilic attack of methyl cations on benzene or toluene, or by the electrophilic insertion of phenyl cations into aliphatic C–H bonds, as carried out most recently under flowing-afterglow conditions (Wang et al., 2018). Another, experimental and complementary bimolecular approach to analyze such gaseous arenium ions and their constitutional isomers makes use of their different gas-phase acidity or, in turn, the different gas-phase basicity of the conjugate arenes or cyclo-olefins. Many of these thermodynamic data have been determined and compiled over the past decades (Lias et al., 1988; Hunter & Lias, 1998; Linstrom & Mallard, 2018), but the challenge to elucidate the nature of gaseous $C_7H_9^+$, $C_8H_{11}^+$ and related ions has led our group to contribute some gas-phase proton basicity (*GB*) and *PA* data on simple carbocyclic hydrocarbons and a few other benzene derivatives (Mormann, Salpin, & Kuck, 1999; Mormann et al., 2000; Salpin et al., 2003; Mormann & Kuck, 2007).

As mentioned above, the interconversion of *ortho*-, *meta*-, and *para*-xylenium ions by 1,2-methyl shifts along the benzenium ring is a well-known isomerization channel. In 1997, Grützmacher et al. showed that the mixture of such constitutionally different $C_8H_{11}^+$ ions—each of which existing as a set of fast interconverting tautomers—can be analyzed by controlled bimolecular deprotonation within the cell of a Fourier transform ion cyclotron resonance (FT-ICR) mass spectrometer (Büker et al., 1997). In this semiquantitative gas-phase titration, a set of volatile basic compounds of increasing gas-phase basicity is used to afford the proton transfer from $C_8H_{11}^+$ ions of decreasing gas-phase acidity. For example, xylenium ions that were generated from *para*-xylene, **15**, by CI with methane as the reactant gas were found to undergo isomerization to a mixture of the three protonated xylenes present in the ratio $\{para\text{-}[C_6H_5(CH_3)_2]^+\}/\{ortho\text{-}[C_6H_5(CH_3)_2]^+\}/[meta\text{-}[C_6H_5(CH_3)_2]^+\}\approx 15{:}25{:}60$. Thus, under such strongly exoergic protonation conditions, repeated 1,2-methyl shifts give rise to the predominance of the conjugate acid of the most basic isomer, *meta*-xylene, similar to isomerization in superacidic solution (Brouwer, 1968), and the relative population of the isomeric xylenium ions seems to reflect their slightly but significantly different gas-phase basicities. Less exoergic but also slightly endoergic protonation was shown to induce less isomerization and it was deduced that the 1,2-methyl shifts occur under kinetic rather than thermodynamic control within the ion/neutral complex formed during the initial protonation of *para*-xylene, **15** (Büker et al., 1997).

Some years later, we performed a detailed study on the gas-phase titration of $C_7H_9^+$ ions formed from toluene, **1**, and its cyclo-olefinic isomers, cycloheptatriene, **2**, norbornadiene, **3**, and 6-methylfulvene, **4** (Mormann, Salpin, & Kuck, 2006). This investigation was inspired by the extended studies of the unimolecular isomerization behavior of the toluenium ions and their constitutional isomers decribed above. The gas-phase basicities and proton affinities of the conjugate bases, hydrocarbons **1**–**4**, were known (Houriet et al., 1986; Hunter & Lias, 1998; Linstrom & Mallard, 2018) or had been determined in the meantime (Mormann, Salpin, & Kuck, 1999; Salpin et al., 2003). As a matter of fact, they differ more strongly than those of the isomeric xylenes: *GB*(**1**) = 756 kJ/mol, *GB*(**2**) = 798 kJ/mol, *GB*(**3**) = 820 kJ/mol, and *GB*(**4**) = 842 kJ/mol. Protonation of these neutral C_7H_8 precursors was performed under CI conditions using either isobutane or methane, that is, under slightly endoergic and strongly exoergic protonation conditions, respectively. Four volatile bases of increasing gas-phase basicity were employed for the stepwise deprotonation of the $C_7H_9^+$ ion populations formed: methyl formate (*GB* = 752 kJ/mol), ethyl acetate (*GB* = 805 kJ/mol), diisopropyl ether (*GB* = 828 kJ/mol), and mesityl oxide (*GB* = 847 kJ/mol) (Linstrom & Mallard, 2018). The deprotonation of the $C_7H_9^+$ ion populations generated from toluene by both CI(isobutane) or CI(methane) revealed that only toluenium ions, [**1**+H]$^+$, were formed. Use of the weakest base, methyl formate, gave rise to complete deprotonation and the deprotonation kinetics were monomodal (Mormann, Salpin, & Kuck, 2006). Thus, even protonation with CH_5^+ ions in the CI(methane) plasma does not give rise to long-lived rearrangement products.

All of the cyclo-olefinic isomers of toluene behave differently, as illustrated in Fig. 9. Mild protonation of cycloheptatriene, **2**, by CI(isobutane) generates a $C_7H_9^+$ ion mixture that consists of three components of different acidity: toluenium ions, [**1**+H]$^+$ (~20%), dihydrotropylium ions, [**2**+H]$^+$ (~60%), and 6-methylfulvenium ions, [**4**+H]$^+$ (~20%). Thus, the major fraction of the [**2**+H]$^+$ ions generated in the protonation step did not suffer skeletal rearrangement under these conditions. Since the deprotonation curves obtained by use of ethyl acetate and diisopropyl ether are quite similar, the presence of significant amounts of protonated norbornadiene, [**3**+H]$^+$, or the nortricyclyl ion [**3'**+H]$^+$ (see below), can be excluded. Obviously, the excitation of the $C_7H_9^+$ ions is not sufficiently strong to allow the [**2**+H]$^+$ ions to rearrange into these isomers. In contrast, use of methane as the CI reactant gas gives rise to much more isomerization: The toluenium ions, [**1**+H]$^+$, dominate (~50%) and only a minor fraction (~15%) of dihydrotropylium ions, [**2**+H]$^+$, survive. In this case, 6-methylfulvenium ions, [**4**+H]$^+$, are formed in increased relative amounts (~30%), and even a small fraction of protonated norbornadiene, [**3**+H]$^+$, was detected (~5%). Most remarkable is the finding that, under both CI conditions, protonation of cycloheptatriene, **2**, leads to ring contraction to toluenium ions, [**1**+H]$^+$, and also to methylfulvenium ions, [**4**+H]$^+$. Thus, the doubly ring-contracted, five-membered ring

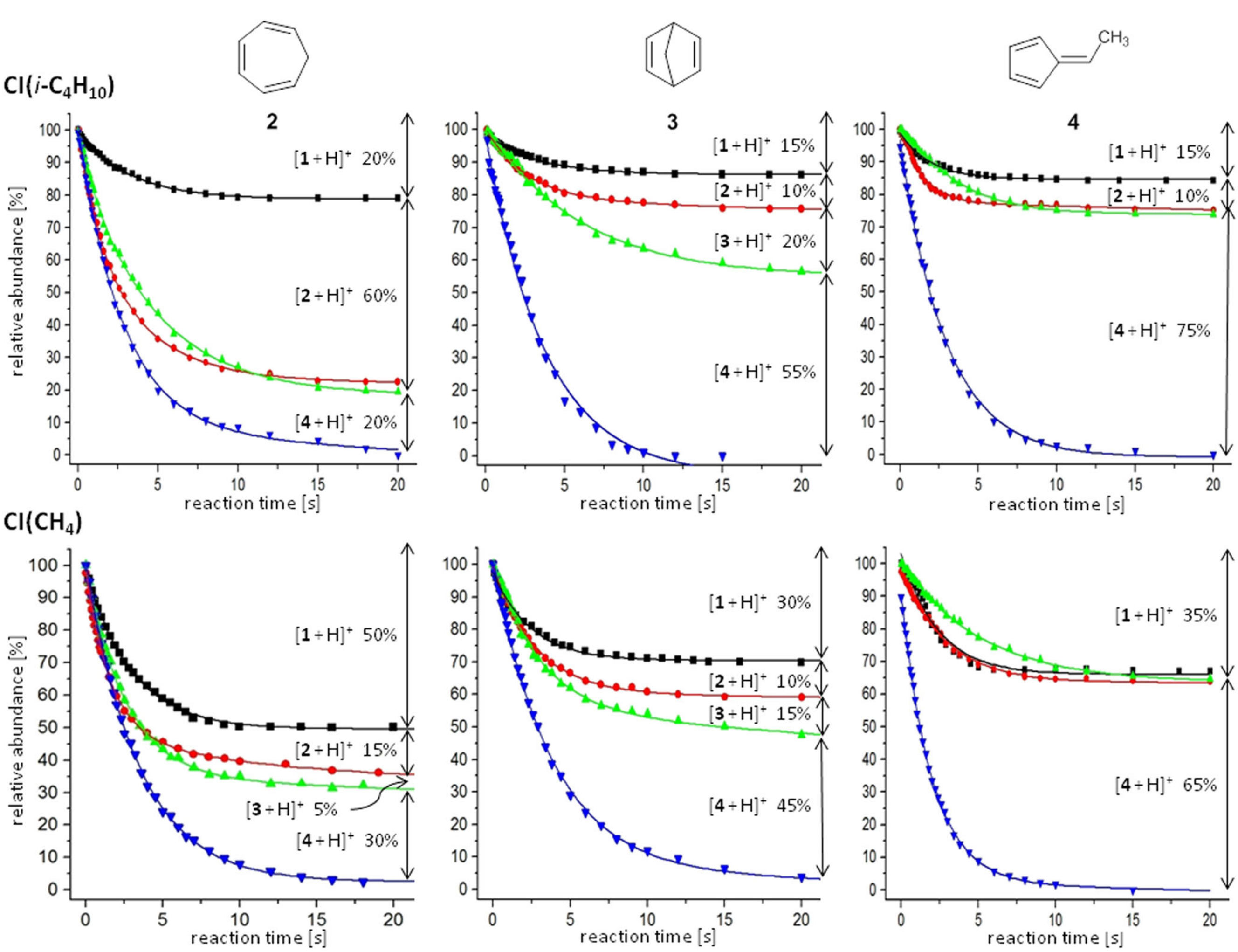

FIGURE 9. Gas-phase titration of $C_7H_9^+$ ion mixtures generated from cycloheptatriene, **2**, norbornadiene, **3**, and 6-methylfulvene, **4**, by CI(isobutane) and CI(methane) in the external ion source of an FT-ICR mass spectrometer. The ion mixtures were deprotonated by use of bases with increasing gas-phase basicity: methyl formate (black lines), ethyl acetate (red), diisopropyl ether (green) and mesityl oxide (blue). The fractions of isomeric $C_7H_9^+$ ions that were deprotonated by a given base are assigned by their respective percentages (Mormann, Salpin, & Kuck, 2006). Adapted from ref. Mormann, Salpin, & Kuck (2006) with permission of Elsevier.

isomer is easily accessible by protonation of **2**. From these results, it may be suspected that the fulvenium structure of ions $[\mathbf{4}+H]^+$ is not attained by stepwise ring contraction via toluenium ions as intermediates but rather by at least one independent isomerization channel (see below). When norbornadiene, **3**, was protonated under the same CI(isobutane) and CI (methane) conditions, minor fractions of surviving ions $[\mathbf{3}+H]^+$ or, rather, $[\mathbf{3'}+H]^+$ were found (~20% and ~15%, respectively), but the major fractions of $C_7H_9^+$ ions consisted of 6-methylfulvenium ions, $[\mathbf{4}+H]^+$ (~55% and ~45%, respectively). The relative amounts of toluenium ions, $[\mathbf{1}+H]^+$ were surprisingly small (~15% and ~30%) and the dihydrotropylium ions, $[\mathbf{2}+H]^+$, were generated in only 10% yield in either case. It appears that proton-induced skeletal rearrangement of the bi- or tricyclic framework in ions $[\mathbf{3}+H]^+$ or $[\mathbf{3'}+H]^+$, respectively, leads to both toluenium and methylfulvenium ions, $[\mathbf{1}+H]^+$ and $[\mathbf{4}+H]^+$, with a marked preference for the latter isomer. Finally, protonation of 6-methylfulvene, **4**, is quite telling. The $C_7H_9^+$ ion mixture produced under both CI conditions consisted mostly of the pristine 6-methylfulvenium ions, $[\mathbf{4}+H]^+$ (~75% and ~65%, respectively), while the 3-nortricyclyl ions, $[\mathbf{3'}+H]^+$, are not formed at all. Rearrangement of the fulvene structure leads mostly to toluenium ions, $[\mathbf{1}+H]^+$ (~15% and ~35%, respectively), while dihydrotropylium ions, $[\mathbf{2}+H]^+$, are formed in minor relative amounts (~10%) only under mild CI conditions.

Some interesting conclusions can be drawn from all these findings: (i) Both toluenium ions, $[\mathbf{1}+H]^+$, and 6-methylfulvenium ions, $[\mathbf{4}+H]^+$, are formed preferably in all three cases. This agrees with the results obtained from a combined experimental and theoretical study, according to which C^1-protonated 6-methylfulvene, ion 1-$[\mathbf{4}+H]^+$, is less stable than *para*-protonated toluene, ion *p*-$[\mathbf{1}+H]^+$ by only 43 kJ/mol (Mormann, Salpin, & Kuck, 1999) (see also refs. Bouchoux, Yáñez, & Mó, 1999 and Mormann & Kuck, 2007), while the other two $C_7H_9^+$ isomers are much less stable (Schröder et al., 2006; Mormann, Salpin, & Kuck, 2006). (ii) The conversion of ions $[\mathbf{4}+H]^+$ to ions $[\mathbf{1}+H]^+$ occurs particularly easily. In fact, the barrier toward ring expansion of

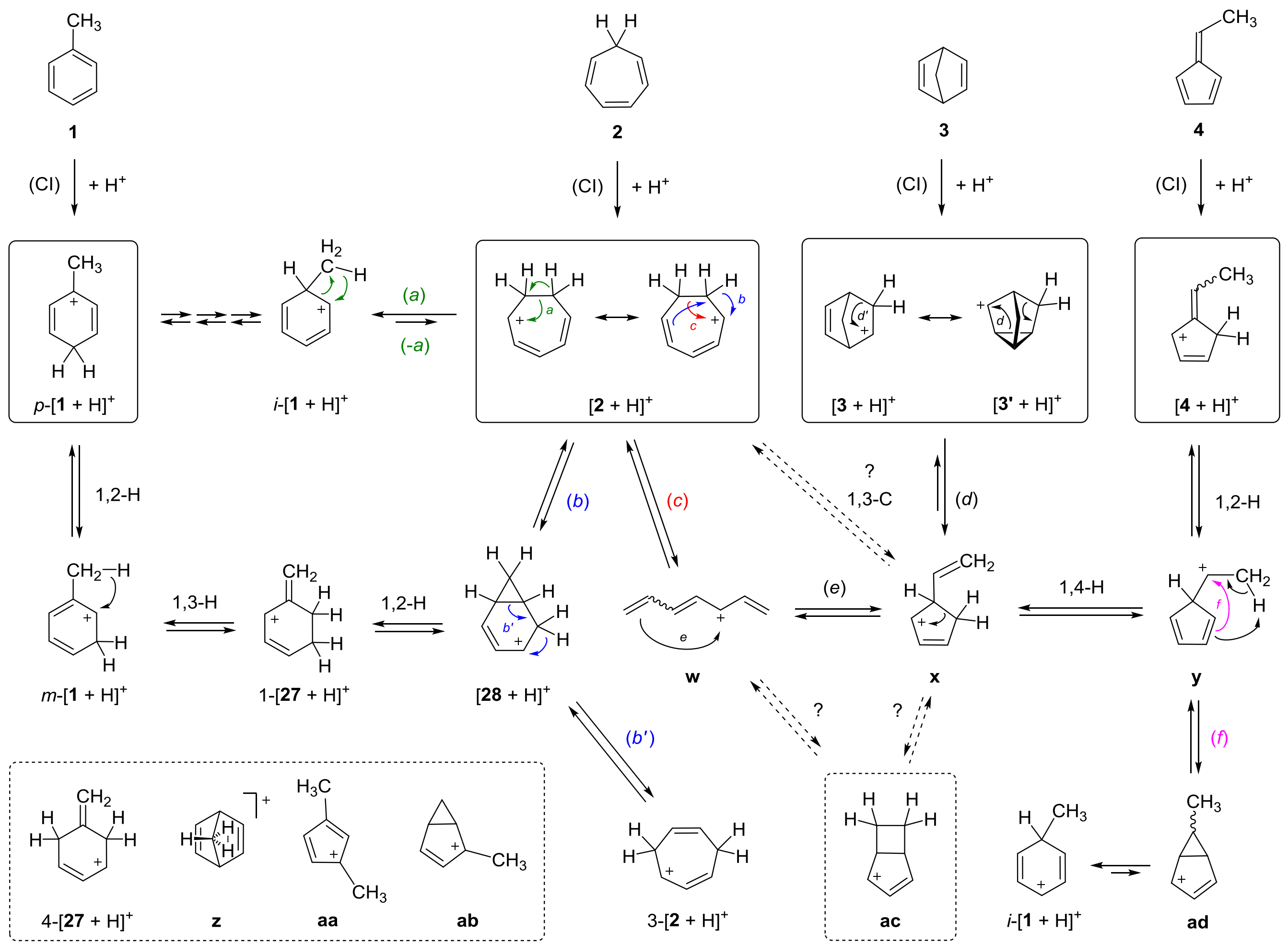

SCHEME 13. Known and potential isomerization pathways of $C_7H_9^+$ ions generated from toluene, **1**, cycloheptatriene, **2**, norbornadiene, **3**, and 6-methylfulvene, **4**, by chemical ionization, with special regard to the gas-phase titration experiments (see Fig. 9). Most structures were characterized at least by computational work, including C^1-protonated *ortho*-isotoluene, 1-[**27**+H]$^+$, and C^4-protonated *ortho*-isotoluene, 4-[**27**+H]$^+$, C^2-protonated norcaradiene, [**28**+H]$^+$, the 1,4-dihydrotropylium ion, 3-[**2**+H]$^+$, ions **w**, **x**, **aa**, **ab** and even the methonium ion **ac**; whereas a few other structures (**y**, **ac** and **ad**) were not and are hypothetical (see also Fig. 10).

ions [**4**+H]$^+$ to ions [**1**+H]$^+$ was calculated to be 170 kJ/mol (Mormann, Salpin, & Kuck, 2006), slightly lower than that for the pair of the parent fulvenium and benzenium ($C_6H_7^+$) ions (179 kJ/mol (Bouchoux, Yáñez, & Mó, 1999)). (iii) Protonated norbornadiene, as the 3-nortricyclyl ion, [**3'**+H]$^+$, is converted most efficiently to the other isomers and, in turn, it is formed in least amounts from them. This is in line with the lowest thermochemical stability of ions [**3'**+H]$^+$ among the four isomeric $C_7H_9^+$ ions (Schröder et al., 2006; Mormann, Salpin, & Kuck, 2006). (iv) It appears that proton-induced formation of the five-membered ring in the fulvenium ion structures [**4**+H]$^+$ from cycloheptatriene, **2**, and norbornadiene, **3**, is independent from the ring contraction to the toluenium ions, [**1**+H]$^+$. This also corresponds to the observation that mild protonation of the 6-methylfulvenium ions, [**4**+H]$^+$, leads to sizeable amounts (~10%) of dihydrotropylium ions, [**2**+H]$^+$, along with toluenium ions, [**1**+H]$^+$, in the $C_7H_9^+$ ion mixture formed. Therefore, as discussed previously (Mormann, Salpin, & Kuck, 2006), additional but unrecognized isomerization channels are opened either within the encounter complex formed upon protonation in the CI plasma or during the lifetime of the $C_7H_9^+$ ions prior to deprotonation—or, at latest, within the ion-molecule complex formed during deprotonation. One of the formal possibilities in this regard is the putative direct interconversion of dihydrotropylium ions, [**2**+H]$^+$, and 6-methylfulvenium ions, [**4**+H]$^+$, by bicyclo[3.2.0]heptane intermediate **ac** (Scheme 13), a mechanism that, to the best of our knowledge, has hitherto never been elucidated (see below). Another, temptingly straightforward isomerization channel of the $C_7H_9^+$ ions could involve completely ring-opened, cyclic isomers, namely heptatrienyl ions **w** (Scheme 13). These isomers were calculated to be similarly stable as ions [**2**+H]$^+$ and considered accessible from either 1-protonated cycloheptatriene, 1-[**2**+H]$^+$, or even directly from the *ipso*-toluenium ions, *i*-[**1**+H]$^+$, but the barriers toward ring opening were calculated to be relatively high (see Fig. 10) (Schröder et al., 2006). Several straightforward as well as multistep isomerization pathways of the $C_7H_9^+$ ion diversity are combined in Scheme 13. Most of them are commented on in the context of the energy profile that emerges from mostly computational work that has been reported in the literature over the past decades and will be presented in the next section.

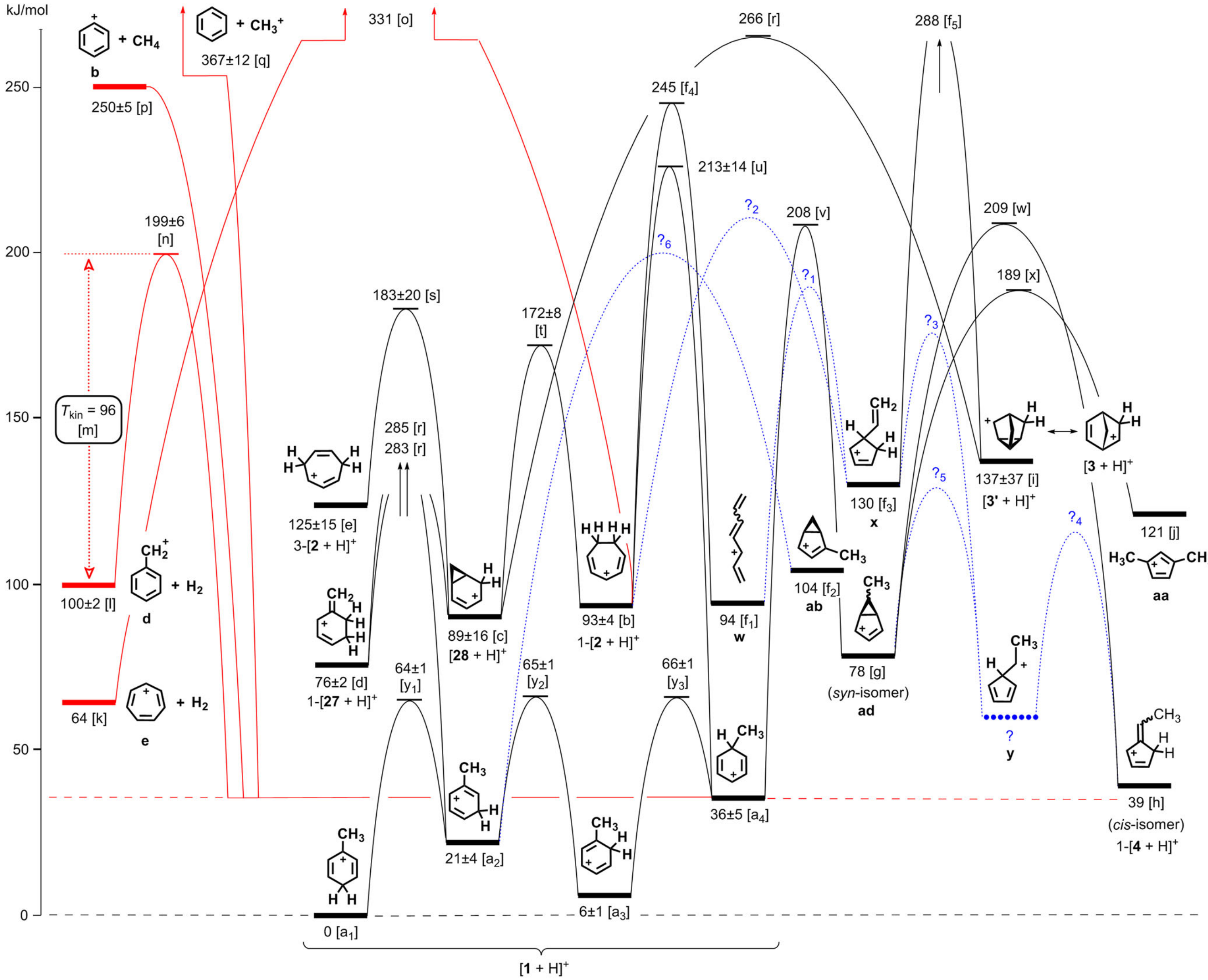

FIGURE 10. Energy profile of the isomerization and fragmentation of gaseous $C_7H_9^+$ ions, as composed from various published computational work (in kJ/mol relative to the level of ion p-$[1{+}H]^+$). The profile represents a semi-quantitative approach where several data are averaged values (e.g., [c]); some conceivable but hitherto unknown mechanistic pathways are included (dashed blue lines and barriers marked by "?$_n$"). The fragmentation paths are shown in red color. Putative but never observed 1,1-elimination of H_2 from the toluenium ions, p-$[1{+}H]^+$, m-$[1{+}H]^+$ and o-$[1{+}H]^+$, that would produce the corresponding tolylium cations (e.g., c) is not included. – References to individual data for $C_7H_9^+$ ions (for $C_6H_7^+$ and $C_8H_{11}^+$ ions in italics): [a] Kuck (1990a), Maksić (1998), Ishikawa (2004), Kuck (2005b), Dopfer (2006), Mormann (2006), Schröder (2006), Chiavarino (2008), Douberly (2008), Mosley (2015), Bouwman (2018), Wang (2018); [b] Salpin (2003), Mormann (2006), Schröder (2006), Sekiguchi (2009), Mosley (2015), Bouwman (2018); [c] Salpin (2003), Mormann (2006), Schröder (2006), Mosley (2015); [d] Mormann (2006), Schröder (2006), Bouwman (2018); [e] Salpin (2003), Schröder (2006), Mosley (2015), Bouwman (2018); [f] Schröder (2006); [g] Bouchoux (1999), Arstad (2004), Mormann (2006); [h] Mormann (2006), Mosley (2015); [i] Mormann (2006), Schröder (2006), Mosley (2015); [j] Mosley (2015); [k] Kuck, Schneider, Grützmacher (1985), Schröder (2006); [l] Kuck, Schneider, Grützmacher (1985), Ignatev (2004), Dopfer (2006), Schröder (2006), Sekiguchi (2009), Wang (2018); [m] Williams (1974b), Kuck, Schneider, Grützmacher (1985); [n] Ignatev (2004), Schröder (2006), Sekiguchi (2009), Wang (2018); [o] Mormann (2003), Schröder (2006); [p] Dopfer (2006), Schröder (2006), Sekiguchi (2009), Wang (2018); [q] Ishikawa (2004), Wang (2018); [r] Mormann (2006); [s] Salpin (2003), Schröder (2006); [t] Salpin (2003), Mormann (2006), Schröder (2006); [u] Mormann (2003), Arstad (2004), Schröder (2006), Sekiguchi (2009); [v] Bouchoux (1999), Arstad (2004), Mormann (2006); [w] Salpin (2003); [x] Arstad (2004); [y] Kuck (1990a), Maksić (1998), Ishikawa (2004), Kuck (2005b), Mormann (2006), Schröder (2006), Wang (2018).

VIII. MERGED INSIGHTS ON THE $C_7H_9^+$ ENERGY HYPERSURFACE FROM A POTPOURRI OF EXPERIMENTAL INSIGHTS AND THEORETICAL CALCULATIONS

The results of the gas-phase titration experiments deserve further discussion in the light of various theoretical calculations performed mostly in view of the unimolecular isomerization and fragmentation of $C_7H_9^+$ ions but also in connection of the bimolecular formation of the ions under flowing afterglow conditions, as detailed in the preceding paragraphs. Even calculations on higher analogs, such as on some $C_8H_{11}^+$ ions mentioned above, can be associated with these considerations. Figure 10 combines the available data in a semiquantitative approach, including some extrapolations and mechanistic bridges that have not been considered (and studied by computational approach) before. Whereas the relative energies of the various $C_7H_9^+$ intermediates and the respective transitions states converge in many cases, considerable deviations between individual features have to be admitted. Nevertheless, the isomerization energy profile largely agrees with both the unimolecular fragmentation channels, that is, the elimination of H_2 and CH_4, and the major observations obtained from the gas-phase titration experiments. The respective literature sources of the computed data are also collected in Figure 10.

Extended and repeated computational work on the energy profile of the 1,2-hydride (or 1,2-proton) shifts along the rim of the protonated benzene ring has been carried out decades ago (Kuck, 1990a, 2005b) and till to date (see below). As far as the gaseous tautomeric toluenium ions are concerned, the order of stability elucidated early by ICR measurements by Hehre and his associates in 1976 (Devlin et al., 1976) was found to match well with that obtained by calculations that also appeared, starting even earlier (Isaacs & Cvitas, 1971; Devlin et al., 1976; Heidrich, Grimmer, & Sommer, 1976). Since then and following Dewar's AM1 semiempirical work published in 1986 (Dewar & Dieter, 1986), numerous further computational studies have accompanied experimental investigations. The following stability order with some margins has been established over the years: *p*-[**1**+H]$^+$ (≡ 0 kJ/mol) > *o*-[**1**+H]$^+$ (5–7 kJ/mol) > *m*-[**1**+H]$^+$ (17–26 kJ/mol) > *i*-[**1**+H]$^+$ (31–42 kJ/mol) (Maksić & Eckert-Maksić, 1998; Ishikawa et al., 2004; Dopfer et al., 2006; Mormann, Salpin, & Kuck, 2006; Schröder et al., 2006; Chiavarino et al., 2008; Sekiguchi et al., 2009; Mosley, Young, & Duncan, 2015; Wang et al., 2018) (Fig. 10, [a_1]–[a_4]). The transition states have been calculated in most of these studies to lie in the range of 64–66 kJ/mol above the level of the most stable tautomer, *p*-[**1**+H]$^+$ (Fig. 10, [y_1]–[y_3]). Lower barriers (32–54 kJ/mol) were reported in our own papers (Mormann, Salpin, & Kuck, 2006; Sekiguchi et al., 2009). Experimental values for the barriers towards 1,2-H shifts in benzenium and alkylbenzenium ions determined in superacid solution and in the gas phase are in the range of 32–40 kJ/mol (Olah et al., 1972; Olah et al., 1978; Kuck, 1990a; Cacace, Crestoni, & Fornarini, 1992). The barriers towards 1,2-methyl shifts in gaseous xylenium ions were also elucidated by experiment and computational approach and found to lie in the range of 83–92 kJ/mol starting from the *ipso*-tautomer of the xylenium ions, *i*-[**15**+H]$^+$ (Büker et al., 1997; Arstad, Kolboe, & Swang, 2004). Of course, the barriers vary for the individual cases.

A simple and well-established conclusion can be drawn from these data: Any $C_7H_9^+$ ions (as well as homologous and analogous ions $C_{7+n}H_{9+2n}^+$, $n = -1$ and $n \geq 1$) formed even with relatively low internal excitation energies undergo the fast conversion between the ring-protonated tautomeric forms with greatest ease, as compared to all other isomerization channels (see below). In this respect, is satisfying to note that the fast and complete intraannular H/D equilibration in toluenium ions, [**1**+H]$^+$, was clearly recognized as an independent process besides other scrambling reactions (Fig. 4) (Kuck, Schneider, & Grützmacher, 1985), as a characteristic element of the composite scrambling scenario (Kuck & Bäther, 1986; Kuck, 2002). In turn, the facile proton ring walk can be used as a mechanistic and structural probe since it represents a ubiquitous reaction behavior of protonated arenes (Kuck, 1990a, 1992, 2002). Notwithstanding the fast and complete intraannular H/D exchange in gaseous toluenium ions, there is no doubt that the *para*- and *ortho*-tautomers, *p*-[**1**+H]$^+$ and *o*-[**1**+H]$^+$, strongly prevail in mixtures of gaseous $C_7H_9^+$ ions, in analogy to the situation in superacid solutions (Fărcaşiu, Melchior, & Craine, 1977; Fărcaşiu, 1982). This latter detail was experimentally corroborated by elucidating the site-selectivity of the D/H exchange within complexes of perdeuterated toluenium ions, formed from [D_8]-toluene with D_3^+ ions under γ-radiolysis, with selected Brønsted acids (Chiavarino et al., 2008).

The combined experimental and computational information clearly indicates that toluenium ions, [**1**+H]$^+$, undergo skeletal rearrangements only after high excitation but stay intact at lower internal energies. There is no doubt that ring expansion to 1,2-dihydrotropylium ions, 1-[**2**+H]$^+$, is the energetically easiest isomerization channel but it requires far more excitation than the intraannular 1,2-H shifts (Fig. 10). According to theoretical calculations, excitation by 197–226 kJ/mol is required to convert *p*-[**1**+H]$^+$ ions into 1,2-dihydrotropylium ions, 1-[**2**+H]$^+$ (Schröder et al., 2006; Sekiguchi et al., 2009). Starting from the *ipso*-tautomer, *i*-[**1**+H]$^+$, the 1,3-H shift from the methyl group to one of the *ortho*-positions still needs 159–183 kJ/mol (reverse path -*a*, Scheme 13) (Schröder et al., 2006; Sekiguchi et al., 2009). Calculations on the analogous process in *para*-xylenium ions, *p*-[**15**+H]$^+$, gave similar results (Arstad, Kolboe, & Swang, 2004). Conversely, ring contraction of ions 1-[**2**+H]$^+$ via path *a* is energetically relatively facile (106–135 kJ/mol) (Schröder et al., 2006; Sekiguchi et al., 2009). An alternative ring expansion via the *meta*-toluenium ions, *m*-[**1**+H]$^+$, by a stepwise process involving the C^1-protonated *ortho*-isotoluene [**27**+H]$^+$ and protonated norcaradiene, [**28**+H]$^+$, isomers was calculated to require even 285 kJ/mol (Scheme 13, Fig. 10) (Mormann, Salpin, & Kuck, 2006).

Protonation of cycloheptatriene, **2**, may occur at positions C^1, C^2, and C^3 and the relative stabilies and transitions states for the interconversions of the corresponding isomers were calculated (Schröder et al., 2006; Mormann, Salpin, & Kuck, 2006). There is some discrepancy about the relative stabilities of the 1,2-dihydrotropylium ion, 1-[**2**+H]$^+$, formed by protonation at C-1 of cycloheptatriene, and protonated norcaradiene, [**28**+H]$^+$, formed by protonation at C-2 (Schröder et al., 2006; Mormann, Salpin, & Kuck, 2006). However, there is no doubt that the latter, bicyclic isomer plays a central role in the isomerization of ions [**2**+H]$^+$ to other $C_7H_9^+$ ions. As shown in Scheme 13 (path *b*), ions [**28**+H]$^+$ may react further by 1,2-H shift to 1,4-dihydrotropylium ions, 3-[**2**+H]$^+$, which were calculated to be somewhat less stable that the other forms of protonated cycloheptatriene (Schröder et al., 2006). Interestingly, 1,2-H shifts along the rim of dihydrotropylium ion require higher energies than 1,2-H shift in the benzenium ring, namely 89–112 kJ/mol; nevertheless, such barriers fall short of those towards ring contraction of the 1,2-dihydrotropylium ions to the toluenium isomers mentioned above (Schröder et al., 2006). This means that complete or incomplete hydrogen scrambling may take place in protonated cycloheptatriene, [**2**+H]$^+$, prior to ring contraction to the toluenium ions, [**1**+H]$^+$, whereas complete scrambling of the ring hydrogens precedes the reverse process.

A noteworthy extension of the scenario can be based on the possible ring opening isomerization of 1,2-dihydrotropylium ions, 1-[**2**+H]$^+$, to acyclic hepta-1,3,5-trien-7-yl ions, **w** (Scheme 13, path *c*). In fact, this process has never been observed by experiment. However, calculations suggest that the barrier towards ring opening of the bis-allylic C–C single bond in the 1-[**2**+H]$^+$ ion requires only little more energy than ring contraction to toluenium ions (154 kJ/mol) (Schröder et al., 2006). Also, these calculations suggest the acyclic isomers to be only negligibly less stable than the cyclic precursor. Thus, quite exothermic protonation of cycloheptatriene by, for example, CH_5^+ ions in the CI(CH_4) plasma may well open this experimentally hidden isomerization channel. Moreover, recyclization of the hepta-1,3,5-trien-7-yl ions, **w**, by ring closure between C^1 and C^5 can open the way to the vinylcyclopentenyl ion **x** and the 6-methylfulvenium isomers, [**4**+H]$^+$ (Scheme 13, path *e*). Notably, neither this path has been studied by experiment or by theory, nor has the direct interconversion of 1,2-dihydrotropylium ions, [**2**+H]$^+$, and vinylcyclopentenyl ions **x** by 1,3-C shift been investigated (Scheme 13, dashed arrows).

Some detailed mechanistic and energetic information has also been accumulated for the role of protonated norbornadiene, [**3**+H]$^+$, in the isomerization scenario of gaseous $C_7H_9^+$ ions. It can be inferred from many classical solvolysis studies of norbornene and nortricyclane derivatives that protonation of the bicyclic diene **3** at C-2 generates 3-nortricycyl (tricyclo-[2.2.1.0^{2,6}]hept-3-yl) cations, [**3'**+H]$^+$, by transannular C–C bond formation (Roberts, Bennett, & Armstrong, 1950; Winstein, Walborsky, & Schreiber, 1950; Olah & Liang, 1975; Saunders, Jarrett, & Pramanik, 1987; Jarrett et al., 1988; Moss et al., 2004; Moss et al., 2005). This stabilizing effect certainly affects the known gas-phase basicity and PA of hydrocarbon **3** (Houriet et al., 1986). Also, it is worth noting that the norbornenyl-nortricyclyl system is known to undergo facile C-scrambling even in solution. As mentioned above, cation [**3'**+H]$^+$ is undoubtedly the least stable among the gaseous $C_7H_9^+$ isomers studied by experiment. Calculations place its heat of formation at 97 kJ/mol (Mormann, Salpin, & Kuck, 2006), 103 kJ/mol (Mosley, Young, & Duncan, 2015) and even 173 kJ/mol (Schröder et al., 2006) above that of the *para*-toluenium ion, *p*-[**1**+H]$^+$. As shown in Scheme 13 (path d), the tricyclic ion [**3'**+H]$^+$ formed by protonation of norbornadiene, **3**, can undergo ring opening to give the 4-vinylcyclopent-1-en-3-yl cation, **x**. Calculations suggest that this isomerization is exoergic by 43 kJ/mol and takes place over a relatively low activation barrier (114 kJ/mol), much lower than the barrier towards isomerization to the *ipso*-toluenium ion, *i*-[**1**+H]$^+$, which would occur via the nonclassical methonium ion **z** (Scheme 13) (Schröder et al., 2006). On the other hand, there should be alternative pathways for the 4-vinylcyclopent-1-en-3-yl cation, **x**, to rearrange to the other $C_7H_9^+$ isomers. Neither of these has been studied by computation so far. Both ring opening to the acyclic ion **w** (reverse path *-e*) and the probably more facile 1,3-C shift to generate ions 1-[**2**+H]$^+$ appear conceivable. As mentioned above, the latter process corresponds to a direct isomerization channel connecting the five- and seven-membered-ring $C_7H_9^+$ isomers (Scheme 13). However, a facile 1,4-H (proton) transfer from the protonated ring of ion **x** to the vinyl residue would give rise to the secondary cyclopentadien-5-yl)ethyl cation, **y** (Scheme 13). This intermediate could easily isomerize by ring expansion to the *ipso*-toluenium ion, *i*-[**1**+H]$^+$, via the 6-methylbicyclo[3.1.0]hex-2-en-4-yl cation, **ad** (Scheme 13, path *f*). As mentioned above, the reverse of this type of isomerization was suggested for the conversion of benzenium ions to fulvenium ions (Bouchoux, Yáñez, & Mó, 1999; Arstad, Kolboe, & Swang, 2004). In fact, a simple 1,2-H shift connects the cyclopentadien-5-yl)ethyl cation **y** with the most stable tautomer of protonated 6-methylfulvene, ion 1-[**4**+H]$^+$ (Scheme 13). The conversion of the 6-methylbicyclo[3.1.0]hex-2-en-4-yl cation, **ad**, to the toluenium ion, *i*-[**1**+H]$^+$, and to the 6-methylfulvenium ion, 1-[**4**+H]$^+$, were also assessed by computational approach (Mormann, Salpin, & Kuck, 2006).

Finally, the gas-phase chemistry of protonated 6-methylfulvene, [**4**+H]$^+$, deserves some comments. After all, this $C_7H_9^+$ ion is only slightly less stable than the toluenium ions, [**1**+H]$^+$. From the experimentally determined gas-phase basicity of 6-methylfulvene, **4**, the heat of formation of ions [**4**+H]$^+$ was found to exceed that of ions *p*-[**1**+H]$^+$ by 43 kJ/mol (Mormann, Salpin, & Kuck, 1999). In line with this, independent computational work on these $C_7H_9^+$ ions gave a difference of 39 kJ/mol (Mormann, Salpin, & Kuck, 2006; Mosley, Young, & Duncan, 2015), and the stabilities of the parent fulvenium and benzenium isomers, $C_6H_7^+$, were calculated to differ by 40 kJ/mol (Bouchoux, Yáñez, & Mó, 1999). It should be noted that the above-mentioned nonconjugated tautomer of ion [**4**+H]$^+$, the 4-vinylcyclopent-1-en-3-yl cation, **x**, was calculated to be much less stable than [**4**+H]$^+$ and the formally anti-aromatic ethylcyclopentadienyl isomer, C_2H_5-*cyclo*-$C_5H_4^+$ (not shown in Scheme 13) would be even more so (Schröder et al., 2006). As also mentioned above, the barrier between the isomers [**4**+H]$^+$ and [**1**+H]$^+$ is only modestly high. Calculations for the mechanistically most facile path for the ring expansion of ion [**4**+H]$^+$ via the 6-methylbicyclo[3.1.0]hex-2-en-4-yl cation, **ad**, to the *ipso*-toluenium ion, *i*-[**1**+H]$^+$, was calculated to be 160 kJ/mol only (Mormann, Salpin, & Kuck, 2006). In the case of the parent $C_6H_7^+$ ions, the corresponding barrier was also calculated (179 kJ/mol) (Bouchoux, Yáñez, & Mó, 1999).

A $C_7H_9^+$ isomer that had been overlooked in all the efforts undertaken over several decades was suggested some years ago by Duncan et al. (Mosley, Young, & Duncan, 2015), who detected the 1,3-dimethylcyclopentadienyl cation **aa** in the mixture with other $C_7H_9^+$ isomers by infrared spectroscopy (see below and Fig. 10). Calculations placed the heat of formation of this isomer at 121 kJ/mol above the level of the *para*-toluenium ion, *p*-[**1**+H]$^+$, that is, considerably above that of the 3-nortricyclyl cation, [**3'**+H]$^+$. A mechanistic access to ions **aa** was suggested to involve elimination of dihydrogen from norbornyl cations, $C_7H_{11}^+$, but remains rather obscure (Mosley, Young, & Duncan, 2015). An independent and more direct access to ion **aa** from a well defined precursor was not pursued. However, energetically accessible skeletal rearrangement channels leading from the *ipso*-tautomer *i*-[**15**+H]$^+$ by ring contraction via stereoisomeric dimethylbicyclo[3.1.0]hexenyl intermediates, that is, higher analogs of ion **ad**, to the 1,3-cyclopentadienyl framework of ion **aa** were calculated for the case of the xylenium ions (Arstad, Kolboe, & Swang, 2004).

Notwithstanding these insights, a more critical view on the energy profile of the $C_7H_9^+$ ions with regard to the results of the gas-phase titration of protonated toluene, **1**, cycloheptatriene, **2**, 2,5-norbornadiene, **3**, and 6-methylfulvene, **4**, should also been given here. Figure 10 compiles some of these multifaceted aspects. The transition state ([u] in Fig. 10) for the ring expansion of ions *i*-[**1**+H]$^+$ to ions 1-[**2**+H]$^+$ was calculated to be significantly but not much lower than the level of the elimination of CH_4 ($\Delta E \approx -37 \pm 14$ kJ/mol). As mentioned above, this is in agreement with the composite C-scrambling observed by experiment. The subsequent steps connecting ion 1-[**2**+H]$^+$ with its isomers, protonated norcaradiene, [**28**+H]$^+$, and the 1,4-dihydrotropylium ion, 3-[**2**+H]$^+$, have lower barriers, [t] and [s]. On the other hand, ion 1-[**2**+H]$^+$ may undergo ring opening to the hepta-1,3-5-trien-7-yl cations, **w**, across the barrier [f_4] that lies close to the fragmentation level of CH_4 elimination ($\Delta E \approx -5$ kJ/mol). The conceivable subsequent ring closure to the vinylcyclopentenyl cation **x** via an unknown transition state (marked by [$?_1$] in Fig. 10) has not been calculated but the barrier may be relatively low. Alternatively, ion 1-[**2**+H]$^+$ may rearrange directly to the latter doubly ring-contracted isomer **x** via an unknown barrier (marked [$?_2$]). Two further isomerization steps by 1,4-H and 1,2-H shifts, both of hitherto unknown height (marked [$?_3$] and [$?_4$]), may eventually lead to the most stable form of the 6-methylfulvenium ion, the C^1-protonated form, 1-[**4**+H]$^+$, which has been calculated to be only $\Delta E \approx +3$ kJ/mol less stable than the *ipso*-toluenium ion, *i*-[**1**+H]$^+$. Whereas this sequence connects the protonated cycloheptatriene species with those of protonated 6-methylfulvene, another sequence enables the direct conversion of the toluenium ions to the protonated fulvenes. The first step, namely ring contraction of ion *i*-[**1**+H]$^+$ to the *syn*-6-methylbicyclo[3.1.0]hexenyl cation **ad** via the barrier [v], was calculated to require relatively little energy and thus lies far below the level CH_4 elimination ($\Delta E \approx -42$ kJ/mol). Isomerization by such ring contraction occurring in competition to ring expansion was suggested to be a key to the isomerization of xylenium ions, such as [**15**+H]$^+$, prior to the elimination of ethene (Arstad, Kolboe, & Swang, 2004). The methylbicyclo-[3.1.0]hexenyl cation, **ad**, may easily rearrange by cleavage of the strained three-membered ring and subsequent 1,2-H shift to the 6-methylfulvenium ion 1-[**4**+H]$^+$. Again, this conceivable path has never been studied in detail and the barriers involved (marked [$?_5$] and [$?_4$]) are unknown, but it closely resembles the isomerization scenario calculated for the xylenium ions (Arstad, Kolboe, & Swang, 2004). It is also interesting to note that the above-mentioned 1,3-dimethylcyclopentadienyl cation **aa**, the previously overlooked $C_7H_9^+$ isomer, may also be accessible from ions [**1**+H]$^+$ via the 6-methylbicyclo[3.1.0]hex-2-en-4-yl cation **ad**. Although this path has not been studied so far, the corresponding transition state [x] can be estimated to lie considerably lower than the exit level to CH_4 elimination ($\Delta E \approx -61$ kJ/mol), when compared to the calculated isomerization scenario of the xylenium ions (Arstad, Kolboe, & Swang, 2004). Finally, the connection of the so-far-discussed isomerization of the $C_7H_9^+$ ions to the third isomer studied by gas-phase titration, protonated norbornadiene, [**3**+H]$^+$, deserves attention. As mentioned above, there is no doubt that ions [**3**+H]$^+$ exist preferably as a resonance hybride with a high contribution of the 3-nortricyclyl structure, [**3'**+H]$^+$, and that it represents the least stable of all the $C_7H_9^+$ isomers discussed here. To the best of our knowledge, only two mechanisms concerning conversions of ions [**3**+H]$^+$ ≡ [**3'**+H]$^+$ have been studied by computational approach. The isomerization barrier [r] (Fig. 10) between the 3-nortricyclyl cations, [**3'**+H]$^+$, and the bicyclo[4.1.0]hept-2-en-4-yl cations, [**28**+H]$^+$, and thus to the isomer sub-family of the dihydrotropylium, [**2**+H]$^+$, and toluenium ions, [**1**+H]$^+$, was calculated to lie slightly above the exit to CH_4 loss ($\Delta E \approx +16$ kJ/mol). The other mechanistic bridge connects ion [**3'**+H]$^+$ to the vinylcyclopentenyl cation **x**, and thus to the 6-methylfulvenium ions, [**4**+H]$^+$, via a barrier [f_5] that was calculated to lie considerably above the energy required for elimination of CH_4 ($\Delta E \approx +38$ kJ/mol) (Schröder et al., 2006). Another conceivable isomerization path connects the *meta*-toluenium ion, *m*-[**1**+H]$^+$, with the relatively stable 2-methylbicyclo[3.1.0]hex-2-en-4-yl cation **ab** via an unknown barrier (marked [$?_6$] in Fig. 10). It may also be added that the energy levels calculated for the elimination of H_2 and CH_4 from ion *i*-[**1**+H]$^+$ agree quite well. This holds also true for the calculated barrier [n] towards the former channel, which lies significantly below the level of CH_4 loss ($\Delta E \approx -51$ kJ/mol). The large reverse activation energy barrier of the H_2 elimination provides almost the whole amount of the high kinetic energy release ($T_{\text{kin}} = 96$ kJ/mol)—the observation of which, as a key feature fertilized the whole field of gaseous $C_7H_9^+$ ions back in 1974 (Williams & Hvistendahl, 1974b; Kuck, Schneider, & Grützmacher, 1985). Also in this special context, it is worth noting that the corresponding barrier [o] towards the elimination of H_2 from the 1,2-dihydrotropylium ion, 1-[**2**+H]$^+$, proposed in the early days, was calculated to exceed the barrier [n] towards the H_2 elimination from the *ipso*-toluenium ion, *i*-[**1**+H]$^+$, by far ($\Delta E \approx +132$ kJ/mol) (Schröder et al., 2006; Mormann & Kuck, 2003).

Finally, it should be noted that the energy profile displayed in Figure 10 relies to strictly unimolecular processes. It clearly ignores the additional mechanistic channels and internal energies that may become available in the ion-molecule complexes formed during the deprotonation reactions formed upon gas-phase titration. Clear indications for the importance of such ion-molecule complexes for intra-complex isomerization processes where reported for the (comparably simple) 1,2-methyl shifts occurring during gas-phase titration of xylenium ions, [**15**+H]$^+$ (Büker et al., 1997). In even more general terms, we should also keep in mind at this point that the method of generation of the $C_7H_9^+$ ions, be it by EI-induced fragmentation, CI-mediated protonation or ion-molecule reactions, as well as the varying ion lifetimes have certainly a significant effect on their reactivity. This appears to be of particular relevance in view of the very complex energy profile discussed above. Thus, while often precise values are available from the various studies, the different energy contents of the given $C_{7+n}H_{9+2n}^+$ ions may complicate comparisons. Nevertheless, it appears striking to note the recurring similarity of such features as

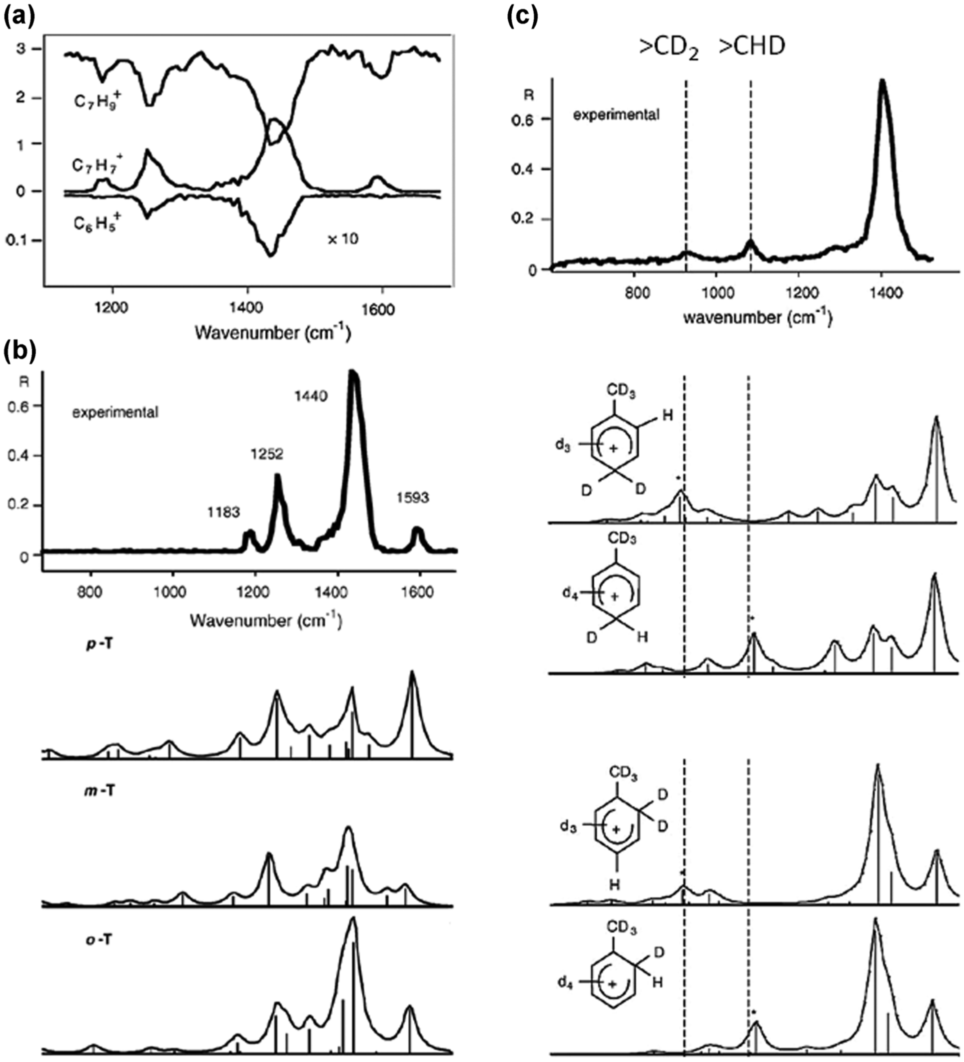

FIGURE 11. IRMPD spectra of toluenium ions generated by CI(CH_4) of toluene and [D_8]-toluene: (a) Decrease of ions $C_7H_9^+$ (*m/z* 93) in favor of the fragment ions $C_7H_7^+$ (*m/z* 91, loss of H_2) and $C_6H_5^+$ (*m/z* 77, loss of CH_4, magnified); (b) Comparison of the experimental IR spectrum with those calculated for the *para*-, *meta*- and *ortho*-tautomers of [**1**+H]$^+$ (spectrum for *ipso*-tautomer not shown here); (c) Comparison of the experimental IR spectrum of ions $C_7HD_8^+$ with those calculated for two selected isotopomers of the *para*- and *ortho*-tautomer, each of which bear either a CD_2- or CHD group (Dopfer et al., 2006). Reproduced (a), (c) or adapted (b) from ref. Dopfer et al. (2006) with permission of Elsevier (b), (c).

branching ratios and the extent of hydrogen and carbon scrambling of methylbenzenium ions and their cyclo-olefinic isomers.

IX. INFRARED SPECTROSCOPY OF GASEOUS TOLUENIUM IONS AND SOME ISOMERS

In the past two decades, the introduction of infrared spectroscopy for the identification and characterization of gaseous ions has increasingly contributed to our present knowledge on the gas-phase chemistry of $C_7H_9^+$ ions, although most efforts have been limited to the toluenium ions. With regard to the latter, "arenium-type" isomers, the focus was mostly put on the structure and interconversion of the benzenium and, in part, of the toluenium ion tautomers, including electronically excited states (Solcà & Dopfer, 2002; Jones et al., 2003; Solcà & Dopfer, 2003; Dopfer, 2006; Douberly et al., 2008; Rode et al., 2009; Esteves-López et al., 2015). The σ-complex structure of gaseous protonated benzene, that is, the prototypical arenium ion, *cyclo*-$C_6H_7^+$, was proven directly by spectroscopy and, thus, confirmed an impressive series of in-depth studies by computational methods (Sieber, Schleyer, & Gauss, 1993; Glukhovtsev et al., 1995; del Río, López, & Sordo, 1997; Jack & Levy, 1999; Maksić, Kovačević, & Lesar, 2000; Sumathy & Kryachko, 2002; Ascenzi et al., 2003). As a further detail, the origin of the regioselective stabilizing effect of the methyl group in the four toluenium tautomers, [**1**+H]$^+$, was suggested (Jack & Levy., 1999). Notwithstanding the existing knowledge, it was claimed in the early IR spectroscopic publications that "only indirect and often inconclusive structural information" (Solcà & Dopfer, 2002) had been provided by mass spectrometric methods. In any case, the wealth of insights elaborated by fragmentation studies, in combination with chemical synthesis and theoretical approaches, has undoubtedly been complemented by the applying IR spectroscopy to gas-phase ion structural analysis. Moreover, such spectroscopic methodology has contributed many additional, independent insights into the gas-phase chemistry of protonated arenes in general and to the long-debated case of the gaseous benzenium ion (Mason, Fernandez, & Jennings, 1987; Kuck, 1990a, 2000; Schröder et al., 2004; Schröder et al., 2006).

The first infrared spectroscopic study of gaseous toluenium ions, [**1**+H]$^+$, by Fornarini and her associates appeared in 2006 (Dopfer et al., 2006). In fact, in a sense this work can be considered a complement to Olah's study using NMR spectroscopy in solution and Reed's solid-state structural analysis obtained by X-ray diffraction (Fig. 1) (Olah et al., 1972; Reed et al., 2003). The IRMPD mass spectrum of gaseous toluenium ions is shown in Figure 11. It was obtained by tracing the fragmentation of mass-selected and thermally relaxed $C_7H_9^+$ ions generated by protonation of toluene in the cell of an FT-ICR mass spectrometer. As shown in Figure 11a, irradiation in the fingerprint region gave rise to both the elimination of H_2 and of CH_4 in wavelength-dependent ratios (~10–25) which, nevertheless, is reminiscent of the fragmentation of metastable toluenium ions studies in a sector-field mass spectrometer (Fig. 2) (Kuck, Schneider, & Grützmacher, 1985). Similar observations were obtained in the IRMPD study by Schröder, Roithová and their associates, also published in 2006 almost simultaneously with the first paper (Schröder et al., 2006). The experimental IRMPD spectrum exhibits a characteristic absorption band at 1252 cm^{-1} which matches with the strong absorption calculated for the CH_2 scissor modes of all three tautomers *p*-[**1**+H]$^+$, *m*-[**1**+H]$^+$ and *o*-[**1**+H]$^+$. This band is absent in the calculated spectrum of ion *i*-[**1**+H]$^+$ (not shown in Fig. 11), in line with the absence of a CH_2 group. The relatively weak absorption at 1593 cm^{-1} in the experimental spectrum, assigned to the C–C stretching mode of the pentadienyl subunits, is representative for all of the four tautomers. Moreover, the most intense absorption in the experimental spectrum appearing at 1440 cm^{-1} was calculated to be strongest in the case of the *ortho*-tautomer, *o*-[**1**+H]$^+$. Overall, and nevertheless, the experimental spectrum compared "well with calculated IR absorption spectra for the *ortho*-, *meta*-, and *para*-toluenium isomers, suggesting a mixture rich in the *ortho*/*para* isomers" (Dopfer et al., 2006). In fact, Figure 11b does reflect this mixture but obviously does not provide unequivocal information about prevailing tautomers, with the exception that the *ipso*-tautomer, *i*-[**1**+H]$^+$, which is known to be least stable, should be absent. On the other hand, IRMPD spectroscopy of the $C_7HD_8^+$ ions formed by protonation of [D$_8$]-toluene was more instructive. As shown in Figure 11c, weak but significant absorption bands were found at 1083 cm^{-1} and 928 cm^{-1} and clearly reflect the scissor modes of CHD and CD_2 groups, respectively. Whereas the former absorption was expected for protonation at any ring site of the [D$_8$]-toluenium or, more specifically, CD_3-$C_6HD_5^+$ ions, the appearance of the weak band at 928 cm^{-1} can be taken as an independent—and actually the first—spectroscopic proof for the ubiquitous proton ring walk in the benzenium unit of ions [**1**+H]$^+$ (Dopfer et al., 2006). In fact, the fast and undoubtedly complete scrambling known to involve all the six *ring*-hydrons in any alkylbenzenium ion (Kuck, 1990a, 2002, 2005a), including ions [**1**+H]$^+$, can be considered the origin of the tautomer-unspecific experimental IRMPD spectrum reported (Fig. 11b). This conclusion is also

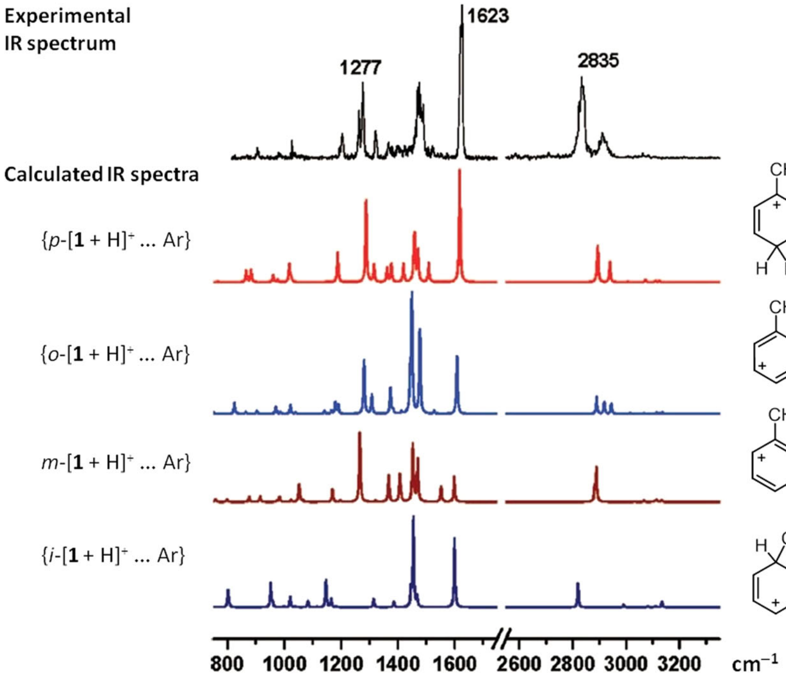

FIGURE 12. IRPD action spectrum of toluenium ions tagged with a weakly bound argon atom, {[**1**+H]$^+$ ··· Ar}, generated by electric discharge of mixture of H_2, Ar, and traces of toluene after supersonic expansion and comparison with the calculated spectra for the Ar-tagged *para*-, *meta*- and *ortho*-tautomers of [**1**+H]$^+$ (Douberly et al., 2008). Adapted with permission from *The Journal of Physical Chemistry A* 2008;112:4869–4874. Copyright 2020 American Chemical Society.

corroborated by the onset of the elimination of H_2, HD and D_2 at ~1300 cm^{-1} in the IRMPD spectrum of $C_7H_6D_3^+$ ions generated by CI(H_2O) of [α,α,α-D_3]-toluene and of the considerable broadening of the absorption bands when more excited $C_7H_9^+$ ions were generated from (unlabeled) toluene under more exothermic conditions, namely by CI(H_2O) instead of CI(*i*-C_4H_{10}) (Schröder et al., 2006).

Two years later, Duncan and his associates reported an alternative approach, employing single-photon IR photodissociation spectroscopy (IRPD) of gaseous benzenium and toluenium ions tagged with a weekly bound argon atom (Douberly et al., 2008). The $C_7H_9^+$ ions were generated in a pulsed-electric-discharge supersonic-expansion ion source yielding cold adducts {[**1**+H]$^+$···Ar} (*m/z* 133) at temperatures below 100 K. The low binding energy to the noble gas atom (200 cm^{-1} = 2.4 kJ/mol) does not perturb the IR-active vibrational modes of the organic cation in the fingerprint region but allows a very facile detachment of the noble gas atom upon single-IR-photon excitation achieved by use of tunable laser. The negligibly small effect of the Ar-tagging was demonstrated for the case of the benzenium ions and this holds also true for the fingerprint region of the toluenium ions (Douberly et al., 2008). The IRPD spectrum of argon-tagged $C_7H_9^+$ ions generated from toluene is depicted in Figure 12 together with the spectra calculated for the four tautomeric adduct ions {[**1**+H]$^+$···Ar}. Based on the increased spectral resolution of these measurements, all experimentally observed IRPD bands were assigned to individual vibrational modes for the *para*-toluenium ion, *p*-[**1**+H]$^+$, and good spectroscopic agreement was achieved. For example, the intense absorption band at 1623 cm^{-1} was attributed to the asymmetric C–C–C stretching motions of the endocyclic pentadienyl unit and interpreted as a general characteristic feature of alkylbenzenium ions (Douberly et al., 2008). This resonance was even related to one of the unidentified infrared bands (UIBs) in interstellar clouds at 1613 cm^{-1} (6.2 μm) (Le Page et al., 1997; Snow et al., 1998; Hudgins et al., 2001; Beegle, Wdowiak, & Harrison, 2001). The absorption band at 1277 cm^{-1} was attributed to the scissor motion of the CH_2 group of the benzenium core and the complex band at

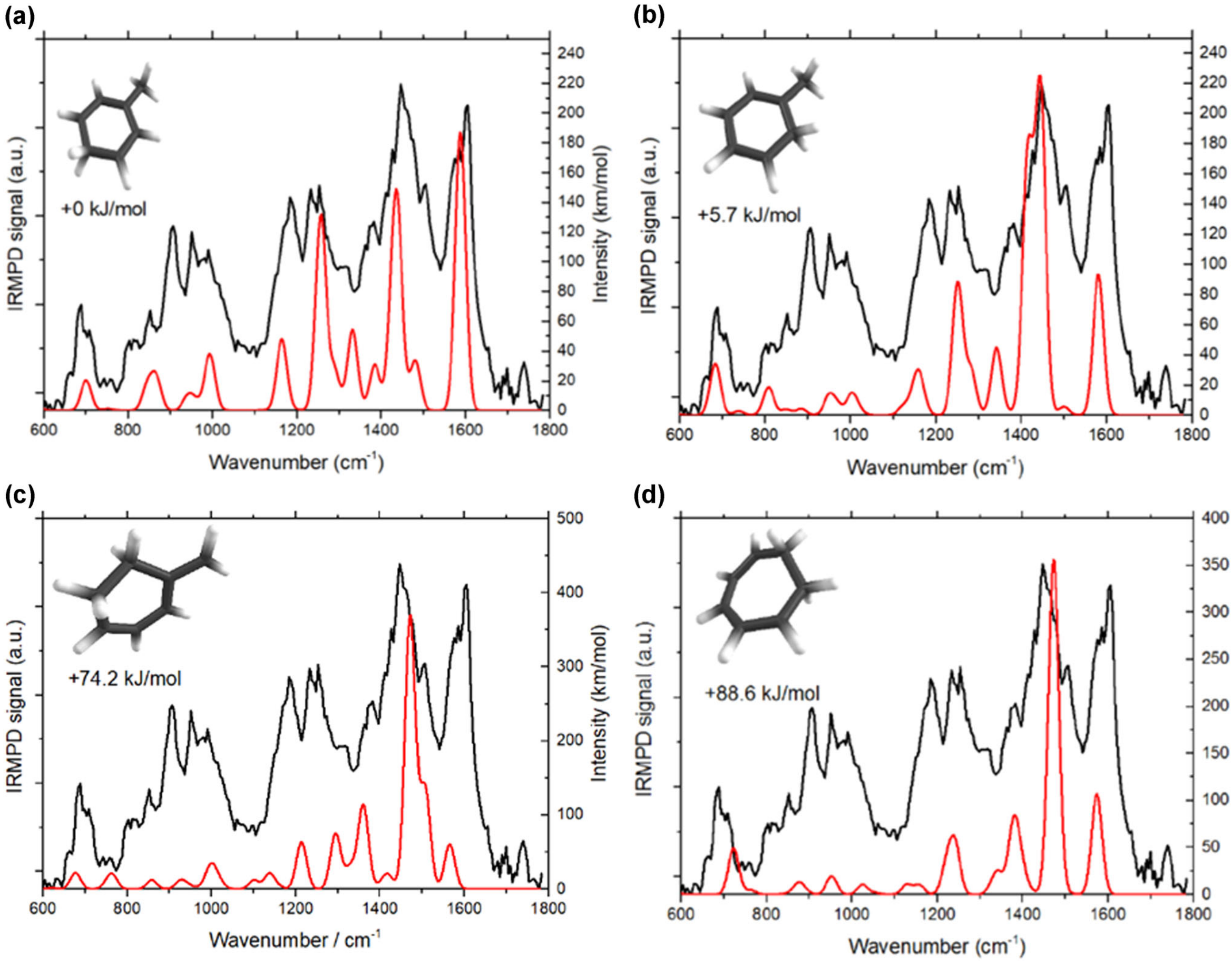

FIGURE 13. IRMPD spectrum of $C_7H_9^+$ ions generated by EI-induced fragmentation of adamantane (black) compared to the calculated IR spectra (red) of the toluenium ions (a) *p*-[**1**+H]$^+$ and (b) *o*-[**1**+H]$^+$, of (c) C^1-protonated 5-methylenecyclohexa-1,3-diene, [**27**+H]$^+$, the most stable isotoluenium ion, and of (d) the 1,2-dihydrotropylium ion 1-[**2**+H]$^+$; reproduced from ref. Bouwman, Horst, & Oomens (2018).

$2835\,cm^{-1}$ was assigned to its asymmetric and symmetric CH_2 stretching modes. Based on the excellent agreement between the experimental and the calculated spectra, this work clearly demonstrates that "vast majority" of gaseous toluenium ions at the low temperatures achieved in these experiments exist in the *para*-tautomeric form, *p*-[**1**+H]$^+$, or, strictly speaking, {*p*-[**1**+H]$^+$···Ar}. However, the presence of small concentrations of the *ortho*-tautomer, *o*-[**1**+H]$^+$, cannot be excluded completely due to the fact that several resonances of the *ortho*-isomer were calculated to be very close of those of the *para*-tautomer. Needless to mention that, neither in the IRMPD nor in the IRPD studies addressed here, any hints were found for $C_7H_9^+$ isomers other than those of the toluenium ion family.

It is obvious from many results discussed in the previous sections that only an access to the tautomeric toluenium ions, [**1**+H]$^+$, at higher energy levels can provide a chance to observe dihydrotropylium ions, [**2**+H]$^+$, and other constitutional isomers. In fact, Schröder, Roithová et al. reported the IRMPD spectrum of $C_7H_9^+$ ions generated by CI(H_2O) of cycloheptatriene, **2** (Schröder et al., 2006). In spite of its low resolution, this spectrum suggested the presence of ions [**2**+H]$^+$, due to a characteristic albeit heavily overlapping absorption band at $1470\,cm^{-1}$, in a mixture containing mostly the toluenium ions *p*-[**1**+H]$^+$ and *o*-[**1**+H]$^+$. This facet not only represented the first spectroscopic detection of gaseous dihydrotropylium ions, [**2**+H]$^+$, but also nicely illuminates the facile ring contraction of these seven-membered-ring isomers that had been deduced previously from a wealth of independent experimental work, as discussed in the above sections.

A very recent spectroscopic work IRMPD work yielded another insight into more than the toluenium branch of the extended family of gaseous $C_7H_9^+$ ions. Again, the access to the ions of interest was quite energetic. As an extension of their study on the dissociative ionization of adamantane, which generates $C_7H_9^+$ ions as one of the prevailing fragment ions (Candian et al., 2018), Bouwman et al. assigned some structures of these and related $C_{6+n}H_{7+2n}^+$ ions by comparing their IRMPD spectra to the IR spectra calculated for an extended set of potential constitutional isomers in the range of $600–1800\,cm^{-1}$ (Bouwman, Horst, & Oomens, 2018). As a side note with regard to previous work discussed in the preceding sections, it is rewarding that the experimental spectrum of the lowest analog, $C_6H_7^+$ ($n = 0$), was compared not only to the calculated IR spectrum of the benzenium ions but also to those of both 1- and 2-protonated fulvene and of the methylcyclopentadienyl cation, that is, the isomers that had been studied computationally by Bouchoux and his associates in 1999 (Bouchoux, Yáñez, & Mó, 1999). The recent IRMPD study allowed the authors to restrict the population of $C_6H_7^+$ ions formed by EI from adamantane to the benzenium structure and to largely exclude even the moderately (by ~40 kJ/mol) less stable 1-fulvenium ion (Bouchoux, Yáñez, & Mó, 1999; Bouwman, Horst, & Oomens, 2018). The IRMPD spectrum of the $C_7H_9^+$ ions produced from adamantane was compared to a larger set of calculated IR spectra than in the previous studies. Selected comparisons are illustrated in Figure 13. Besides the four toluenium ion tautomers, four protonated isotoluenes, derived from 5-methylene-1,3-cyclohexadiene (*ortho*-isotoluene, **27**) and 3-methylene-1,4-cyclohexadiene (*para*-isotoluene), as well as a bicyclic isomer, were calculated. The most stable of these "isotoluenium ions" is certainly C^1-protonated *ortho*-isotoluene, [**27**+H]$^+$, calculated to be 75 kJ/mol above the $C_7H_9^+$ stabilomer, *p*-[**1**+H]$^+$ (Fig. 10) (Schröder et al., 2006; Bouwman, Horst, & Oomens, 2018). Reasonably, none of the IR spectra calculated for the isotoluenium ions matches with the experimental spectrum. Among the isomeric dihydrotropylium ions considered, the IR spectrum of the 1,2-isomer, 1-[**2**+H]$^+$, gave a slightly better match than that of the isotoluenium ion [**27**+H]$^+$ mentioned above—in spite of its somewhat lower calculated stability (Fig. 13c and d). However, it was concluded that, here again, the experimental IRMPD spectrum of the $C_7H_9^+$ ions can be best explained with the presence of a mixture of the two most stable toluenium ions, *p*-[**1**+H]$^+$ and *o*-[**1**+H]$^+$ (Fig. 13a and b) but assuming possible contributions of ion 1-[**2**+H]$^+$. Notably, this isomer was calculated to be formed via the lowest barrier upon fragmentation of the adamantane precursor (Candian et al., 2018; Bouwman, Horst, & Oomens, 2018). Unfortunately, neither the bicyclic form of C^2-protonated cycloheptatriene, the bicyclo[4.1.0]hept-2-en-3-yl cation, [**28**+H]$^+$ (Fig. 11), calculated to be relatively energetically close to the 1,2-dihydrotropylium ion, 1-[**2**+H]$^+$, nor the methyl-substituted fulvenium ions, such as ion 1-[**4**+H]$^+$, were considered as candidates (Bouwman, Horst, & Oomens, 2018). Nevertheless, it appears that the $C_7H_9^+$ fragment ion mixture generated from adamantane by EI-induced fragmentation may contain a minor fraction of dihydrotropylium ions.

This conclusion agrees with insights obtained from the analysis of $C_7H_9^+$ ion mixtures generated independently by other EI-induced fragmentation routes. In particular, it has been known since the early days of organic mass spectrometry that the EI mass spectra of monoterpenes exhibit intense (and mostly even the base) peaks at *m/z* 93, reflecting the $C_7H_9^+$ ions (Reed, 1963; Budzikiewicz, Djerassi, & Williams, 1964; Beynon, Saunders, & Williams, 1968). Later, the nature of the $C_7H_9^+$ ions generated from large sets of monoterpenes was addressed by applying collision-induced dissociation (CID), kinetic-energy release measurements and charge-stripping mass spectrometry (Schwarz, Borchers, & Levsen, 1976; Basic & Harrison, 1991). In fact, these studies did not allow clear-cut differentiation between the possible $C_7H_9^+$ isomers. Nevertheless, as a most remarkable result, the charge stripping experiments pointed to the presence of dihydrotropylium ions, [**2**+H]$^+$, rather than toluenium ions, [**1**+H]$^+$, in the mixture of $C_7H_9^+$ ions (Basic & Harrison, 1991). Much in contrast, the gas-phase titration study discussed above provided more detailed insight (Mormann, Salpin, & Kuck, 2006). Increasingly exothermic deprotonation of the $C_7H_9^+$ ions generated by EI-induced fragmentation of α-pinene and of the two enantiomeric limonenes, using the same set of four differently strong bases mentioned above, revealed that the mixture of long-lived $C_7H_9^+$ ions consists far dominantly (≥85%) of toluenium ions, [**1**+H]$^+$. However, a small fraction (≤10%) of dihydrotropylium ions, [**2**+H]$^+$, probably admixed with the least acidic 6-methylfulvenium ions, was detected as well (Mormann, Salpin, & Kuck, 2006). It appears to be fruitful and rewarding to have such a multitude of independent methods at hand, at least potentially nowadays and hopefully still in the future.

X. METHYLBENZENIUM IONS IN METHANOL-TO-HYDROCARBON (MTH) REACTIONS

It has become evident from the very beginning of this review that studies on protonated toluene and various isomeric

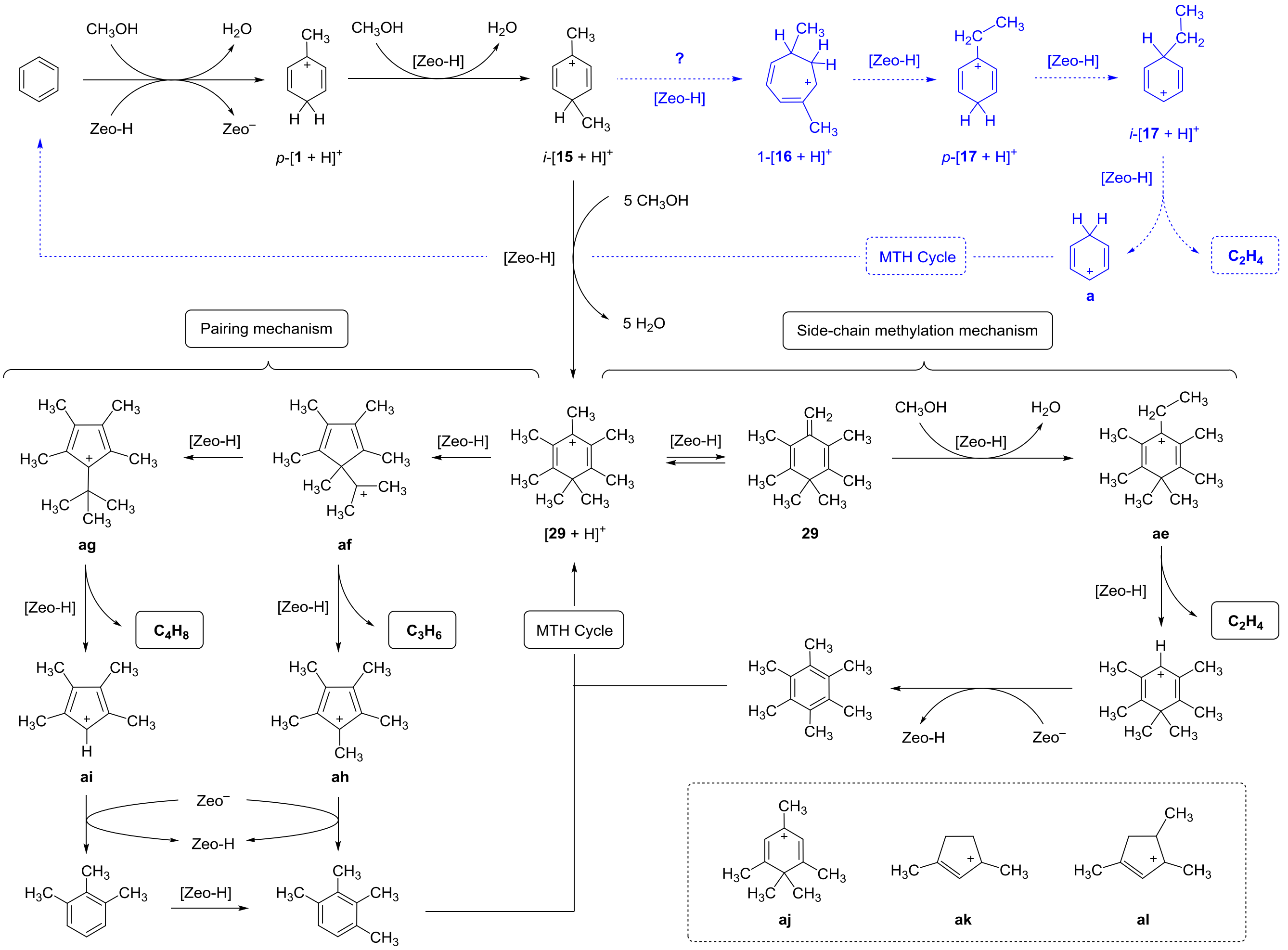

SCHEME 14. Selected mechanistic pathways of the methanol-to-hydrocarbon (MTH) reactions. Multiple methylation steps of arenes (mostly benzene and methylbenzenes) present in the zeolite hydrocarbon pool generate, besides lower analogs, such as ions **aj**, the heptamethylbenzenium ion, [**29**+H]$^+$. This ion is a key intermediate in both the side-chain methylation mechanism, that involves the neutral *para*-isotoluene derivative **29** and yields ethene via ion **ae**, and the pairing mechanism, yielding higher olefins (e.g., propene and isobutene). Another conceivable MTH cycle shows the connection of xylenium ions, such as *i*-[**15**+H]$^+$, with ring-expanded isomers, such as ion 1-[**16**+H]$^+$, and subsequent generation of ethene, involving the ethylbenzenium ions, such as *p*-[**17**+H]$^+$, is added and highlighted in blue.

$C_7H_9^+$ ions as well as their analogs have covered all states of matter and that their structures and reactions are central to fundamental organic chemistry. There is even an overlap to the chemistry of natural compounds through the early appearance of m/z 93 peaks indicating analytically diagnostic $C_7H_9^+$ ions in conventional EI mass spectrometry. In this last section, it will be shown that toluenium ions and their isomers, as well as the corresponding $C_{7+n}H_{9+2n}^+$ analogs, play a crucial role in technical chemistry. Amusingly, this completes a parabolic journey—with $C_7H_9^+$ ions in its focus—from Georg Hvistendahl's work in the 1970's in Dudley Williams' laboratory in Cambrigde, UK (Williams & Hvistendahl, 1974a, 1974b; Hvistendahl & Williams, 1975) to a collaboration between Stein Kolboe and Einar Uggerud and their associates at the University of Oslo with the author's group in Bielefeld one generation later (Svelle et al., 2006a; Sekiguchi et al., 2009).

The conversion of methanol to hydrocarbons (MTH reaction) is known for more than forty years now since its discovery (Meisel et al., 1976; Chang and Silvestri, 1977). Many reviews on this industrially highly important process have appeared (Chang, 1983, 1984; Haw, 2002; Haw et al., 2003; Olsbye et al., 2005; McCann et al., 2008; Olsbye et al., 2012; Wang, Xu, & Deng, 2020). They all reflect the broad and, in the same time, in-depth fundamental research on the complex mechanistic course by which several C_1 building blocks grow into various valuable hydrocarbon products with concomitant elimination of water, mainly according to the gross reaction n $CH_3OH \rightarrow (CH_2)_n + n$ H_2O. Although a discussion of this topic would be far beyond the scope of this review, it appears worth highlighting the role of toluenium ions and other methylbenzenium ions as key reactive intermediates in the MTH processes in view of our present knowledge of their established gas-phase chemistry. A very limited mechanistic rationalization of the proposed MTH processes is depicted in Scheme 14, in combination with a speculative extension based on the ring-expansion mechanism deduced from the studies on gaseous toluenium and xylenium ions.

The key mechanistic insight of the MTH reaction is based on the fact that aromatic species, such as benzene and methylbenzenes, are formed from the original C_1 feed (e. g., methanol) within the acidic cavities of the zeolites during an incubation period. The so-called hydrocarbon pool (Dahl & Kolboe, 1994a, 1994b) present in the cavities reacts as a cocatalyst to the given zeolite (Haw et al., 2003). Once a benzenium ion is generated and bound to an anionic site of the zeolite framework, methylation of the benzene nucleus starts and leads to a mixture of various oligomethylbenzenium ions, up to the heptamethylbenzenium ion [**29**+H]$^+$. This ionic key species and a lower analog, the 1,3,5,6,6-pentamethylcyclohexadienyl cation **aj**, as well as several dimethyl- and trialkylsubstituted cyclopentenyl cations, such as ions **ak** and **al** (see box in Scheme 14), were detected in the solid state by magic angle spinning NMR spectroscopy (Xu et al., 1998; Song et al., 2002; Wang et al., 2014, 2015a, 2015b; Xiao et al., 2017). The spectroscopic observation of five-membered cyclo-olefins corroborated the course of skeletal isomerization by ring contraction, and the reversibility of this step, giving rise to the MTH cycle and leading back to benzenium intermediates, was discovered by extensive ^{13}C and deuterium labeling experiments (Mole, Bett, & Seddon, 1983; Bjørgen et al., 2004, 2007)—a technique reminiscent of the experimental strategies used in gas-phase ion chemistry. It was suggested that the mechanistic route leading to ethene is separated from those that produce the higher olefins (Svelle et al., 2006b). More recently, lower degrees of methylation on the benzenium ring was associated with the generation of ethene, while higher degrees of methylation were attributed to the generation of propene and higher olefins (Scheme 14) (Wang et al., 2015a).

From all this, it is clear that understanding of the complex mechanisms that govern the MTH reaction is still growing. While two major reaction mechanisms based on the heptamethylbenzenium ion [**33**+H]$^+$ and other highly methylated analogs that bear a geminal dimethyl grouping, namely the "pairing mechanism" and the "side-chain methylation mechanism" (Scheme 14), are accepted in the literature, lower analogs, such as the xylenium ions, are still under debate as intermediates on the way to ethene production. Also, current mechanistic models invoke ring-contraction pathways involving methyl-substituted bicyclo[3.1.0]hex-2-en-4-yl ions, i. e., analogs of such as **ab** and **ad** (Scheme 13) and the cyclopentenyl cations **ak** and **al** as intermediates (Haw et al., 2003; Wang, Xu, & Deng, 2020). On this basis, a complete catalytic cycle including the energy profile and rate constants was developed by combining theory with experiment (McCann et al., 2008). Ring contraction of ions [**29**+H]$^+$ leads to ion **af** and alkyl-substituted cyclopentadienyl ions, such as ions **ag–ai**, as other important intermediates of the paring mechanism suggested for the MTH process. Notably, ring-expanded intermediates, such as dihydrotropylium ions, [**2**+H]$^+$, were never observed in the experiments. However, in view of the potential relevance to the MHT chemistry, theoretical work was invested to understand the gas-phase isomerization and fragmentation of xylenium and ethylbenzenium ions, $C_8H_{11}{}^+$ (Arstad, Kolboe, & Swang, 2004; Sekiguchi et al., 2009; Kolboe, Svelle, & Arstad, 2009).

The close formal relation of various mechanistic steps of the MTH reactions to the reaction paths of $C_8H_{11}{}^+$ ions in the highly diluted gas phase of a mass spectrometer initiated two collaborative projects based on mass spectrometric investigations. In the first one, the fragmentation of long-lived methyl-substituted benzenium ions, $C_{6+n}H_{7+2n}{}^+$ ($n = 0–7$), was studied (Svelle et al., 2006a). The ions were generated either by protonation of the corresponding hydrocarbon in the CI(CH_4) plasma or by methylation employing chloromethane as a reactant gas [CI(CH_3Cl)]. Both the spontaneous and the CID were studied

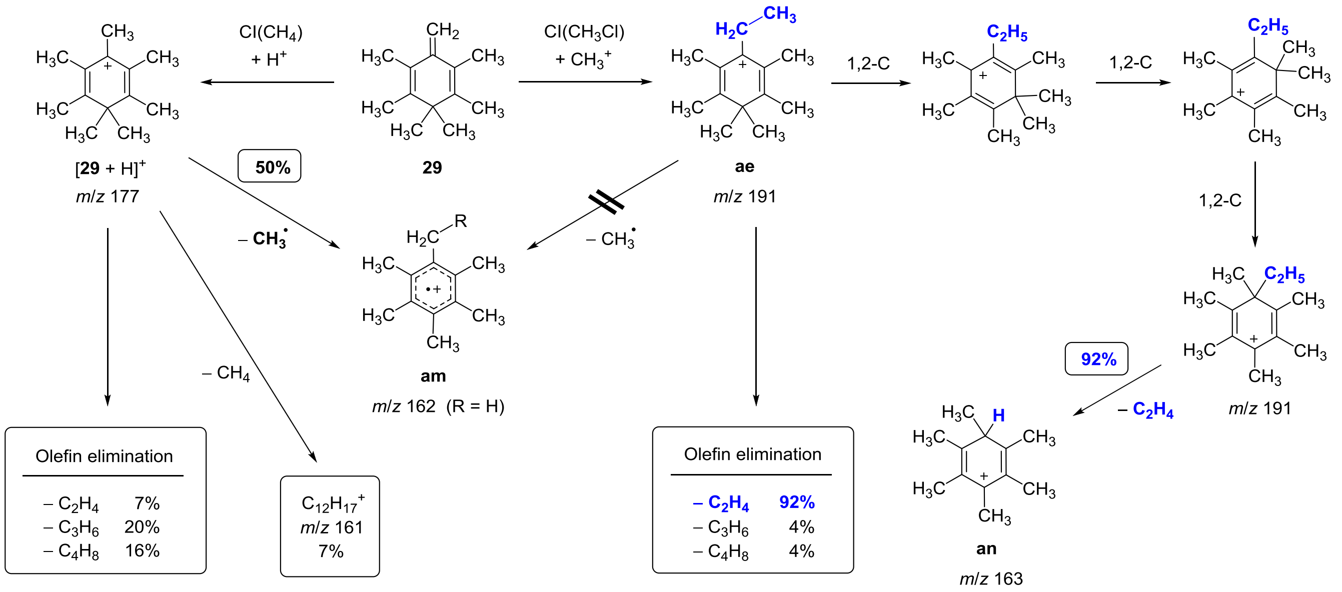

SCHEME 15. Comparison of the mass spectrometric fragmentation routes of the heptamethylbenzenium ion [**29**+H]$^+$ (*m/z* 177) and the ethyl(hexamethyl)benzenium ion **ae** (*m/z* 191) generated by exocyclic protonation and methylation, respectively, of the hexamethyl-*para*-isotoluene **29**. Note that loss of $CH_3^•$ occurs exclusively in the former case and that elimination of C_2H_4 dominates in the latter (Svelle et al., 2006a).

by MIKE and CID-MIKE spectrometry, respectively. As shown in Scheme 15, protonation of the 3-methylenecyclohexa-1,4-diene **29**, a hexamethyl-*para*-isotoluene, generated the heptamethylbenzenium ion, [**29**+H]$^+$, $C_{13}H_{21}{}^+$ ($n = 7$). Under CI(CH_3Cl) conditions, even a homolog, the 3-ethyl-1,2,4,5,6,6-hexamethylbenzenium ion, **ae**, $C_{14}H_{23}{}^+$ ($n = 8$), was generated by methylation of the exocyclic methylene group of isotoluene **29**—in strict analogy to the key mechanism of the side-chain methylation mechanism of the MHT reaction.

Some clear trends were found in the series of long-lived, metastable methyl-substituted benzenium ions. The expulsion of dihydrogen decreases in favor of the elimination of methane with increasing methyl substitution. In the same time, homolytic C–C bond cleavage giving rise to the loss of a methyl radical to produce the corresponding radical cations strongly increases. As shown in Scheme 15, this process is the dominating fragmentation channel in the case of the heptamethylbenzenium ion, [**29**+H]$^+$ (m/z 177), giving ion **am** (R = H, m/z 162, 50%). This homolytic dissociation process is attributed to the particularly low ionization energy of hexamethylbenzene (Svelle et al., 2006a). Ion [**29**+H]$^+$ also undergoes elimination of olefins in minor abundance, with propene prevailing (20%). Minor loss of methane (7%) is surprising because of the absence of mobile ring hydrogen atoms. Similar to the elimination of olefins, loss of CH_4 may point to deep-seated rearrangements of the heptamethylbenzenium ion; hwoever, it may also be assumed that the [**29**+H–CH_4]$^+$ ion is simply the pentamethylbenzylium ion, $(CH_3)_5C_6$–$CH_2{}^+$. More interestingly, the ethyl(hexamethyl) benzenium ion **ae** generated by exocyclic methylation, loses neither $CH_3{}^•$ nor CH_4 but almost exclusively C_2H_4 to give the hexamethylbenzenium ion **an** (m/z 163)—in analogy to the side-chain methylation mechanisms suggested for the production of C_2H_4 in the MTH processes. It appears likely that the olefin is lost after repeated methyl ring walk by energetically facile 1,2-C shifts, as mentioned above.

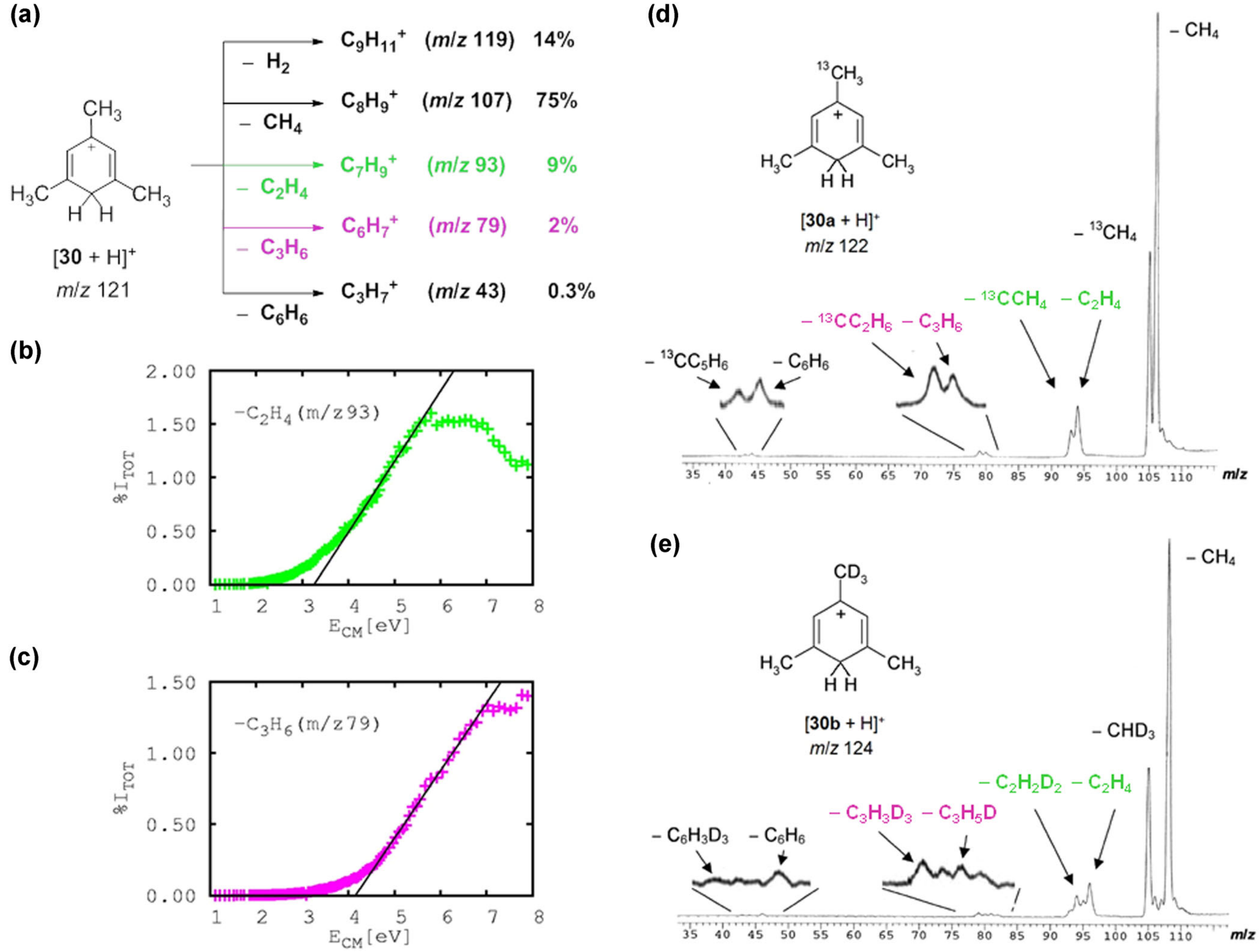

FIGURE 14. Fragmentation of metastable mesitylenium ions, [**30**+H]$^+$, and two isotopologs, with the two MTH-relevant reactions being highlighted. (a) Branching ratios of the five fragmentation channels for metastable ions. (b) and (c) Fractions of the total ion signal due to the loss of C_2H_4 and C_3H_6, respectively, as a function of the center-of-mass collisional energy. (d) and (e) MIKE spectra of the ^{13}C-labeled isotopolog [**30a**+H]$^+$and the [α,α,α-D_3]-labeled isotopolog [**30b**+H]$^+$, both reflecting the relatively low degree of C- and H-scrambling prior to the elimination of methane and ethene (Sekiguchi et al., 2009). Adapted from ref. Sekiguchi et al., (2009) with permission of SAGE Publishing.

Another mass spectrometric investigation that was also inspired by the obvious parallels between gas-phase chemistry of gaseous methylbenzenium ions and the MTH reactions focused on the energetics of the fragmentation of toluenium, xylenium, and mesitylenium ions, as well as on the scrambling reactions of the latter ions (Sekiguchi et al., 2009). In contrast to the indirect experimental and the vast amount of computational data available in the literature, almost no directly acquired experimental data on the energetics of the fragmentation of methylbenzenium ions is known. From early appearance energy measurements, the difference between the barriers towards H_2 and CH_4 elimination from toluenium ions, $[\mathbf{1}+H]^+$, was found to be 37 ± 10 kJ/mol (Kuck, Schneider, & Grützmacher, 1985), which is close to the values obtained by later calculations (51 ± 10 kJ/mol, see Fig. 10). In the latest work, Sekiguchi, Uggerud et al. determined the energy requirements for the major fragmentation reactions of toluenium, *ortho*- and *meta*-xylenium and ethylbenzenium ions by variable-collision-energy mass spectrometry (Sekiguchi et al., 2009). A hybrid instrument equipped with a quadrupole/hexapole/time-of-flight sequence was used. Mass-selected ions (*m/z* 93, *m/z* 107, and *m/z* 121, respectively) with varying kinetic energy of $E_{\mathrm{lab}} = 0.2$–20 eV were subjected to CID. The onsets for the elimination of H_2 and CH_4 from toluenium ions, $[\mathbf{1}+H]^+$, were estimated to be at $E_{\mathrm{CM}} = 1.8$ eV = 174 kJ/mol and 2.2 eV = 212 kJ/mol, respectively. While these thresholds appear to be somewhat too low as compared to the available experimental and theoretical potential energy surface (Fig. 10), the difference (0.4 eV = 39 kJ/mol) agrees well with the early appearance energy measurements (Kuck, Schneider, & Grützmacher, 1985). Furthermore, it was inferred from the quite different slopes of the energy dependences that the transitions states of the formal 1,2-elimination of H_2 from ions $[\mathbf{1}+H]^+$ is much tighter than that for the 1,1-elimination of CH_4. Overall, the variable-collision-energy measurements with toluenium ions were found to be both in line with theory and also our early experimental results. Thus, the computational finding that the barrier towards reversible ring expansion of ions *i*-$[\mathbf{1}+H]^+$ to ions $[\mathbf{2}+H]^+$ is only 40–50 kJ/mol below the exit to CH_4 loss (Fig. 10) was invoked as a rationalization for the composite scrambling behavior deduced for toluenium ions from the early labeling study (Kuck, Schneider, & Grützmacher, 1985; Sekiguchi et al., 2009). Similar variable-energy measurements with *ortho*- and *meta*-xylenium ions gave energy thresholds of $E_{\mathrm{CM}} = 1.9$ eV = 183 kJ/mol and 2.6 eV = 251 kJ/mol, respectively, for the losses of H_2 and CH_4. Thus, the two barriers towards fragmentation slightly increase with increasing methyl substitution of the benzenium core, as does the energy difference between them (0.5 eV = 48 kJ/mol). This parallels the clearly attenuated scrambling behavior of long-lived *para*-xylenium ions, $[\mathbf{15}+H]^+$, as compared to toluenium ions, $[\mathbf{1}+H]^+$, as shown above. Variable-energy CID measurements of ethylbenzenium ions, $[\mathbf{17}+H]^+$, yielded the particularly low threshold of only $E_{\mathrm{CM}} = 1.1$ eV = 106 kJ/mol for the characteristic elimination of C_2H_4. This finding is in clear accordance with the fact that the conversion of xylenium (and methyldihydrotropylium) ions to ethylbenzenium ions is irreversible, as deduced from the labeling studies with various $C_8H_{11}{}^+$ ions discussed above.

Finally, the fragmentation of the highest analog, the mesitylenium ion, $[\mathbf{30}+H]^+$ ($C_9H_{13}{}^+$, *m/z* 121) should be presented (Sekiguchi et al., 2009). These ions are interesting since they are at half-way to the high-methyl benzenium ions discussed above in view of the mechanisms of the MTH reaction. Long-lived, metastable ions $[\mathbf{30}+H]^+$ were found to eliminate H_2, CH_4, C_2H_4 and C_3H_6 in the ratio of 14.2:74.8:9.4:1.6. Even C_6H_6 (undoubtedly as benzene) is formed in minute but characteristic relative amounts (Fig. 14a). Thus, olefins are generated in significant abundances and necessarily after repeated skeletal isomerization to ethyltoluenium and even *n*-propylbenzenium ions, $[\mathbf{23}+H]^+$ and $[\mathbf{22}+H]^+$, respectively. The thresholds for these fragmentation reactions were determined to be $E_{\mathrm{CM}} = 2.2$ eV = 212 kJ/mol (H_2 loss), $E_{\mathrm{CM}} = 2.7$ eV = 261 kJ/mol (CH_4 loss), $E_{\mathrm{CM}} = 2.3$ eV = 222 kJ/mol (C_2H_4 loss), and $E_{\mathrm{CM}} = 3.0$ eV = 290 kJ/mol (C_3H_6 loss). The barriers towards H_2 and CH_4 loss are again higher than those of the lower congeners. However, it is worth noting that the energy requirements for the MTH-relevant elimination reactions producing C_2H_4 and C_3H_6 have been determined experimentally for the first time here (Fig. 14b and c). A labeling study of mesitylenium ions $[\mathbf{30a}+H]^+$ and $[\mathbf{30b}+H]^+$ bearing either one $^{13}CH_3$- or one CD_3-group, respectively, clearly reflects the relatively low degree of skeletal and hydrogen scrambling prior to methane loss. Even the elimination of ethene is rather specific and the propene loss is dominated by the contribution of the $C_3H_3D_3$ isotopomer (Fig. 14d and e). All this shows that the isomerization by repeated skeletal rearrangements in gaseous protonated trimethylbenzenes is a relatively slow process but occurs with a high degree of irreversibility (Sekiguchi et al., 2009).

Overall, the experimental study of the energetics of the fragmentation of long-lived toluenium, xylenium, and mesitylenium ions agrees well with the overall energy profile and mechanistic scenario. Both the isomerization behavior preceding the fragmentation of gaseous mesitylenium ions, $[\mathbf{30}+H]^+$, as that of even more highly methylated benzenium ions resembles that of such species present in the hydrocarbon pool of the MTH reaction occurring in the cavities of zeolites. It is also clear that carbon and hydrogen scrambling is a characteristic feature of methylbenzenium ions both in the gas phase and in the solid-state zeolite catalysts. On the other hand, it remains unclear whether the production of ethene and higher olefins in the course of MTH reactions takes place by reversible ring contraction to five-membered species, by ring expansion processes or even in competition of both isomerization processes. To the best of our knowledge, the studies on the MTH reactions have never included the fate of cycloheptatriene, **2**, methylfulvenes such as **4**, or other cyclo-olefinic isomers and analogs upon protonation in the zeolites at high temperatures. Whereas the reasons for this fact are obvious, feeding MTH reactors with such compounds should be informative, as is feeding mass spectrometers with suitably designed precursors has been so often in the past decades.

XI. CONCLUSIONS

Protonated methylbenzenes, such as toluenium and xylenium ions, represent apparently simple and prototypical intermediates in a central field of organic chemistry. Their structures in the solid and liquid phase are well understood. The chemistry of gaseous toluenium ions and their higher analogs has also been well rationalized in depth by various mass spectrometric techniques, and complemented by infrared photodissociation spectroscopy of mass-selected ions. However, this concerns mainly the thermochemistry as well as regioselective protonation/deprotonation and hydrogen equilibration by proton (or hydride) ring-walk occurring at low excitation energies. At higher internal energies that allow fragmentation in the gas phase, toluenium ions undergo various reversible ring expansion and ring contraction processes that generate dihydrotropylium and methylfulvenium isomers, respectively. Even protonated norbornadiene, as 3-nortricyclicyl cations, may be formed under such conditions. A multitude of other isomeric, mostly cyclo-olefinic structures interfere and the complex isomerization scenario gives rise to composite carbon and hydrogen scrambling prior to fragmentation. Labeling experiments comprising not only isotopologous toluenium and other methylbenzenium ions but also isomeric carbenium ions generated from labeled cyclo-olefinic precursors clearly revealed the complex interplay between protonated methylbenzenes and isomeric protonated cycloheptatrienes, norbornadienes and methylfulvenes. Owing to the combination of a multitude of experimental methods, including deprotonation ("gas-phase titration") and regioselective protonation, radiolysis experiments, bimolecular covalent adduct formation, flowing afterglow techniques, infrared spectroscopy of the gaseous ions, and various theoretical approaches, a rather complex picture has emerged over the past four decades. As a particular facet of the chemistry of toluenium, higher methylbenzenium and the isomeric cyclo-olefinic carbenium ions, it has become evident that, while the arenium-type isomers represent the stabilomers of the large family of isomers, their structural conversion to the cyclo-olefinic isomers has been recognized as the key step in the MTH process. Thus, understanding a considerable part, but by far not the whole of the complex chemistry of gaseous methylbenzenium ions has been an exciting challenge of research with relevance in fundamental, analytical and industrial organic chemistry. Maybe future research will bring even more detailed insights and understanding into this field, where mass spectrometry has played a central und fruitful role over many decades already.

ACKNOWLEDGMENTS

I remember with joy many fruitful and encouraging discussions with various colleagues and friends in the field: Hans-Friedrich Grützmacher (Bielefeld), Wilhelm J. Richter (Basel) see (Kuck et al., 1989), Charles H. DePuy (Boulder), Veronica Bierbaum (Boulder) and, last not least, Einar Uggerud (Oslo). In particular, I would like to express my gratitude and memory to several intense, inspiring and encouraging discussions with Chuck DePuy on the chemistry of gaseous toluenium ions, starting in 1990 on a symposium in Rome and continued over many years (see (Kuck, 1992) and (Wang et al., 2018)). Early encounters with Georg Hvistendahl (Oslo) and Dudley Williams (Cambridge, UK) are also recalled with great joy. The invaluable work by Dr Michael Mormann (now at Münster) and Dr Jean-Yves Salpin (now at Évry), see (Kuck et al., 2001), based on their great competence and enthusiasm, as well as of a few more students and coworkers at Bielefeld University, whose names appear in the references, has enabled many contributions to the topic of this review. To all of them go my respect and gratefulness.

REFERENCES

Angelini G, Sparapani C, Speranza M. 1984. Reactions of phenylium ions with gaseous hydrocarbons. 1. Methane, ethane, and propane. Tetrahedron 40:4865–4871.

Arstad B, Kolboe S, Swang O. 2004. Theoretical study of protonated xylenes: Ethene elimination and H,C-scrambling reactions. J Phys Org Chem 17:1023–1032.

Ascenzi D, Bassi D, Franceschi P, Tosi P, Di Stefano M, Rosi M, Sgamellotti A. 2003. Reactions of phenylium ions with D_2. J Chem Phys 119:8366–8372.

Ausloos P. 1982. Structure and isomerization of $C_7H_7^+$ ions formed in the charge-transfer-induced fragmentation of ethylbenzene, toluene, and norbornadiene. J Am Chem Soc 106:5259–5265.

Basic C, Harrison AG. 1991. A mass-spectral study of some $C_{10}H_{16}$ monoterpenes. Can J Appl Spectrosc 2:33–40.

Beauchamp JL. 1975. Reaction mechnisms of organic and inorganic ions in the gas phase. In: P Ausloos, editor, Interaction between ions and molecules., pp. 413–444. New York: Plenum Press.

Beegle LW, Wdowiak TJ, Harrison JG. 2001. Hydrogenation of polycyclic aromatic hydrocarbons as a factor affecting the cosmic 6.2 micron emission band. Spectrochim Acta, Part A 57:737–744.

Benezra SA, Hoffman MK, Bursey MM. 1970. Electrophilic aromatic substitution reactions. An ion cyclotron resonance study. J Am Chem Soc 92:7501–7502.

Berthomieu D, Audier HE, Denhez JP, Monteiro C, Mourgues P. 1991. [C_6H_6, $C_3H_7^+$] and [$C_6H_7^+$, C_3H_6] ion-neutral complexes intermediate in the reactions of protonated propylbenzenes. Org Mass Spectrom 26:271–275.

Beynon JH, Saunders RA, Williams AE. 1968. The mass spectra of organic molecules, New York: Elsevier.

Bierbaum VM. 2015. Go with the flow: Fifty years of innovation and ion chemistry using the flowing afterglow. Int J Mass Spectrom 377:456–466.

Bjørgen M, Olsbye U, Petersen D, Kolboe S. 2004. The methanol-to-hydrocarbons reaction: Insight into the reaction mechanism from [^{12}C] benzene and [^{13}C]methanol coreactions over zeolite H-beta. J Catal 221:1–10.

Bjørgen M, Svelle S, Joensen F, Nerlov J, Kolboe S, Bonino F, Palumbo L, Bordiga S, Olsbye U. 2007. Conversion of methanol to hydrocarbons over zeolite H-ZSM-5: On the origin of the olefinic species. J Catal 249:195–207.

Bouchoux G, Nguyen MT, Salpin JY. 2000. Condensation reactions between 1,3-butadiene radical cation and acetylene in the gas phase. J Phys Chem A 104:5778–5786.

Bouchoux G, Yáñez M, Mó O. 1999. Isomerization and dissociation processes of protonated benzene and protonated fulvene in the gas phase. Int J Mass Spectrom 185/186/187:241–251.

Bouwman J, Horst S, Oomens J. 2018. Spectroscopic characterization of the product ions formed by electron ionization of adamantane. Chem Phys Chem 19:3211–3218.

Brookhart M, Anet FAL, Winstein S. 1966. The behavior of the 3-phenyl-2-butanols in SO_2-FSO_3H-SbF_5. J Am Chem Soc 88:5657–5659.

Brouwer DM. 1968. Kinetics of rearrangements of methylbenzenium ions in HF. Recl Trav Chim Pay-Bas 87:611–622.

Budzikiewicz H, Djerassi C, Williams DH. 1964. Structure elucidation of natural products by mass spectrometry, part II, San Francisco: Holden-Day.

Bursey JT, Bursey MM, Kingston DGI. 1973. Intramolecular hydrogen transfer in mass spectra. I. Rearrangements in aliphatic hydrocarbons and aromatic compounds. Chem Rev 73:191–234.

Büker HH, Grützmacher HF, Crestoni ME, Ricci A. 1997. Proton induced methyl group shifts in gaseous xylenium ions. Distinguishing isomers by gas-phase titration. Int J Mass Spectrom Ion Process 160:167–181.

Cacace F. 1982. On the formation of adduct ions in gas-phase aromatic substitution. J Chem Soc Perkin Trans 2:1129–1132.

Cacace F. 1988. The radiolytic approach to gas-phase ion chemistry. Acc Chem Res 21:215–222.

Cacace F, Crestoni ME, Fornarini S. 1992. Proton shifts in gaseous arenium ions and their role in the gas-phase aromatic substitution by free Me_3C^+ and Me_3Si^+ cations. J Am Chem Soc 114:6776–6784.

Cacace F, Giacomello P. 1978. Aromatic substitutions by $[^3H_3]$Methyl decay ions. A comparative study of gas- and liquid-phase attack on benzene and toluene. J Chem Soc Perkin Trans 2:652–658.

Candian A, Bouwman J, Hemberger P, Bodi A, Tielens AGGM. 2018. Dissociative ionisation of adamantane: A combined theoretical and experimental study. Phys Chem Chem Phys 20:5399–5406.

Chang CD. 1983. Hydrocarbons from methanol. Catal Rev Sci Eng 25:1–118.

Chang CD. 1984. Methanol conversion to light olefins. Catal Rev Sci Eng 26:323–345.

Chang CD, Silvestri AJ. 1977. Conversion of methanol and other o-compounds over zeolite catalysts. J Catal 47:249–259.

Chiavarino B, Crestoni ME, Di Rienzo B, Fornarini S, Lanucara F. 2008. Site-selectivity of protonation in gaseous toluene. Phys Chem Chem Phys 10:5507–5509.

Cooks RG, Beynon JH, Bertrand M, Hoffmann K. 1973. Ion structural studies by ion kinetic energy spectrometry: $[C_7H_7]^+$, $[C_7H_8]^{+\bullet}$, $[C_7H_7OCH_3]^{+\bullet}$. Org Mass Spectrom 7:1303–1312.

Dahl IM, Kolboe S. 1994a. On the reaction mechanism for propene formation in the MTO reaction over SAPO-34. Catal Lett 20:329–336.

Dahl IM, Kolboe S. 1994b. On the reaction mechanism for hydrocarbon formation from methanol over SAPO-34: I. Isotopic labeling studies of the co-reaction of ethene and methanol. J Catal 149:458–464.

DePuy CH, Gareyev R, Fornarini S. 1997. Generation and assay of $C_6H_xD_{(7-x)}{}^+$ (x = 1−6) benzenium ions: A flowing afterglow-selected ion flow tube study. Int J Mass Spectrom Ion Processes 161:41–45.

Devlin JL, III, Wolf JF, Taft RW, Hehre WJ. 1976. The proton affinities of toluene. J Am Chem Soc 98:1990–1992.

Dewar MJS. 1946. The kinetics of some benzidine rearrangements, and a note on the mechanism of aromatic substitution. J Chem Soc 777–781.

Dewar MJS, Dieter KM. 1986. Evaluation of AMI calculated proton affinities and deprotonation enthalpies. J Am Chem Soc 108:8075–8086.

Doering WvE, Saunders M, Boynton HG, Earhart JW, Wadley EF, Edwards WR, Laber G. 1958. The 1,1,2,3,4,5,6-Heptamethylbenzenonium Ion. Tetrahedron 4:178–185.

Dopfer O. 2006. IR spectroscopic strategies for the structural characterization of isolated and microsolvated arenium ions. J Phys Org Chem 19:540–551.

Dopfer O, Lemaire J, Maître P, Chiavarino B, Crestoni ME, Fornarini S. 2006. IR spectroscopy of protonated toluene: Probing ring hydrogen shifts in gaseous arenium ions. Int J Mass Spectrom 249–250:149–154.

Douberly GE, Ricks AM, Schleyer PvR, Duncan MA. 2008. Infrared spectroscopy of gas phase benzenium *ions*: Protonated benzene and protonated toluene, from 750 to 3400 cm^{-1}. J Phys Chem A 112:4869–4874.

Dunbar RC. 1975. Nature of the ions from toluene parent ion photodissociation. J Am Chem Soc 97:1382–1384.

Esteves-López N, Dedonder-Lardeux C, Jouvet C. 2015. Excited state of protonated benzene and toluene. J Chem Phys 143:074303.

Fornarini S, Crestoni ME. 1998. Gaseous arenium ions at atmospheric pressure: Elementary reactions and internal solvation effects. Acc Chem Res 31:827–834.

Friedman L, Wolf AP. 1958. Electron impact dissociation of camphene-8-C^{13}. J Am Chem Soc 80:2424–2426.

Fărcaşiu D. 1982. Protonation of simple aromatics in superacids. A reexamination. Acc Chem Res 15:46–51.

Fărcaşiu D, Melchior MT, Craine L. 1977. *Ortho-para* protonation of toluene and ethylbenzene in super acids. Angew Chem Int Ed 16:315–316.

Glukhovtsev MN, Pross A, Nicolaides A, Radom L. 1995. Is the most stable gas-phase isomer of the benzenium cation a face-protonated π-complex? J Chem Soc Chem Commun 22:2347–2348.

Grubb HM, Meyerson S. 1963. Mass spectra of alkylbenzenes. In McLafferty FW editor., Mass spectrometry of organic ions. New York: Academic Press, Chap. 10, pp. 453–527.

Gäumann T, Zhao G, Zhu Z. 1994. Photofragmentation in Fourier-transform ion cyclotron resonance: Use or misuse? Rapid Commun Mass Spectrom 8:1–9.

Harrison AG, Haynes P, McLean S, Meyer F. 1965. The mass spectra of methyl-substituted cyclopentadienes. J Am Chem Soc 87:5099–5105.

Haw JF. 2002. Zeolite acid strength and reaction mechanisms in catalysis. Phys Chem Chem Phys 4:5431–5441.

Haw JF, Song W, Marcus DM, Nicholas JB. 2003. The mechanism of methanol to hydrocarbon catalysis. Acc Chem Res 36:317–326.

Heidrich D. 2002. Do isopropyl and *tert*-butyl cations form π-complexes with benzene? Angew Chem Int Ed 41:3208–3210.

Heidrich D, Grimmer M, Sommer B. 1976. Quantenchemische Untersuchungen zum Mechanismus der Elektrophilen Substitution—III. Zur Stabilität und Struktur von $[H,CH_3]$-σ-Komplexen (*Ipso*-Addukten) protonierter Methylbenzole. Tetrahedron 32:2027–2032.

Herman JA, Harrison AG. 1981. Effect of protonation exothermicity on the chemical ionization mass spectra of some alkylbenzenes. Org. Mass Spectrom 26:423–427.

Herman JA, Herman K, McMahon TB. 1991. Formation of $C_6H_7{}^+$ ions in ion-molecule reactions in vinyl chloride. Can J Chem 69:2038–2043.

Houriet R, Schwitzguebel T, Carrupt PA, Vogel P. 1986. Experimental and theoretical studies on the homoconjugation in bicyclic carbenium and oxonium ions in the gas phase. Tetrahedron Lett 27:37–40.

Howe I, McLafferty FW. 1971. Metastable ion characteristics. XVII. Unimolecular decomposition of toluene and cycloheptatriene molecular ions. Variation of the degree of scrambling and isotope effect with internal energy. J Am Chem Soc 93:99–105.

Hudgins DM, Bauschlicher CW, Jr, Allamandola LJ. 2001. Closed-shell polycyclic aromatic hydrocarbon cations: A new category of interstellar polycyclic aromatic hydrocarbons. Spectrochim Acta, Part A 57:907–930.

Hunter EP, Lias SG. 1998. Evaluated gas phase basicities and proton affinities of molecules: An update. J Phys Chem Ref Data 27:413–656.

Hvistendahl G, Williams DH. 1975. Partitioning of reverse activation energy between kinetic and internal energy in reactions of some simple organic ions. J Chem Soc Perkin Trans 2:881–885.

Ignatyev IS, Schaefer HF, III. 2004. Dihydrogen and methane elimination from adducts formed by the interaction of carbenium and silylium cations with nucleophiles. J Am Chem Soc 126:14515–14526.

Isaacs NS, Cvitas D. 1971. Molecular orbital calculations on organic molecules—II. CNDO solutions for polymethylbenzenes and benzenonium ions. Tetrahedron 27:4139–4151.

Ishikawa Y, Yilmaz H, Yanai T, Nakajima T, Hirao K. 2004. Direct ab initio molecular dynamics study of $CH_3{}^+$ plus benzene. Chem Phys Lett 396:16–20.

Jack B, Levy. A. 1999. Quantum chemical and electrostatic study of alkyl and substituted benzenonium cations and related molecules: The effect of atomic charge distribution on carbocation energy and geometry. Struct Chem 10:121–127.

Jarrett RM, Veniero JC, Bryne TP, Saunders M, Laidig KE. 1988. Kinetics of degenerate rearrangements in nortricyclyl cation. J Am Chem Soc 110:8287–8791.

Jones W, Boissel P, Chiavarino B, Crestoni ME, Fornarini S, Lemaire J, Maître P. 2003. Infrared fingerprint of protonated benzene in the gas phase. Angew Chem Int Ed 42:2057–2059.

Kolboe S, Svelle S, Arstad B. 2009. Theoretical study of ethylbenzenium ions: The mechanism for splitting off ethene, and the formation of a π complex of ethene and the benzenium ion. J Phys Chem A 113:917–923.

Kuck D. 1990a. Mass spectrometry of alkylbenzenes and related compounds—part II: Gas phase ion chemistry of protonated alkylbenzenes (alkylbenzenium ions). Mass Spectrom Rev 9:583–630.

Kuck D. 1990b. Mass spectrometry of alkylbenzenes and related compounds—part I: Gas phase ion chemistry of alkylbenzene radical cations. Mass Spectrom Rev 9:181–233.

Kuck D. 1992. Gaseous $[M - H]^+$ ions of α,ω-diphenylalkanes: Cyclization to $[M + H]^+$ type ions of benzocycloalkanes as recognized by chain-length dependent proton exchange. Int J Mass Spectrom. Ion Processes 117:441–455.

Kuck D. 2000. Thermochemical data of organic ions obtained from investigations in the more or less “diluted” gas phase. Angew Chem Int Ed 39:125–130.

Kuck D. 2002. Half a century of scrambling in organic ions: Complete, incomplete, progressive and composite atom interchange. Int J Mass Spectrom 213:101–144.

Kuck D. 2005a. H/D exchange in hydrocarbon ions. In: Nibbering NMM editor., Encyclopedia of Mass Spectrometry, Vol. 4, Topic B20. Amsterdam: Elsevier. pp 270–286.

Kuck D. 2005b. Protonated aromatics and arenium ions. In: Nibbering NMM editor., Encyclopedia of mass spectrometry, Vol. 4, Topic B16. Amsterdam: Elsevier. pp 229–242.

Kuck D. 2005c. Tropylium and related ions. In: Nibbering NMM editor., Encyclopedia of mass spectrometry, Vol. 4, Topic B12. Amsterdam: Elsevier. pp. 199–214.

Kuck D. 2007. Scrambling versus specific processes in gaseous organic ions during mass spectrometric fragmentation: Elucidation of mechanistic origins by isotope labeling—An overview. J Label Comp Radiopharm 50:360–365.

Kuck D. 2012. Concomitant hydride and proton transfer: An essay on competing and consecutive key reactions occurring in gaseous ion/neutral complexes. Eur J Mass Spectrom 18:161–181.

Kuck D. 2015. From fragmentation to construction—from void to massive: Fascination on organic mass spectrometry and the synthesis of novel three-dimensional polycyclic aromatic hydrocarbons. Chem Rec 15:1075–1109.

Kuck D, Bäther W. 1986. Inter- and intra-annular proton exchange in gaseous benzylbenzenium ions (protonated diphenylmethane). Org Mass Spectrom 21:451–457.

Kuck D, Bäther W, Grützmacher HF. 1979. Intramolecular ring-to-ring proton transfer in gaseous (ω-phenylalkyl)-benzenium ions. J Am Chem Soc 101:7154–7157.

Kuck D, Bäther W, Grützmacher HF. 1985. Interannular proton exchange in protonated long-chain 1,ω-diphenylalkanes. Int J Mass Spectrom Ion Processes 67:75–91.

Kuck D, Ingemann S, de Koning LJ, Grützmacher HF, Nibbering NMM. 1985. Proton exchange between arenium ions and arenes in the gas phase. Angew Chem Int Ed Engl 24:693–695.

Kuck D, Mormann M, Salpin JY, Nguyen MT. 2001. Skeletal rearrangements of protonated hydrocarbons: *Para*-xylenium-, 7-methyldihydrotropylium and 6,6-dimethylfulvenium ions. Adv Mass Spectrom 15:715–716.

Kuck D, Mormann M. 2000. Mass spectrometry and gas-phase ion chemistry of dienes and polyenes. In: Z Rappoport, editor, The chemistry of functional groups: The chemistry of dienes and polyenes, Vol. 2. New York: Wiley. Chapt. 1, pp 1–57.

Kuck D, Prior G, Grützmacher HF, Müller DR, Richter WJ. 1989. Protonated arenes in the gas phase: Xylenium and related $C_8H_{11}^+$ ions. Adv Mass Spectrom 11A:750–751.

Kuck D, Schneider J, Grützmacher HF. 1985. A study of gaseous benzenium and toluenium ions generated from 1,4-dihydro- and 1-methyl-1,4-dihydrobenzoic acids. J Chem Soc Perkin Trans 2:689–696.

Leung HW, Harrison AG. 1977. Hydrogen migrations in mass spectrometry IV—Formation of $[C_6H_7]^+$ in the chemical ionization mass spectra of alkylbenzenes? Org Mass Spectrom 12:582–586.

Leung HW, Ichikawa H, Li YH, Harrison AG. 1978. Concerning the mechanism of dehalogenation of halobenzene derivatives by gaseous brønsted acids. J Am Chem Soc 100:2479–2484.

Lias SG, Ausloos P. 1985. Structures of $C_6H_7^+$ ions formed in unimolecular and bimolecular reactions. J Chem Phys 82:3613–3624.

Lias SG, Bartmess JE, Liebman JF, Holmes JL, Levin RD, Mallard WG. 1988. Gas-phase ion and neutral thermochemistry. J Phys Chem Ref Data 17. Suppl. 1.

Lifshitz C. 1994. Tropylium ion formation from toluene: Solution of an old problem in organic mass spectrometry. Acc Chem Res 27:138–144.

Linstrom PJ, Mallard WG, editors. 2018. Linstrom PJ, Mallard WG, editors., NIST Chemistry WebBook. NIST Standard Reference Database Number 69, National Institute of Standards and Technology, Gaithersburg MD, 20899, https://doi.org/10.18434/T4D303

Maksić ZB, Eckert-Maksić M. 1998. Intrinsic proton affinity of substituted aromatics. In Parkanyi C editor., Theoretical organic chemistry. Theoretical and computational chemistry, Vol. 5. Chichester: Elsevier. pp 203–231.

Maksić ZB, Kovačević B, Lesar A. 2000. Protonation of archetypal aromatic and antiaromatic systems—G2 studies of benzene and cyclobutadiene. Chem Phys 253:59–71.

March J. 1992. Advanced organic chemistry—reactions, mechanisms, and structure. 4th Ed., p. 534. New York: John Wiley & Sons.

Mason RS, Fernandez MT, Jennings KR. 1987. Thermodynamics of some proton-transfer reactions—dynamic ion structures and the measurement of entropies of ‘internal translation’. J Chem Soc, Faraday Trans 2 83:89–109.

Mason RS, Williams CM, Anderson PDJ. 1995. The face-centred π complex isomer of the benzenium ion is probably the most stable form in the gas phase: Experimental evidence. J Chem Soc Chem Commun 1027–1028.

McCann DM, Lesthaeghe D, Kletnieks PW, Guenther DR, Hayman MJ, Van Speybroeck V, Waroquier M, Haw JF. 2008. A complete catalytic cycle for supramolecular methanol-to-olefins conversion by linking theory with experiment. Angew Chem Int Ed 47:5179–5182.

Meisel SL, McCullough JP, Lechthaler CH, Weisz PB. 1976. Gasoline from methanol in one step. ChemTech 6:86–89.

Meyer F, Harrison AG. 1965. Unimolecular fragmentation of the toluene molecule ion. J Chem Phys 43:1778–1782.

Mole T, Bett G, Seddon D. 1983. Conversion of methanol to hydrocarbons over ZSM-5 zeolite: An examination of the role of aromatic hydrocarbons using ^{13}carbon and deuterium-labeled feeds. J Catal 84:435–445.

Mormann M, Bashir S, Derrick PJ, Kuck D. 2000. Gas-phase basicities of the isomeric dihydroxybenzoic acids and gas-phase acidities of their radical cations. J Am Soc Mass Spectrom 11:544–552.

Mormann M, Decker B, Kuck D. 2007. Composite C- and H-scrambling and fragmentation of long-lived 6-methylfulvene and 6,6-dimethylfulvene—alternative entry to the gas-phase chemistry of gaseous toluenium ($C_7H_9^+$) and xylenium ($C_8H_{11}^+$) ions. Int J Mass Spectrom 267:148–158.

Mormann M, Kuck D. 1999. Protonated 1,3,5-cycloheptatriene and 7-alkyl-1,3,5-cycloheptatrienes in the gas phase: Ring contraction to the isomeric alkylbenzenium ions. J. Mass Spectrom 34:384–394.

Mormann M, Kuck D. 2001. Interconversion of gaseous bicyclo[3.2.1]oct-2-en-4-yl cations and protonated 7-alkylcycloheptatrienes: [5 + 2] cycloreversion in competition with fragmentation by way of alkylbenzenium ions. Int J Mass Spectrom 210/211:531–544.

Mormann M, Kuck D. 2002a. Loss of methane and ethene from long-lived gaseous xylenium ions (protonated xylene) after “composite” scrambling. Int J Mass Spectrom 219:497–514.

Mormann M, Kuck D. 2002b. Synthesis of 1-[^{13}C]-*para*-xylene and 2-[^{13}C]-*para*-xylene. J Label Comp Radiopharm 45:601–610.

Mormann M, Kuck D. 2003. Hydride abstraction from 1,3,5-cycloheptatriene by gaseous carbenium ions, as studied by Fourier transform ion cyclotron resonance kinetics and deuterium labeling. J Phys Org Chem 16:746–752.

Mormann M, Kuck D. 2007. The gas-phase basicity and proton affinity of 7-methyl-1,3,5-cycloheptatriene as determined by the thermokinetic method. J Mass Spectrom 42:263–265.

Mormann M, Salpin JY, Kuck D. 1999. The gas-phase basicities of 6-methylfulvene and 6,6-dimethylfulvene. Eur J Mass Spectrom 5: 441–447.

Mormann M, Salpin JY, Kuck D. 2006. Gas-phase titration of $C_7H_9^+$ on mixtures by FT-ICR mass spectrometry: Semiquantitative determination of ion populations generated by CI-induced protonation of C_7H_8 isomers and by EI-induced fragmentation of some monoterpenes. Int J Mass Spectrom 249–250:340–352.

Morrison JD, Stanney K, Tedder JM. 1981a. The reaction of CH_4^+, CH_3^+, and other simple carbocations with benzene in the gas phase. J Chem Soc Perkin Trans 2:838–841.

Morrison JD, Stanney K, Tedder JM. 1981b. The reactions of some common electrophiles, CH_3^+, NO^+, NO_2^+, and $O_2NCH_2^+$, with monosubstituted benzenes in the gas phase. J Chem Soc Perkin Trans 2:967–969.

Mosley JD, Young JW, Duncan MA. 2015. Infrared detection of the 1,3-dimethylcyclopentadienyl cation, an isomer of protonated toluene. Int J Mass Spectrom 378:322–327.

Moss RA, Fu X, Sauers RR, Wipf P. 2005. Endo entry to the nortricyclyl-norbornenyl cation system: Stereochemistry in the fragmentation of *endo*-5-norbornenyl-2-oxychlorocarbene. J Org Chem 70:8454–8460.

Moss RA, Ma Y, Sauers RR, Madni M. 2004. Nortricyclyl–norbornenyl cation system accessed by carbene fragmentation. J Org Chem 69:3628–3634.

Munson MSB, Field FH. 1966. Chemical ionization mass spectrometry. I. General introduction. J Am Chem Soc 88:2621–2630.

Munson MSB, Field FH. 1967. Chemical ionization mass spectrometry. IV. Aromatic hydrocarbons. J Am Chem Soc 89:1047–1052.

Nefedov VD, Sinotova EN, Akulov GP, Korsakov MV. 1970. Radiochemical study of free methyl-cation reactions with aromatic compounds. J Org Chem USSR 6:1220–1224.

Nelson NA, Fassnacht JH, Piper JU. 1961. Cycloheptatrienes from the solvolysis of 1,4-dihydrobenzyl p-toluenesulfonates. J Am Chem Soc 83:206–213.

Olah GA. 1965. Stable carbonium ions. 9. Methylbenzenonium hexafluoroantimonates. J Amer Chem Soc 87:1103–1108.

Olah GA. 1971. Aromatic substitution. XXVIII. Mechanism of electrophilic aromatic substitutions. Acc Chem Res 4:240–248.

Olah GA, Liang G. 1975. Stable carbocations. CLXXVI. 3-Nortricyclyl cations. Question of charge delocalization in rigid cyclopropylcarbinyl systems. J Am Chem Soc 97:1920–1927.

Olah GA, Schlosberg RH, Porter RD, Mo YK, Kelly DP, Mateescu GD. 1972. Stable carbocations. CXXIV. The benzenium ion and monoalkylbenzenium ions. J Am Chem Soc 94:2034–2043.

Olah GA, Staral JS, Asencio G, Liang G, Forsyth DA, Mateescu GD. 1978. Stable carbocations. 215. ^{13}C nuclear magnetic resonance spectroscopic study of the benzenium, naphthalenium, and anthracenium ions. J Am Chem Soc 100:6299–6308.

Olsbye U, Bjørgen M, Svelle S, Lillerud KP, Kolboe S. 2005. Mechanistic insight into the methanol-to-hydrocarbons reaction. Catalysis Today 106:108–111.

Olsbye U, Svelle S, Bjørgen M, Beato P, Janssens TVW, Joensen F, Bordiga S, Lillerud KP. 2012. Conversion of methanol to hydrocarbons: How zeolite cavity and pore size controls product selectivity. Angew Chem Int Ed 51:5810–5831.

Le Page V, Keheyan Y, Bierbaum VM, Snow TP. 1997. Chemical constraints on organic cations in the interstellar medium. J Am Chem Soc 119:8373–8374.

Reed CA, Kim KC, Stoyanov ES, Stasko D, Tham FS, Mueller LJ, Boyd PDW. 2003. Isolating benzenium ion salts. J Am Chem Soc 125:1796–1804.

Reed I. 1963. Mass spectra of terpenes. In: FW McLafferty, editor, Mass spectrometry of organic ions, pp. 637–699. New York: Academic Press. Chap. 10.

Reed RI 1963. Mass spectra of terpenes. In McLafferty FW editor., Mass spectrometry of organic ions. Academic Press: New York. Chapt. 13, pp 637–699.

Roberts JD, Bennett W, Armstrong R. 1950. Solvolytic reactivities of nortricyclyl, dehydronorbornyl and norbornyl halides. Possible steric requirements for hyperconjugative resonance. J Am Chem Soc 72:3329–3333.

Rode MF, Sobolewski AL, Dedonder C, Jouvet C, Dopfer O. 2009. Computational study on the photophysics of protonated benzene. J Phys Chem A 113:5865–5873.

del Río E, López R, Sordo TL. 1997. A theoretical study of the H_2 elimination from $C_6H_7^+$: An example of the role of back-donation in carbocation chemistry. J Phys Chem A 101:10090–10094.

Salpin JY, Mormann M, Tortajada J, Nguyen MT, Kuck D. 2003. The gas-phase basicity and proton affinity of 1,3,5-cycloheptatriene—energetics, structure and interconversion of dihydrotropylium ions. Eur J Mass Spectrom 9:361–376.

Saunders M, Jarrett RM, Pramanik P. 1987. Nortricyclyl-norbornenyl cation. Isotopic perturbation and isotopic scrambling. J Am Chem Soc. 109:3735–3739.

Schröder D, Loos J, Schwarz H, Thissen R, Dutuit O. 2004. Protonated benzene: A case for structural memory effects? J Phys Chem A 108:9931–9937.

Schröder D, Schwarz H, Milko P, Roithova J. 2006. Dissociation routes of protonated toluene probed by infrared spectroscopy in the gas phase. J Phys Chem A 110:8346–8353.

Schwarz H, Borchers F, Levsen K. 1976. Collisional activation mass spectrometry of monoterpenes and isomerisation of gaseous $C_7H_9^+$ ions. Z Naturforsch B 31:935–940.

Sekiguchi O, Meyer V, Letzel MC, Kuck D, Uggerud E. 2009. Energetics and reaction mechanisms for the competitive losses of H_2, CH_4 and C_2H_4 from protonated methylbenzenes—Implications to the methanol-to-hydrocarbons (MTH) process. Eur J Mass Spectrom 15:167–181.

Sieber S, Schleyer PvR, Gauss J. 1993. The accurate C_2, phenonium and benzenonium ion structures confirmed by correlated GIAO-MP2 NMR chemical shift calculations. J Am Chem Soc 115:6987–6988.

Snow T, Le Page V, Keheyan Y, Bierbaum VM. 1998. The interstellar chemistry of PAH cations. Nature 391:259–260.

Solcà N, Dopfer O. 2002. Protonated benzene: IR spectrum and structure of $C_6H_7^+$. Angew Chem Int Ed 41:3628–3631.

Solcà N, Dopfer O. 2003. Interaction of the benzenium ion with inert ligands: IR spectra of $C_6H_7^+–L_n$ cluster cations (L = Ar, N_2, CH_4, H_2O). Chem Eur J 9:3154–3163.

Song W, Nicholas JB, Sassi A, Haw JF. 2002. Synthesis of the heptamethylbenzenium cation in zeolite-β: In situ NMR and theory. Catal Lett 81:49–53.

Speranza M. 1992. Kinetics and mechanisms in gas-phase ion chemistry by radiolytic methods. Mass Spectrom Rev 11:73–117.

Speranza M, Sefcik MD, Henis JMS, Gaspar PP. 1977. Phenylium ($C_6H_5^+$) ion-molecule reactions studied by ion cyclotron resonance spectroscopy. J Am Chem Soc 99:5583–5589.

Sumathy R, Kryachko ES. 2002. Multiprotonation of benzene: A theoretical study. J Phys Chem A 106:510–519.

Svelle S, Bjørgen M, Kolboe S, Kuck D, Letzel M, Olsbye U, Sekiguchi O, Uggerud E. 2006a. Intermediates in the methanol-to-hydrocarbons (MTH) reaction: A gas phase study of the unimolecular reactivity of multiply methylated benzenium cations. Catal Lett 109:25–35.

Svelle S, Joensen F, Nerlov J, Olsbye U, Lillerud KP, Kolboe S, Bjørgen M. 2006b. Conversion of methanol into hydrocarbons over zeolite H-ZSM-5: Ethene formation is mechanistically separated from the formation of higher alkenes. J Am Chem Soc 128:14770–14771.

Taylor R. 1990. Electrophilic aromatic substitution. Chichester, UK: John Wiley & Sons Ltd.

Wang C, Chu Y, Zheng A, Xu J, Wang Q, Gao P, Qi G, Gong Y, Deng F. 2014. New Insight into the hydrocarbon-pool chemistry of the methanol-to-olefins conversion over zeolite H-ZSM-5 from GC-MS, solid-state NMR spectroscopy, and DFT calculations. Chem Eur J 20:12432–12443.

Wang C, Xu J, Deng F. 2020. The mechanism of methanol to hydrocarbon catalysis mechanism of methanol-to-hydrocarbon reaction over zeolites: A solid-state NMR perspective. Chem Cat Chem 12:1–17.

Wang C, Xu J, Qi G, Gong Y, Wang W, Gao P, Wang Q, Feng N, Liu X, Deng F. 2015a. Methylbenzene hydrocarbon pool in methanol-to-olefins conversion over zeolite H-ZSM-5. J Catal 332:127–137.

Wang C, Yi X, Xu J, Qi G, Gao P, Wang W, Chu Y, Wang Q, Feng N, Liu X, Zheng A, Deng F. 2015b. Experimental evidence on the formation of ethene through carbocations in methanol conversion over HZSM-5 zeolite. Chem Eur J 21:12061–12068.

Wang ZC, Thomsen DL, Motell EL, Robinson MS, Garrey R, Bierbaum VM, DePuy CH. 2018. The gas-phase methylation of benzene and toluene. Int J Mass Spectrom 429:6–13.

Watson JT, Sparkman OD. 2007. Introduction to mass spectrometry, applications and strategies for data interpretation. 4th Edn., pp. 355–363. Chichester: Wiley.

Williams DH, Hvistendahl G. 1974a. Kinetic energy release in relation to symmetry-forbidden reactions. J Am Chem Soc 96:6753–6755.

Williams DH, Hvistendahl G. 1974b. Kinetic energy release as a mechanistic probe. The role of orbital symmetry. J Am Chem Soc 96:6755–6757.

Winstein S, Walborsky HM, Schreiber K. 1950. Driving force of the homoallylic rearrangement in acetolysis of *exo*-dehydronorbornyl *p*-bromobenzenesulfonate. J Am Chem Soc 72:5795.

Woodward RB, Hoffmann R. 1969. The conservation of orbital symmetry. Angew Chem Int Ed Engl 8:781–853.

Xiao D, Han X, Bao X, Hou G, Blanc F. 2017. Direct structural identification of carbenium ions and investigation of host–guest interaction in the methanol to olefins reaction obtained by multinuclear NMR correlations. Chem Sci 8:8309–8314.

Xu T, Barich DH, Goguen PW, Song W, Wang Z, Nicholas JB, Haw JF. 1998. Synthesis of a benzenium ion in a zeolite with use of a catalytic flow reactor. J Am Chem Soc 120:4025–4026.

Zhu Z, Gäumann T. 1993. Structures of product Ions $C_6H_7^+$ and $C_6H_9^+$ of ion-molecule reactions with allyl bromide. Org Mass Spectrom 28:1111–1118.

Zins EL, Pepe C, Schröder D. 2010. Methylene-transfer reactions of benzylium/tropylium ions with neutral toluene studied by means of ion-trap mass spectrometry. Faraday Discuss 145:157–169.

Dietmar Kuck studied chemistry at the University of Hamburg from 1968 to 1972. He earned his doctoral degree at the newly founded Bielefeld University in 1976 under the supervision of Hans-Friedrich Grützmacher. Working as an Akademischer Direktor in Bielefeld throughout till his retirement, he pursued independent research on gas-phase ion chemistry and mass spectrometry as well as in the field of novel polyaromatic compounds. The latter work earned him the habilitation at the University of Paderborn in 1995 and the title of a Privatdozent. He joint Nico Nibbering's group at the University of Amsterdam in 1983 for a short research stay and was honored by the *Mattauch-Herzog Award for Mass Spectrometry* of the *German Mass Spectrometry Society* (*DGMS*) in 1988. After his return to Bielefeld, he was deputized Professor in 2002. Dietmar Kuck served on the Boards of *DGMS* (1995-1998 and 2002-2014) and the *International Mass Spectrometry Foundation* (IMSF, 2006-2012). He retired in 2014 but is still contributing to both of his fields.